Manipulating Histone H3 Methylation During Development: A Caenorhabditis Elegans Approach Toward Modeling Kabuki Syndrome.

Manipulating Histone H3 Methylation During Development: a *Caenorhabditis elegans* Approach Toward Modeling Kabuki Syndrome.

A Thesis in the Field of Biology

for the Degree of Master of Liberal Arts and Sciences in Extension Studies

Harvard University

November 2020

Abstract

Sophisticated and highly coordinated mechanisms regulate histone methylation during development. In a diseased state this can give rise to multi-organ system congenital disorders such as Kabuki syndrome. The *Caenorhabditis elegans* animal model provides unique control in recapitulating genetic conditions relevant to disease states, as its genes are widely homologous to humans' and its cellular development is well characterized. With this in mind, an experimental approach was designed to selectively depletion the key epigenetic regulators SET-16 or UTX-1, homologous in function to human KMT2D and KDM6A, respectively, malfunctions in which underly Kabuki syndrome. The auxin inducible degron (AID) system was shown to reliably induce targeted proteasomal degradation of SET-16 and UTX-1 resulting in changes to gene expression regulated by these factors, identified through transcriptomic analysis. The extent of auxin-induced depletion depended on both the concentration of auxin applied and the amount of time the animals were exposed. Early depletion of either SET-16 or UTX-1 consistently reduced the number of oocytes present, as well as overall fecundity. Genomic analysis indicates common changes in the expression patterns of at least 390 genes between both depletion scenarios, providing a list of potential genetic candidates for targeted treatment of Kabuki syndrome.

Acknowledgments

It is important to note that this project would not have been possible without funding through the Roya Kabuki Program and the aid of its collaborators.

I would like to extend my appreciation to Dr. Maxwell Heiman, who served as my research instructor and mentor, for both supplying the strains and devoting the time and attention to teaching me how to work with *C. elegans* in the laboratory, as well as how to perform a multitude of tasks that were critical to performing experiments and accumulating the necessary data for this project. I could not have accomplished much with regard to the following thesis project without his patience and devotion to teaching aspiring scientists, especially given the global circumstances of early 2020. The access I was given to state of the art technologies and materials was truly a privilege and the techniques I was taught will aid my future research for decades to come.

Also, I would like to offer a special thank you to both Dr. Christina Hung and Dr. Alan Jiao for their time and patience. Everything I know with regard to proper handling of RNA samples and purification techniques I credit to Dr. Hung. Her encouragement was absolutely necessary when attempting to master such a delicate process.

Dr. Jiao had no obligation to allow me to shadow him as he worked in order to learn from his techniques, but he happily volunteered his time and attention. His passion and drive is something that I fully intend to mirror throughout my career, and I greatly appreciate the first hand lessons that he showed me.

Table of Contents

List of Tables

List of Figures

Chapter I.

Introduction

Kabuki syndrome is a relatively unfamiliar condition in the modern medical field. Those diagnosed face a multitude of hurdles through life. Symptoms such as congenital heart defects, mental impairment, and immune deficiency are typically associated with this genetic disorder. Therefore, establishing a firm grasp on the underlying biological mechanisms is critical to developing more effective diagnostic protocols and ameliorative treatments. While it was first officially described in 1981, molecular data underlying the syndrome was only uncovered as recently as 2010 [Ng et al., 2010]. This is attributed to a variety of factors that make Kabuki syndrome difficult to clinically diagnose. First, the condition is thought to be somewhat rare, occurring in fewer than 1/32,000 [Cheon et al., 2015]. However, given the scarcity of diagnostic methods population statistics are subject to debate. Second, phenotypes typical of the condition, such as characteristic physiognomy (lateral sparseness of the eyebrow and eversion of the lower eyelid; prominent ears with a depressed nasal tip; etc.), tend to lose conspicuousness as the children age and grow [Matsumoto and Niikawa, 2003]. This means that unless identified early, the condition may go undetected into adulthood. Lastly, Kabuki syndrome can arise from various mutations in the *kmt2d* gene and sometimes in the *kdm6a* gene [Cocciadiferro et al., 2018]. However, these mutations are most often *de novo* which results in a lack of family history and a large amount of heterogeneity between cases, compounding the difficulties associated with recognizing the syndrome by phenotype alone.

Because information regarding the molecular genetics of this condition were virtually non-existent until only a decade ago, much remains to be done in terms of exploring the pathology and etiology of this disease. Through whole exome sequencing it was determined that *kmt2d* is the most frequently mutated gene in cases of Kabuki syndrome, with only a small percentage of patients possessing mutations in *kdm6a* [Ng et al., 2010]. KMT2D, histone-lysine *N*-methyltransferase 2D, belongs to a family of histone H3 lysine 4 (H3K4) methyltransferases that play various roles in regulating gene expression during development. This family is largely conserved, with homologs discovered in the genomes of invertebrates such as *Drosophila* and even in fungi, such as yeast [Froimchuk et al., 2017]. KDM6A, histone-lysine demethylase 6A, belonging to a family of histone H3 lysine 27 (H3K27) demethylases, claims a similar degree of conservation across species [Maures et al., 2011]. Fortunately, these genetic similarities allow for the use of well-characterized model organisms to more closely study the role histone methylation plays during cellular development, as well as to understand how mutations that affect chromatin remodeling can result in such a plethora of symptoms across multiple organ systems, typical of Kabuki syndrome.

Understanding the effect reduced activity by KMT2D or KDM6A has on development will be useful in determining the pathogenic mechanisms underlying Kabuki syndrome. Determining the importance and specificity of histone methylation by KMT2D and KDM6A interactions throughout development will serve to address several questions that persist regarding Kabuki syndrome: where and at what point in development must a mutation occur? And, why are some, indeed most, organ systems effected, but not all?

In order to address these points of interest, *Caenorhabditis elegans* has been employed as an animal model for either *kmt2d* or *kdm6a* haploinsufficiency. In order to experimentally determine the minimum threshold for reduced expression to produce characteristic phenotypes, an auxin inducible degron (AID) system has been engineered to selectively deplete products of the homologous genes *set-16* (*kmt2d*) or *utx-1* (*kdm6a*) in either somatic or germ-line tissues [Zhang et al., 2015]. This system is advantageous in that it allows for the conditional depletion of a specific protein product in defined tissues, and this study shows the extent of depletion can be modulated based on the concentration of auxin. Importantly, this system is reversible—removing auxin restores homeostatic protein levels and activity. Having temporal and spatial control of KMT2D/KDM6A levels allows for the selective manipulation of target histone methylation during different windows of development and within different tissue types. This is critical to understanding the timetable of Kabuki syndrome occurrence and progression. Tissue specificity also makes it possible to address organ systems in isolation, parsing out symptoms that are a direct result of the developmental disorder, versus the result of indirect interactions with other affected organs.

Despite its potential, the AID system is still a relatively new tool and much remains to be tested and refined regarding its application. While initial studies that employed AID have been carried out in various animal models ranging from fruit flies to zebrafish, to date the degree of control in manipulating protein levels has not been fully addressed. Previous studies focused on showing that endogenous protein depletion is efficient, rapid, and reversible but did not fully evaluate to what extent depletion can be

manipulated [Nishimura et al., 2009; Morawska et al., 2013; Zhang et al., 2015; Daniel et al., 2018; Sathyan et al., 2019].

As stated, Kabuki syndrome is a multi-organ system congenital disorder caused by *de novo* mutations in either *kmt2d* (*set-16*) or *kdm6a* (*utx-1*) resulting in the haploinsufficient expression of KMT2D/SET-16 or KMD6A/UTX-1, respectively. Yet, how the transcriptome responds to partial depletion of these factors remains to be studied in depth. The following series of experiments demonstrate that exposure to progressively elevated concentrations of auxin produces titratable depletion of AID-tagged SET-16 and UTX-1 in somatic and germline tissues, mirroring the reduced gene dosage effects in Kabuki syndrome. Transcriptomic analysis was used to evaluate the genomic response to reduced levels of SET-16 or UTX-1 throughout early embryonic development. Results demonstrate that some genes follow a trend in changed expression proportional to elevating levels of auxin, while others produce a more exaggerated trend, reminiscent of a binary, on-or-off response.

Kabuki Make-Up Syndrome

History and Discovery

While the name "Kabuki-makeup syndrome" was officially coined in 1981, harkening to the traditional make-up used in Kabuki theater, the condition was observed and documented in the medical literature as far back as 1967 [Niikawa et al., 1981]. It was first described by the Japanese pediatrician Dr. Norio Niikawa, who reportedly encountered multiple young patients as a clinician, all presenting the same or similar unique features (Figure 1). In 1968, a different, independent, group of researchers led by Dr. Yoshikazu Kuroki examined five patients all exhibiting the same unique set of symptoms [Kuroki et al., 1981]. These parallel findings led both teams of researchers to independently conclude that their patients possessed a previously undescribed condition. Dr. Niikawa initially presented his findings in 1979 to the Japanese Dysmorphology Conference, before coordinating with Dr. Kuroki and establishing the condition as "Kabuki make-up syndrome," despite reservations by editors at the *Journal of Pediatrics* that the name may be too unfamiliar for western scientists [Matsumoto and Niikawa, 2003]. Hence the more common and simpler term "Kabuki syndrome" used predominantly in western literature.

Etiology and Disease Progression

The most common features of this disease are dysmorphic facial appearance (sparseness of the lateral 2/3^{rds} of the brow, long palpebral fissures, upturning or eversion of the outer 1/3rd of the lower eyelid, broad/depressed nasal tip, and large, protruding

ears), skeletal anomalies (scoliosis, stunting, joint laxity, short fifth finger and phalanges), dermatoglyphic abnormalities (presence of finger-tip pads, finger-tip ulnar loop patterns), and both mental and growth retardation [Matsumoto and Niikawa, 2003]. These have been established as the five cardinal diagnostic criteria in identifying the syndrome. However, this method for diagnosis is flawed in that no two cases of Kabuki syndrome are identical, and these symptoms may not all be present or visually apparent in every patient. Also, these phenotypes tend to change or evolve over time, meaning that unless the condition is observed early the cardinal symptoms may no longer be obvious. In such a scenario, it is a short leap to imagine that a later diagnosis may exclusively focus on the individual symptoms, overlooking the entire syndrome. Much of the blame for difficulties in unraveling this disease, or improving screening methods, rests with the fact that the majority of cases are the result of spontaneous *de novo* mutations that introduce either a frameshift, missense or nonsense mutation within the *kmt2d* gene [Ng et al., 2010; Cocciadiferro et al., 2018]. A missense mutation or frameshift may alter the protein structure of KMT2D or its associated complex, whereas an early stop codon can halt expression of the protein entirely. Patients with similar mutations may exhibit similar or divergent phenotypes. It remains unclear if differences in disease presentation are caused by the type of mutation within the gene, at what point during embryo development that mutation occurred, or other environmental or genetic factors [Cocciadiferro et al., 2018].

Current Therapies

Initially, it was believed that the condition must be regional and is likely much less common outside of Japan, but upon further study, it was soon realized that the rate of

occurrence is largely consistent across all populations, albeit still rare [Cheon and Ko, 2015]. It is for this reason that data on the genealogy and molecular physiology of Kabuki syndrome was only first published less than a decade ago. As a consequence, there are tragically few effective therapies for this condition. Because Kabuki syndrome is characterized by congenital deformities across multiple organ systems there is no one therapy that could address all of the symptoms a patient is likely to possess. This is why it is necessary to establish an intimate understanding of the associated mechanisms that are affected by *kmt2d* or *kdm6a* mutations. There is a consensus that therapies designed to target a common denominator mechanism (if there is one), should claim primary focus with regard to research and the development of treatments [Aref-Eshghi et al., 2017].

Caenorhabditis elegans

History and Justification

C. elegans is a soil dwelling nematode. They can be isolated from decaying vegetable or fruit matter and detritus, where they feed off of resident bacteria [De Ley et al., 2011]. It was first put forward as an animal model by Sydney Brenner, in 1963, via a letter to the chairman of the Medical Research Council's Laboratory of Molecular Biology. He reasoned that an approach like that used in studies of bacteria and phages was needed to attack more subtle or mechanistic questions regarding the form and function of the nervous system, gene regulation during development, and other complex metazoan processes [Brenner et al., 1973]. *Drosophila* was already established as an effective animal model by the time of Brenner's letter, but he argued that even they are too large and complex. Therefore, he proposed that a multicellular organism should maintain as much simplicity as possible as is represented in prokaryotic systems. From this, nematodes became a leading candidate. Initially, Brenner suggested the species *C. briggsae*, but later decided on *C. elegans* for technical reasons—mainly for quality of growth in a laboratory environment [Corsi et al., 2015].

Biology, Ecology, and Lifecycle

The nematode is a relatively simple animal, with a rapid life cycle and rudimentary body form (Figure 2). Because they naturally subsist on bacteria in the wild, *C. elegans* can be easily maintained on an agar plate seeded with a lawn of laboratory strain *Escherichia coli*. These hardy organisms can survive starvation for up to six

months by entering what is referred to as a ‘dauer’ state, and can even survive being frozen for long-term storage [Brenner et al., 1973]. Obviously, these are valued traits in an animal model, due to the time constraints and typically harsh environment associated with being in a laboratory. As previously mentioned, other *Caenorhabditis* species were considered for a model, but *C. elegans* grows the healthiest between 20-25˚C (typical laboratory room temperature standard) making it convenient for housing large populations in a single facility [Corsi et al., 2015]. *C. elegans* are developmentally fixed in that the wild-type growth rate does not vary between specimens. This makes the animal a uniquely versatile model for testing molecular mechanisms that are conserved across more complex, less predictable, animals. Perhaps even more advantageous, phenotypes have been catalogued for almost every gene in the *C. elegans* genome [Culetto and Sattelle, 2000]. As for their anatomy, the entire animal is composed of only 959 somatic cells, wherein roughly one-third are neurons. From this simplicity, it was possible to characterize the fate of every embryonic cell starting at fertilization [Sulston et al., 1988]. Another useful advantage to using this animal as a model is their characteristically short lifecycle—taking only about 4-5 days from embryo fertilization to fertile adult. Adding to this, *C. elegans* reproduce by self-fertilization and many phenotypes adhere to a strict Mendelian pattern of inheritance, meaning that mutant stocks can be readily established and maintained [Brenner et al., 1973; Corsi et al., 2015]. Because every cell lineage is known, these animals are useful models to evaluate the effects a particular gene may have on any cell population, through any known mechanism. This is ideal for modeling cancers and developmental disorders, as

researchers are able to watch the effects of altered gene expression during development, in real time, within a whole organism.

Previous Applications

Because of the simplicity, versatility and ease of handling that *C. elegans* allows, this animal has been instrumental in filling informational gaps resulting from the use of more complex organisms. One such example involves a mutagenesis experiment that uncovered a set of genes which governed phagocytosis of apoptotic cells in early embryo development. From their observations, and further genetic studies, researchers identified mechanisms for programmed cell death, which, prior to that experiment, was a process believed to be conferred largely by necrosis [Hedgecock et al., 1983; Ellis and Horvitz et al., 1986]. Another example includes a study that discovered the effectiveness of double-stranded RNA interference (dsRNAi) as a method for controlled depletion of gene products [Fire et al., 1998]. To this day dsRNAi is a staple method used by geneticists and molecular biologists the world over. Since Brenner first made the argument for *C. elegans*' usefulness in the lab, many studies have been carried out using this animal model. Genes that regulate lifespan have been discovered in *C. elegans* [Kenyon et al., 1993] and this animal even served as the first whole-organism in which Channelrhodopsin-2 was demonstrated to be effective in eliciting controlled neuronal activation [Nagel et al., 2005]. The advantages associated with this animal model are such that, in 2002, Sydney Brenner and his colleagues, H. Robert Horvitz and John E. Sulston, were awarded the Nobel Prize in Physiology or Medicine for their work on genetic regulation of organogenesis and mechanisms of apoptosis.

COMPASS/MLL

Overview of Function and Patterns of Expression

Chromatin refers to the basic structural organization of DNA within a eukaryotic cell's nucleus, consisting mainly of tightly packed proteins known as core histones, along with various scaffold-like proteins that provide structural support and kinetic access to transcription-regulating enzymes [Moore et al., 2012]. The nucleosome is the major unit of chromatin, formed from an octamer complex of two of each of the histone core proteins H2A, H2B, H3 and H4, around which ~147 base pairs of DNA are wrapped [Kouzarides et al., 2007]. Each histone subunit possesses an exposed NH_2-terminal tail that can be modified, recruiting transcription-regulating enzymes to the regions of wrapped DNA via patterns of methylation, acetylation and phosphorylation at different amino residues. Various studies using mass spectroscopy and antibody staining have identified key patterns associated with active gene expression and maintenance, as well as gene silencing [Heintzman et al., 2007; Kouzarides et al., 2007; Moore et al., 2012]. Importantly, different extents of methylation have been identified that are unique to specific amino acids: lysines (K) can be marked by either mono-, di-, or trimethylation while arginines (R) only exhibit mono- and dimethylation, for example. Each of these states represent a different form of transcriptional readiness, whereby mono- and dimethylation of lysine is typically associated with enhancer priming, while trimethylation is often an indication of promoter activation [Ruthenburg et al., 2007; Wang et al., 2016]. This is with regard to regulation of developmental and lineage determining genes in eukaryotic cells, but these methylation patterns vary between cell

types and are also believed to play intimate roles in epigenetic regulation after development [Heintzman et al., 2007; Kouzarides et al., 2007; Ruthenburg et al., 2007]. Methylation of lysine residues is carried out by a family of enzymes known as lysine methyltransferases, or KMTs. In humans, KMT2D, often referred to as Mixed Lineage Leukemia 4 (MLL4, also sometimes referred to as MLL2 in some older literature), has been identified as a key regulator of gene expression during development [Lee et al., 2013; Yan et al., 2018]. KMTs in humans exist in the COMPASS/MLL family of complexes, but because of its known role in early development and indications that malfunction of this particular member leads to developmental disorders such as Kabuki syndrome, KMT2D of COMPASS/MLL4 will be the primary subject for discussion [Froimchuk et al., 2017; Cocciadiferro et al., 2018]. An important subunit of the COMPASS/MLL4 complex, KDM6A, or lysine demethylase 6A, has also been shown to play a critical role in promoting stability of the overall complex, as well as in preparing chromatin for KMT2D activity [Wang et al., 2017]. Malfunctions in KDM6A have also been implicated in cases of Kabuki syndrome, although less commonly [Cocciadiferro et al., 2018]. KMT2D specifically deposits methyl groups on the 4th lysine of the H3 core histone, or H3K4 site. As previously mentioned, these modifications can include H3K4me1, H3K4me2, and H3K4me3 and are indicators of enhancer activation (H3K4me1, H3K4me2) and promoter activation (H3K4me3) [Ruthenburg et al., 2007; Lee et al., 2013; Wang et al., 2016]. KDM6A, also commonly referred to as UTX-1, or simply UTX, is a primary H3K27me-1, or demethylator that has been shown to play an important conformational role for KMT2D activity [Zhang et al., 2016; Wang et al., 2017]. However, the exact kinetics of this interaction are not yet well understood. For

example, it has been shown in a *C. elegans* model that KDM6A regulates cellular development and normal growth regardless of its demethylase activity [Vandamme et al., 2012]. It is also required for the recruitment of the H3K27 acetyltransferase (H3K27ac) p300 in an enzymatically independent manner, while loss of KDM6A results in reduced H3K4me1 and p300 binding instability [Wang et al., 2017]. This is curious in that H3K27me1 indicates a "poised" or repressed state of activation, and this methyl group must be removed to allow for activating H3K27ac by p300 [Kouzarides et al., 2007; Fang et al., 2014]. Furthermore, activity by KMT2D at H3K4 requires activity by p300, which in turn enhances activity by p300, however this feedback cycle is initiated by KDM6A in a demethylase-independent manner, suggesting some other mechanism at play in preparing the H3K27 site [Wang et al., 2017].

Structure and Subunits

COMPASS stands for Complex of Proteins Associated with Set1, named for its original discovery in yeast, which only possesses one form of this complex [Roguev et al., 2001]. The human genome possesses six orthologs of the COMPASS family, namely SET1a, SET1b, and MLL1-4, but the MLL4 member has been the most extensively studied to date [Ruthenburg et al., 2007; Takahashi et al., 2011; Shilatifard et al., 2012; Lee et al., 2013; Sze et al., 2016; Froimchuk et al., 2017]. COMPASS/MLL4 contains five main subunits (KMT2D, KDM6A, PTIP, PA1 and NCOA6) along with four associated factors collectively referred to as the sub-complex WRAD (WDR5, RbBP5, ASH2L, and DPY30) [Takahashi et al., 2011; Shilatifard et al., 2012; Sze et al., 2016; Froimchuk et al., 2017]. PTIP and PA1 are unique to COMPASS/MLL4 and its sister

complex COMPASS/MLL3 [Froimchuk et al., 2017]. A visual representation of the estimated structure of this complex is demonstrated in Figure 3. The KMT2D protein, itself, is considered to be the main structural component, and contains an enzymatically active SET domain, which has been shown to be crucial for maintaining the stability and nominal activity of the overall complex [Ruthenburg et al., 2007; Takahashi et al., 2011].

Disease Mechanism(s)

KMT2D, indeed the COMPASS/MLL4 complex in general, has been shown to play critical roles in diverse processes like early embryonic and postembryonic development (maintenance of pluripotency and establishment of cell fate), tumor suppression and even regulation of circadian rhythms [Kim et al., 2014; Kantidakis et al., 2015; Rickels et al., 2016; Wang et al., 2016; Yan et al., 2018; Schwenty-Lara et al., 2019]. Despite numerous findings regarding the functional importance of COMPASS/ MLL4 catalytic domains in selective gene expression, it is notable that a few recent studies determined COMPASS/MLL4 possessing enzymatically deficient KMT2D 1) does not result in a major loss of H3K4me1 at enhancer sites, 2) does not drastically hinder RNA synthesis at associated promoter sequences and 3) does not prevent exiting from a pluripotent state in murine embryonic stem cells [Dorighi et al., 2017; Cao et al., 2018]. This indicates that KMT2D driven monomethylation at enhancers is only a minor portion of the overall capacity by COMPASS/MLL4 to regulate gene expression and aligns with the previously mentioned finding by Wang et al., that enzymatic activity by UTX-1 is also not exclusively required to drive enhancer activation. In all of these cases, complete knockout or removal of the proteins within the complex is necessary to

significantly disrupt normal patterns of expression. Together, such findings represent a serious enigma concerning the etiology of genetic conditions like Kabuki syndrome, whereby mutations in either *kmt2d* or *kdm6a* result in significant developmental defects, but the nature of these mutations are highly variable and neither expression of KMT2D or KDM6A is totally lost [Ng et al., 2010].

C. elegans Homologs

As briefly stated in the introduction, the COMPASS/MLL family of complexes are widely conserved, with human orthologs having been identified in species ranging from single-celled eukaryotes to vertebrates [Froimchuk et al., 2017]. The original discovery of this complex was identified using a yeast model and has been extensively studied in fly as well as nematode models [Roguev et al., 2001; Ruthenburg et al., 2007; Fisher et al., 2010; Greer et al., 2010; Maures et al., 2011; Mohan et al., 2011; Rickels et al., 2016]. Members of the *C. elegans* COMPASS/MLL complex, namely SET-16 (KMT2D homolog) and UTX-1 (KDM6A homolog) have been shown to be critical in regulating developmental processes and lifespan, as well as fertility [Fisher et al., 2010; Greer et al., 2010; Vandamme et al., 2012]. However, a cardinal difference between the *C. elegans* homolog and human COMPASS/MLL4 is that loss of a single allele of SET-16 or UTX-1 has no overt phenotype, in contrast to the severe developmental phenotypes observed upon loss of a single allele of KMT2D or KDM6A in humans [Anderson and Horvitz, 2007]. This makes it impossible to study the basis of haploinsufficiency in *C. elegans*, and requires and new experimental approach.

AID/SCF-TIR1

Natural Context

The auxin inducible degron (AID) system is derived from a pathway in plants—in this case, specifically *Arabidopsis thaliana*—whereby the presence of the plant hormone auxin (IAA17: indole-3-acetic acid 17) is required for initiating target protein proteasomal degradation [Teale et al., 2006]. Degron is short-hand for 'a domain to induce degradation.' In plants, the AID system plays a key role in regulating patterns of gene expression during growth and development by acting as a conditional and selective repressor of protein products, aiding in processes like lateral root formation, orientation, and cellular elongation [Ruegger et al., 1998]. This is accomplished when a degron-tagged protein is marked for proteasomal destruction by the E3 ubiquitin ligase complex SKP1-CUL1-F-Box, or SCF (Skp1: S-phase kinase-associated protein; Cul1: Cullin-1; Rbx1: RING-box protein 1) combined with the F-box protein TIR1 (Transport Inhibitor Response 1), wherein, upon recognition of auxin, this SCF^{TIR1} complex recruits an E2 ligase resulting in polyubiquitylation of the degron, initiating proteasomal destruction of the tagged protein [Teale et al., 2006; Nishimura et al., 2009].

System Usefulness

While TIR1 orthologs have only been discovered in plants, the SCF complex—Skp1 in particular—exists, in some form, in all eukaryotes [Nishimura et al., 2009]. Because the SCF directed proteasomal pathway is so widely conserved, it has been possible to generate other organismal models that efficiently incorporate the AID-tag and

TIR1 constructs, allowing scientists to perform controlled, reversible, protein degradation studies across multiple developmental timepoints and within specified tissue types [Nishimura et al., 2009; Morawska et al., 2013; Zhang et al., 2015; Daniel et al., 2018]. What truly makes this approach unique is the level of control allotted to the user. Other methods of controlled depletion have traditionally relied on the use of genetic disruptors like CRISPR/Cas9 directed DNA mutations or RNAi, however, these methods do not target the protein products directly, and instead act at the level of transcription or translation [Fire et al., 1998; Cong et al., 2013]. Therefore, protein stability *in situ,* as well as its specific role during development, potentially become limiting factors in these types of experiments. This necessarily results in a buffering to the temporal effect of the treatment, and is frequently associated with off-target effects. With this system, though, simply adding purified auxin to the environment, or incorporating it into the food/water supply, reliably induces AID-mediated destruction of target proteins in the model organism. Removal of auxin relieves this effect (Figure 4).

Successful Applications

This degron system was first reengineered and tested in the budding yeast *Saccharomyces cerevisiae*, where researchers demonstrated that both the AID and TIR1 constructs could be inserted into the genome of a non-plant organism and could efficiently reduce endogenous Mcm4 (mini-chromosome maintenance) protein levels, resulting in impaired colony formation [Nishimura et al., 2009]. Later, in another study, also within a yeast model, researchers were able to reduce the size of the AID construct from a 229 amino acid full-length IAA17 protein to just 44 amino acids, reducing the

destabilizing effect induced by fusion of the tag to the target protein [Morawska and Ulrich, 2013]. Following this, the minimized AID construct was successfully inserted into the genome of *C. elegans*, where researchers demonstrated that auxin-inducible degradation of target proteins was efficient and reversible in an animal model [Zhang et al., 2015]. More importantly, though, Zhang *et al.,* (2015) also established generalized tissue specificity by driving TIR1 expression from either the *eft-3* promoter and *unc-54* 3' UTR for somatic tissues or the *sun-1* promoter and 3' UTR for germline tissues, effectively demonstrating controllable depletion within specific tissue types.

Recently, it was demonstrated that the AID/TIR1 system could be employed as a means of controlling reproductive timing in *C. elegans* by using the degron to target a gene that regulates spermatogenesis, *spe-44*, thus allowing researchers to control fertility [Kasimatis et al., 2018]. More work has been done in recent years to refine the specificity of this genetic tool-kit. It was understood upon the initial development of this system that off-target or auxin-independent effects could be a potential issue. Fortunately, researchers determined that co-expressing the PB1 domain of the *Arabidopsis* auxin response factor (ARF) improved the effectiveness of the AID construct, both decreasing the occurrence of auxin-independent degradation and increasing the rate at which auxin-mediated degradation takes place following exposure [Sathyan et al., 2019]. However, this finding is still relatively new and has not yet been incorporated into many other AID oriented studies.

Hypothesis and Research Aims

Controlled temporal and systematic depletion of KMT2D and KDM6A homologs by auxin induced degradation (AID) will demonstrate titratable manipulation of gene expression and identify associated elements of regulated lysine histone methylation, through visible expression and transcriptomic profile.

Experimental Goal

Here, the overarching goal was to demonstrate titratable, spatiotemporal control of gene expression using the AID/TIR1 system, with the added intent of using this system to catalog transcriptional responses to manipulating histone lysine methyltransferase and lysine demethylase activity by KMT2D and KDM6A homologs, respectively. To date, this auxin dependent system has only been employed to induce a total depletion of selected protein targets, using higher concentrations of the hormone to produce the strongest degradative effect. However, previous studies have not exploited the ability of this system to induce controlled reduction of a particular protein to an arbitrary level, as opposed to complete removal, by gauging the concentration of auxin used. Incomplete depletion would be more comparable to pathological cases of haploinsufficiency, in which not all of the protein product is lost or fails to translate, but enough depletion has occurred to generate an aberrant phenotype. As previously mentioned, Kabuki syndrome is caused by haploinsufficiency of either KMT2D or KDM6A. This experiment is intended to model that pathological state in an organism that can be easily monitored and analyzed through each stage of development.

Specific Aim 1

Hypothesis—The AID system, paired with expression of TIR1, can be used to conditionally knock-down KMT2D and KDM6A to arbitrary levels.

While knock-out models have been historically useful for establishing a firm understanding of broad mechanisms across species, many of the more subtle mechanisms involved in a majority of developmental disorders and chronic illnesses cannot be readily addressed through a simple knock-out. Instead, having the ability to conditionally—reversibly—alter product concentration *in vivo* would be far more appropriate. Here, such a model will be demonstrated using four genetic strains of *C. elegans* engineered to co-express AID-tagged SET-16, along with expression of TIR1 either from a somatic or germ-line promoter, as previously described. AID will be expressed from the same promoter of SET-16 along with GFP for visual confirmation of expression—TIR1 is tagged with mRuby and is coexpressed from either the *eft-3* promoter for somatic tissues, or the *sun-1* promoter for germline tissues. Results demonstrate the effective removal of SET-16 from oocyte nuclei in young adults when auxin is present, conditional upon co-expression of TIR1 (data not shown), and that knock-down is reversible upon auxin removal. This experiment is intended to demonstrate a titratable response to auxin and will allow for analysis of phenotypic changes at particular expressive thresholds.

Specific Aim 2

Hypothesis: Transcriptomic analysis of whole organisms at various auxin concentrations will reveal changes to overall expression patterns, identifying developmental targets of KMT2D and KDM6A activity.

Given the expectation that the COMPASS/MLL complex is highly regulated throughout development, interrupted activity by auxin induced degradation is likely to result in detectable changes in the expression of tissue-specific target genes. Whole exome RNA sequencing is a useful method for identifying changes in gene expression. RNA analysis of the entire transcriptome in each hybrid strain, under conditions of varying auxin concentration, and thus, variable KMT2D or KDM6A depletion, will provide a detailed profile of the transcriptional changes that result from a reduction in histone H3K4 mono-, di-, and tri-methylation, as well as from reductions in H3K27 demethylation. These findings are intended to demonstrate the viability of candidate genes as therapeutic targets in treating lysine methyltransferase specific developmental disorders, such as Kabuki syndrome. Importantly, because Kabuki syndrome arises from *de novo* mutations during embryonic development and not familial inheritance, somatic tissues will be targeted for transcriptomic analysis, in an attempt to disentangle the effects of maternal and zygotic altered histone methylation activity.

Chapter II.

Materials and Methods

All experiments were performed in triplicate. Each replicate consisted of freshly made medium and independent synchronized populations of animals. For routine strain maintenance, populations were stored at 20˚C, cultured on standard NGM plates and passaged twice per week to prevent overcrowding or starvation, according to standard protocols [Brenner et al., 1979].

Auxin Preparation

Auxin plates were prepared from a 400mM liquid stock made of auxin, (Indole-3-acetic acid, IAA) (MW=175.19) dissolved in ethanol, prepared fresh monthly. Auxin stocks were stored at 4˚C in the dark and were replaced after 30 days. Auxin plates were prepared using four concentrations: 1.0mM, 0.1mM, 0.01mM, and 0mM (control). To account for additional solvent, all volumes were made to contain a final concentration of 0.25% ethanol. Plates were stored under the same conditions as the 400mM auxin stocks, at 4˚C away from light and were not kept beyond 30 days. Plates were prepared 4-5 days prior to the start of each experiment and new plates freshly prepared for each experimental replication. Any plates showing signs of contamination or chemical breakdown (yellowing of agar, presumably due to auxin decomposition) were not used for experiments. Plates were seeded with laboratory strain *Escherichia coli*, OP50, 2-3 days prior to plate use, allowing for sufficient growth of a feeder lawn. For higher

concentrations of auxin, it was sometimes necessary to first concentrate OP50 stock by centrifugation to yield a higher density for seeding [Zhang et al., 2015].

Population Preparation

All animals used for experiments were synchronized first larval stage (L1) progeny prepared by bleach treatment of gravid adults. Synchronization was accomplished by washing animals into Eppendorf tubes using M9 medium, followed by brief centrifugation and removal of excess solution. Bleaching solution was prepared by mixing sodium hydroxide, sodium hypochlorite, and water in a 1:1:2 ratio. Washed animals were suspended in 2mL bleaching solution for ~4 minutes, with occasional mixing by hand shaking. Once all adults were lysed, remaining embryos were washed up to 5 times in M9 to remove residual bleach from the sample, and suspended in clean M9 medium. Samples were then placed on a rotator overnight. The following morning, hatched L1s were deposited onto standard, seeded NGM plates and allowed to reach the L4 stage before transfer to an auxin containing environment. Their progeny were then selected at either the L4 stage or as day 1 adults, depending on the intended procedure.

Fluorescence Imaging of Germline GFP

Specimens for imaging were mounted onto 2% agarose gel pads and anesthetized using 30uL 100mM sodium azide. Images were acquired using a Deltavision Core imaging system (Applied Precision) with UApo/340 40×1.35NA, PlanApo 60×1.42NA and U- PlanApo 100×1.4NA objectives (Olympus) and a CoolSnap HQ2 camera with settings at 100% transmittance for GFP fluorescence (EX) with 300 msec exposure time. Brightfield (polarized (POL)) images were collected with the exposure time adjusted to 25 msec to compensate for brightness saturation of images. All images were acquired using the 60X objective. Images were taken of L4 stage animals, or 1-day adults with grossly normal appearance and at least four pre-fertilization oocytes with readily discerned nuclei. Brightness differences were calculated using both germline hybrid strains for SET-16, *ieSi64* II; *set-16*(*syb1046*)III, and UTX-1, *ieSi64* II; *utx-1*(*syb1026*)X. See Table 1 for a full list of strains and brief descriptions. All images were processed using Fiji Imaging Software. For each nuclei, three measurements were taken: one of the nucleus center, one of the ventral oocyte cell body, and one of the dorsal oocyte cell body. The average background intensity value was calculated from the two measurements derived from the cell body, and this value was subtracted from the center nucleus measurement. The final calculated value was considered to be the intensity of nuclear GFP expression in germline cells.

Fluorescence imaging of Somatic GFP

Samples were imaged using the same methodology described above. All images were acquired using the 40X objective. Images were taken at the L1 and L2 stages. Brightness differences were calculated using both somatic hybrid strains for SET-16, *ieSi*57 II; *set-16*(syb1046)III, and UTX-1, *ieSi*57 II; utx-1(syb1026)X. See Table 1 for full list of strains and brief descriptions. All images were processed using Fiji Imaging Software. For each animal imaged a total of five measurements were taken of tail nuclei followed by a single measurement from tail background. This background measurement was then subtracted from each nuclear measurement. The final calculated values were considered to be the actual difference in intensity of nuclear GFP expression in the soma.

RNA Purification

For RNA purification, animals from each strain were washed from seeded agar plates using standard M9 buffer solution into 1mL Eppendorf tubes and centrifuged to form a pellet. M9 supernatant was removed and the pellet was washed 2-3 times with clean M9 to remove bacterial contamination. Animals were left suspended in M9 and placed on the rotator for ~30-60 min in order to allow for clearance of the gut. The animals were then washed once more before final removal of the supernatant. Next, around 150-250µL Trizol was added depending on the overall volume of animals recovered, with an estimated ratio of 2:1 Trizol to pellet volume. The solution was then vortexed for 1 minute and submerged in liquid nitrogen until frozen, followed immediately by a water bath at 40˚C. Once thawed, the sample immersed again in a liquid nitrogen bath and this process was repeated at least 5 times to ensure complete rupture of the cuticle and RNA exposure to Trizol. Next, dependent on sample volume, 50-100uL chloroform was added, vortexed for ~30 sec, and centrifuged at 12,000 rpm for 15 min at 4˚C. The upper aqueous layer was transferred to an RNase free Eppendorf tube, and centrifuged once more using the above conditions. The aqueous layer was then transferred to another RNase free eppendorf tube and this process was repeated 2-3 more times, as needed. Next, 125uL 2-propanol was added and mixed gently, without vortexing, followed by centrifugation at 12,000 rpm for 10 min at 4˚C. The supernatant was then removed and discarded and the remaining pellet washed with 250-500uL 70% ethanol (RNase free). The solution was centrifuged at 14,000rpm for 5 min at 4˚C. Ethanol was completely removed and the pellet allowed to dry before dissolving in ~10-25uL RNase free water, again dependent on recovered pellet size.

DNA contamination was removed using an Invitrogen TURBO DNA-*free* Kit (ThermoFisher Scientific) according to User Guide instructions: ~33uL RNase free water was added to an RNase free eppendorf tube, followed by 10ug RNA sample (calculated from the total estimated yield, determined via NanoDrop ND-1000 spectrometer) with the addition of 5uL 10X TURBO DNase Buffer with 1uL TURBO DNase Enzyme. The solution was then mixed gently, without vortexing and incubated at room temperature for 20-30 min. Finally, 1uL of 0.5M EDTA was added to neutralize DNase enzymes and the solution was incubated at 65˚C for ~10 min. The sample was then placed on dry ice and delivered to the Dana-Farber Cancer Institute Molecular Biology Core Facility for sequencing.

Bioinformatics

RNA sequencing was performed on a total set of 24 samples representing somatic depletion of SET-16 and UTX-1 under four auxin concentrations (0mM, 0.01mM, 0.1mM, and 1mM) in three full replicates. RNA sequencing was also performed on a single replicate of eight samples representing germline depletion of SET-16 and UTX-1 under the same four auxin conditions mentioned above.

The resulting fastq files containing the RNA sequencing reads were processed in collaboration with Dr. Jaejoon Choi and Dr. Alice Lee (Roya Kabuki Program at Boston Children's Hospital) using the following analytical pipeline: 1) reads were aligned to the c_elegans.PRJNA13758.WS274 genome (wormbase.org) and HTSeg was used to count the number of aligned reads per gene. 2) DESeq2 was used to determine a list of differentially expressed genes (DEGs) that resulted from developmental exposure to each

auxin condition. 3) A functional enrichment test (https://wormbase.org/tools/enrichment/tea/tea.cgi) was performed on each DEG list to establish which biological functions are related to expression patterns that are altered.

A list of all DEGs that were commonly identified upon somatic depletion of both SET-16 and UTX-1, showing Log2FoldChange and adjusted p-values, can be found in the Supplemental Table Data section (Table S1). No table for germline depletion has been included as only one DEG was identified.

Chapter III.

Results and Interpretation

Oocyte Nuclear GFP Intensity

To determine if intermediate levels of protein depletion can be achieved by titrating auxin concentrations, animals expressing SET-16-AID-GFP or UTX-1-AID-GFP with TIR1 expressed in the germline or soma were cultured on 0mM, 0.01mM, 0.1mM, or 1 mM auxin and the resulting GFP intensity in the germline (pre-fertilization oocytes) or soma (a group of cells in the tail) was measured. Upon calculating nuclear GFP intensity values, a trend in the data was visible for both the germline and somatic depletion strains (Figures 5.1-8.2).

SET-16 germline and soma depletion strains produced linear downward curves in response to increasing auxin concentration, with the highest concentration (1.0mM) yielding the greatest reduction in GFP intensity. For SET-16 germline depletion, the average value of nuclear GFP intensity in the absence of auxin was 201.72±78.62; at 0.01mM, 135.06±88.35; at 0.1mM, 78.39±74.26; and at 1.0mM, -0.187±51.01 compared to background. For SET-16 somatic depletion, the average value of nuclear GFP intensity without auxin was 356.74±129.45; at 0.01mM, 265.37±134.94; at 0.1mM, 86.45±97.21; and at 1.0mM, 4.13±29.66 compared to background.

UTX-1 strains demonstrated a steeper response curve to auxin with GFP intensity being abolished at 0.1mM concentration. The average nuclear GFP intensity value without auxin for UTX-1 germline depletion was 172.6±58.96; at 0.01mM, 34.86±58.96; and at both 0.1mM and 1.0mM, the adjusted intensity value fell below 0 (-28.62±30.55

and -23.69±21.21, respectively) due to higher background autofluorescence in cytoplasm. For UTX-1 somatic depletion the average value of nuclear GFP intensity in the absence of auxin was 361.24±118.30; at 0.01mM, 52.19±54.52; and at both 0.1mM and 1.0mM the signal was essentially absent (10.80±21.38 and -4.23±19.21, respectively).

While SET-16 is the major component of the *C. elegans* COMPASS/MLL complex, UTX-1 appears to show a higher sensitivity to auxin induced depletion (Figures 7.2 & 8.2). This is possibly related to it being a more peripheral component of the complex and thus more accessible to the degradation machinery. However, loss of SET-16 results in a stronger phenotypic response and greater reduction in overall brood-size (Figures 9.1-10.2). These data show that the auxin degron system can be used to deplete a protein of interest to arbitrary levels, in order to study dosage-sensitive effects. Importantly, these results also show that the dose-response curve for depletion needs to be empirically evaluated for each protein under study, as different proteins—even members of the same complex—can exhibit strikingly different response curves.

Transcriptomic Analysis

To determine how partial depletion of SET-16 and UTX-1 affect phenotype, in this case gene expression, transcriptomic analysis was performed on the somatic depletion strains at each auxin concentration. Statistical analysis of RNA-seq data from whole animals identified altered expression of 4047 genes following somatic depletion of SET-16 (1969 upregulated; 2078 downregulated) and 569 genes following somatic depletion of UTX-1 (432 upregulated; 137 downregulated). Among these data sets there were 390 genes with altered expression in both strains that follow approximately the

same trends in response to auxin exposure (Figure 11; Table S1). From that list, there are several candidates that stand out as being the most statistically significant and with the greatest fold change: for example, the uncharacterized gene *Y70C5A.3* had the greatest reduction, showing a -1.9-fold and -2.2-fold decrease in gene expression after SET-16 and UTX-1 depletion, respectively, with an adjusted p-value ≤ 0.00001 in either case. It should also be noted that from transcriptomic analysis of germline strains only a single DEG was identified, *his-63*, with an adjusted p-value of ≤ 0.05 in either case. It is interesting to note this gene was downregulated by both depletion of SET-16 and UTX-1 but was not identified in the somatic depletion data set.

These data contain a few features that are worth addressing further:

1. A greater number of DEGs for both depletions are up-regulated, suggesting that the overall effect of the wild-type COMPASS/MLL complex is to indirectly reduce gene expression during development. This is surprising in that KMT2D and KDM6A promote transcription (through H3K4me and H3K27me, respectively) so their depletion would be expected to result in wide-spread down-regulation, however this was not observed.

2. Some genes demonstrate a steeper response curve to auxin induced depletion, suggesting that the COMPASS/MLL complex must also rely on activity by other transcription regulating factors for the majority of its targets, but that some genes are more dependent on the specific patterns of histone methylation deposited by this complex, possibly highlighting suitable genetic candidates as therapeutic targets. This might demonstrate why Kabuki syndrome can present with so many degrees of severity in patient cohorts, but all cases still maintain those previously described

cardinal features used to identify the condition in a clinical setting, which would indicate a set of genes whose expression is consistently affected by this disease.

3. Gene-set enrichment tests showed that a significant number of down-regulated genes after somatic depletion of SET-16 promote male-like phenotypes, germline development and reproductive system growth (Figure 12.2). Notably, reduced fertility was observed for this strain, noticeable in both the number of oocytes present in mature adults as well as in overall fecundity (Figures 6.1 & 9.1). In both SET-16 and UTX-1 somatic depletions, gene-sets for sensory neurons including the outer labial sensilla, and PVD neurons were up-regulated. This is interesting as neurological disorders are frequently reported in human Kabuki patients.

4. Many of the commonly identified DEGs are members of the same family of genes (for example, 24 out of a total of 39 members from the "*pals*-," or Protein Containing ALS2cr12 Signature family; Figure 14), which are present in the genome as a large gene cluster. This result suggests that the COMPASS/MLL complex possibly regulates gene expression across a chromosomal locus i.e. this complex governs multiple genes on the basis of their physical position in the genome.

5. Lastly, because 390 DEGs were identified by analysis after somatic depletions but only one DEG after germline depletion, this may suggest that the larger number of affected genes seen in somatic depletion suggests a major role for UTX-1 and SET-16 in the ongoing maintenance of gene expression, while the smaller number of affected genes seen in germline depletion suggests that normal expression of these factors within the zygote is sufficient for healthy development.

Chapter IV.

Discussion

Firstly, Specific Aim 1 of this project determined via quantification of GFP intensity that the AID/TIR1 system can induce titrated depletion of a specific gene product at the protein level. Importantly, the extent of protein depletion is directly determined by the concentration of auxin used. This is advantageous in that it allows for arbitrary reduction of *in situ* protein levels that can be readily reversed by simply removing auxin from the environment. Previous methods for producing knockout models focus on eliminating protein expression, yet many human diseases arise from dose-dependent effects that may differ markedly from complete loss of function. Second, transcriptomic analysis using RNA-seq has identified 390 genes (329 upregulated, 61 downregulated) whose expression is altered by both the loss of KMT2D (Kabuki syndrome type 1) and KDM6A (Kabuki syndrome type 2) homologs, potentially establishing candidates that are responsible for the related symptoms between both types of syndrome. Gene-sets responsible for governing the development of the reproductive and neurological systems as well as sex specific phenotypes were mainly affected by these depletion experiments (Figures 12.1-13.2). Whether this is connected to developmental defects in human cases of Kabuki syndrome is yet to be determined, however this data suggests that there is a significant correlation between insufficient expression of KMT2D (SET-16) or KDM6A (UTX-1) and subsequent dysregulation of expression for many members of the same families of genes and gene-sets related to specific roles in development.

Significance

While the AID system has been employed with success in various experimental models, prior to this series of experiments the system has not been used to evaluate intermediate degrees of depletion representative of genetic disorders characterized by the haploinsufficient expression of a protein product. Previous experiments have modeled haploinsufficiency by inactivating a single allele, however there are two issues with this approach. First, unless tissue specific methods are employed, this typically results in the los of the genetic product from the very beginning of development, and does not model a *de novo* mutation that occurs during development. Second, and more importantly, traditional knockout methods are generally limited to producing 50% gene dosage. This may not be the case in patient cohorts, where hypomorphic mutations or genetic compensation may lead to other gene dosages. Further, the threshold concentration to elicit a phenotype may differ between humans and the model organism being used. Therefore, the use of an inducible degradation system is powerful simply because the extent of depletion is readily controlled by the concentration of the induction agent, in this case auxin, and thus any arbitrary gene dosage can be 'dialed-in.'

Here, the effectiveness of the AID system is demonstrated in *C. elegans* by modeling variable depletion of either SET-16 or UTX-1 reminiscent of the genetic disorder Kabuki syndrome, with the added potential for uncovering critical developmental windows in which such a loss can result in differential severity of the condition.

Future Directions

While GFP intensity calculations demonstrated a significant response to auxin inducible degradation and RNA-seq analysis shows a wide genomic response to loss of SET-16 and a mild genomic response to loss of UTX-1, phenotypic analysis and fertility measurements are still incomplete. At a glance, it is clear that higher concentrations of auxin exposure for both the SET-16 somatic depletion and UTX-1 germline depletion strains result in noticeable phenotypic anomalies within either population as well as reduced population density compared to controls (Figures 9.1-10.2). Based on the transcriptomic data, it will be useful to conduct histone immunostaining and western blot experiments to identify the relative changes to patterns of mono-, di-, and trimethylation that result from titrated depletion of SET-16 and UTX-1, as well as to identify where and when these changes are occurring during early development. Adding to this, candidate genes identified through the RNA-seq experiments can then be used to weigh the significance of these changes to normal histone H3 methylation patterns. This will potentially identify therapeutic targets that can be manually up-regulated, down-regulated or supplemented in order to compensate for haploinsufficient expression of the proper COMPASS/MLL4 complex.

Limitations

It is worth noting that previous studies that employed the AID system reported a minor degree of proteasomal degradation induced by the AID-tag in the absence of auxin [Morawska et al., 2013]. While this is not expected to have had an impact on experimental outcomes it is worth keeping in mind that some variability in phenotypic

severity across conditions will be present, even in control groups cultured on standard agar plates. Indeed, morphological defects were occasionally observed even in the absence of auxin, indicating that the tagged proteins may not be fully functional, or that the degron does sometimes initiate auxin-independent proteasomal degradation.

With regard to GFP fluorescence intensity measurements: a substantial amount of variability was observed in the overall brightness of nuclear expression in untreated animals, as well as following auxin exposure. While overall trends in the datasets are visibly and statistically present, it should be noted that measurements taken from the somatic lines demonstrate a greater degree of variability, largely due to difficulty in identifying nuclei that have reduced GFP signal, in combination with a poorer quality appearance of animals at higher auxin concentrations. In such cases, cellular backgrounds tend to appear hazier than control counterparts, returning low but non-zero values, despite no GFP signal being noticeably present in tail nuclei. Adding to this, sodium azide used to anesthetize animals tends to induce vacuoles within tissues after a short period of time, affecting fluorescence.

Conclusions

The purpose of this series of experiments was to demonstrate the effectiveness of the AID system to induce titratable depletion of a protein product to an arbitrarily defined functional level, reminiscent of a disease state caused by haploinsufficiency. This new genetic approach was successful in reducing both SET-16 and UTX-1 proteins in both somatic and germline tissues and the extent of this depletion was directly dependent on the concentration of environmental auxin that animals were raised on. In response to this

depletion, RNA sequencing results show changes, either by up-regulation or down-regulation, of associated genes that correlate with the overall extent of auxin-induced depletion of both SET-16 and UTX-1. Through verification of application of the AID toolkit, it is now possible to model a plethora of genetic illnesses, such as Kabuki syndrome, in particular, that are caused by reduced gene dosage rather than a complete null. Lastly, these series of experiments have demonstrated the critical importance of the COMPASS/MLL family of complexes in development, as even subtle depletion of SET-16 or UTX-1, using 0.01mM auxin, resulted in genome-wide changes in gene expression within the *C. elegans* model, despite animals appearing grossly wild-type. Given the importance of choreographed histone methylation during development among all organisms, diseases that result from impaired function of complexes such as COMPASS/MLL4 should be given more attention in future studies as the individuals who possess these diseases, namely Kabuki syndromes Type I and Type II, face a lifetime of health disparities with few available means of treatment.

Appendix 1.

Table 1. *C. elegans* strains used in study.

Strain Name	**Transgene**	**Description**
CA1352 “GermTIR1”	*ieSi64* II	This strain carries the TIR1 F-box protein expressing in germline tissues.
CA1200 “SomaTIR1”	*ieSi57* II	This strain carries the TIR1 F-box protein expressing in somatic tissues.
CHB3561 “SET-16”	*set-16(syb1046)* III	This strain carries the AID-GFP tagged SET-16 at its endogenous locus.
CHB3564 “UTX-1”	*utx-1(syb1026)* X	This strain carries the AID-GFP tagged UTX-1 at its endogenous locus.
SET-16/GermTIR1	*ieSi64* II; *set-16(syb1046)* III	Strain used for germline depletion of SET-16.
UTX-1/GermTIR1	*ieSi64* II; *utx-1(syb1026)* X	Strain used for germline depletion of UTX-1.
SET-16/SomaTIR1	*ieSi57* II; *set-16(syb1046)* III	Strain used for somatic depletion of SET-16.
UTX-1/SomaTIR1	*ieSi57* II; *utx-1(syb1026)* X	Strain used for the somatic depletion of UTX-1.

Appendix 2.

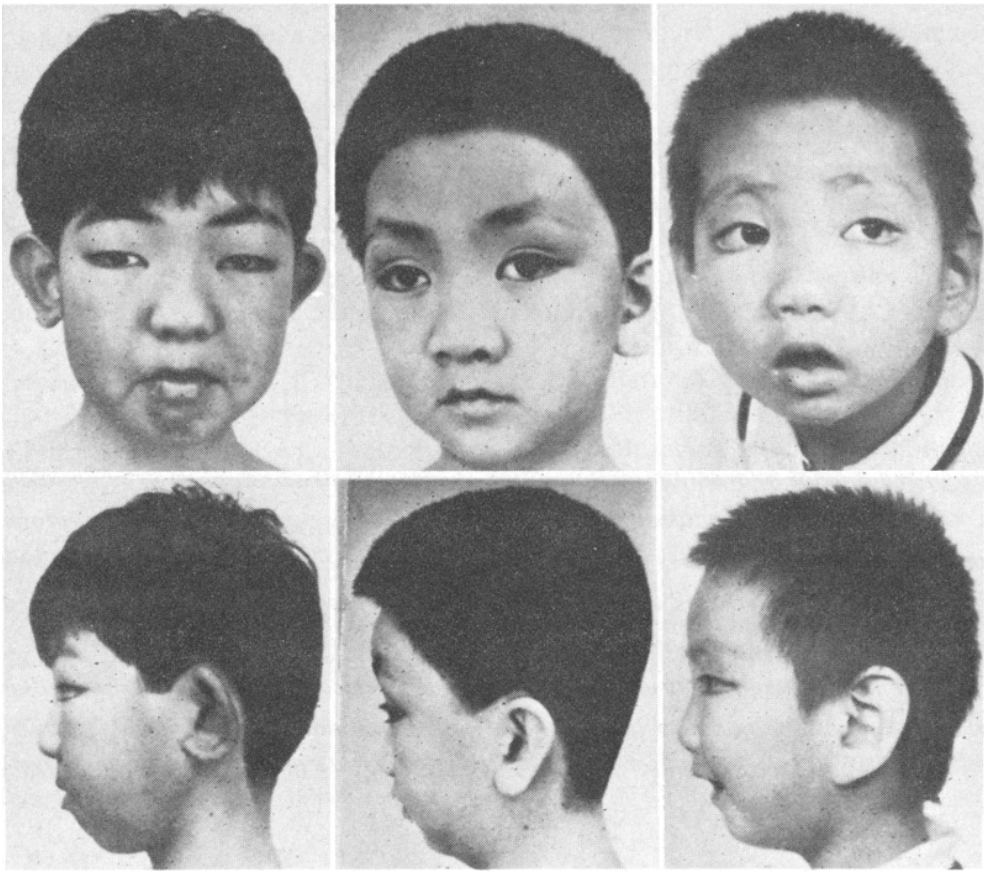

Figure 1. Kabuki Syndrome Patient Appearance from Front and Side.

Images depicted demonstrate each patient exhibits physiognomies consistent with the cardinal features associated with this genetic condition: eversion of the lateral lower eyelid, elongated palpebral fissures, arched eyebrows and a depressed nasal tip (Patient images by Nikawa et al., 1981).

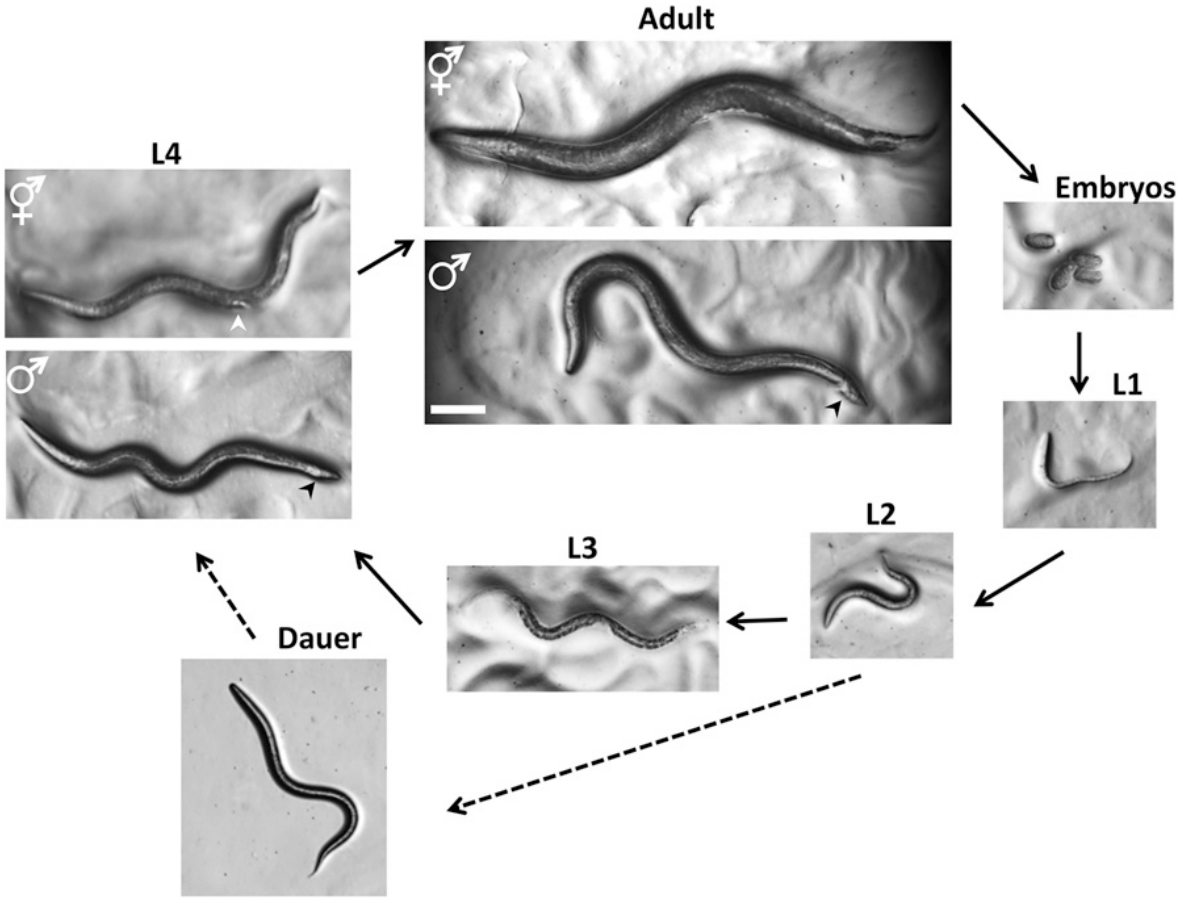

Figure 2. *C. elegans* Life-cycle and Growth Stages.

C. elegans experience six growth stages starting from fertilized embryos, then larval stages L1-L4, and into mature adults. Upon environmental stress or famine L2 larvae can enter into the dauer state, a form of active developmental hibernation, allowing them to survive harsh conditions and without food. The L4 larval stage is distinguishable by the developing vulva in hermaphrodites (white arrow). Males arise less frequently than hermaphrodites and can be distinguished through their smaller size and fanned tail (black arrow). The average life-cycle from embryo to fertile adult is 3 days at 25˚C (Figure by Corsi et al., 2015).

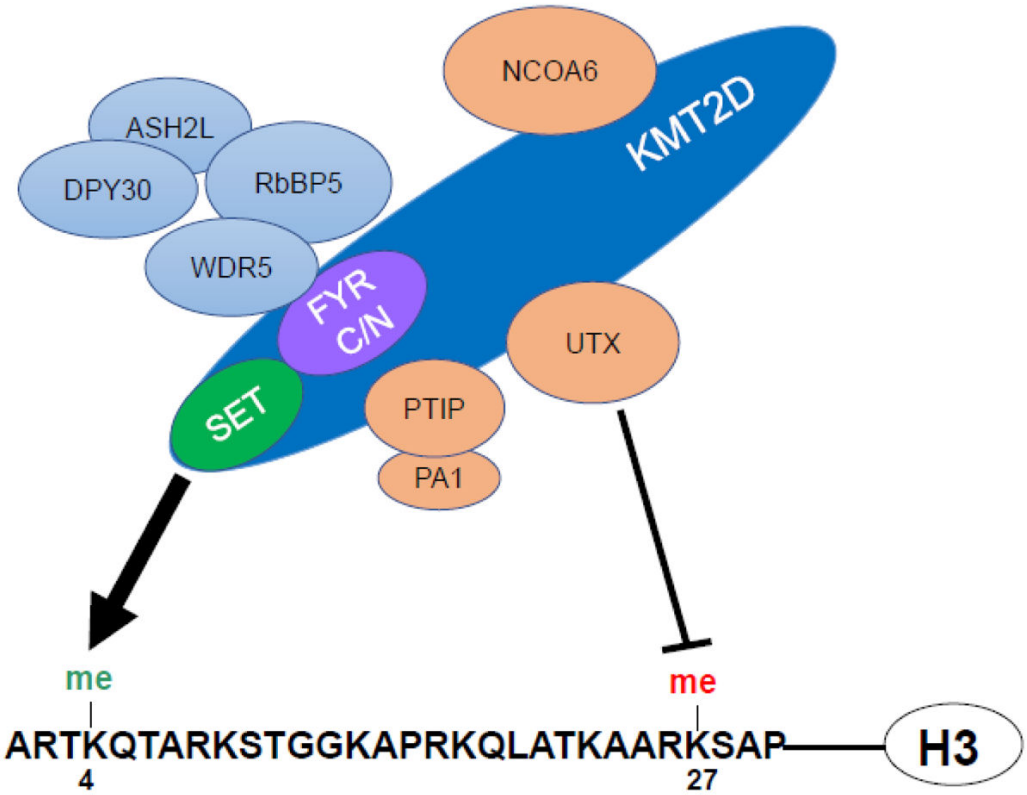

Figure 3. COMPASS/MLL4 Complex and Interaction with H3 Amino Acid Tail.

COMPASS/MLL4 complex (KMT2D, PTIP, PA1, NCOA6 and KDM6A—shown as UTX) associates with WRAD (WDR5, RbBP5, ASH2L and DPY30). Enzymatic activity by the SET domain of KMT2D methylates the fourth lysine (H3K4), associated with gene activation. Methylated H3K27 is associated with gene silencing, and is removed by KDM6A demethylase activity (Figure by Froimchuk et al., 2017).

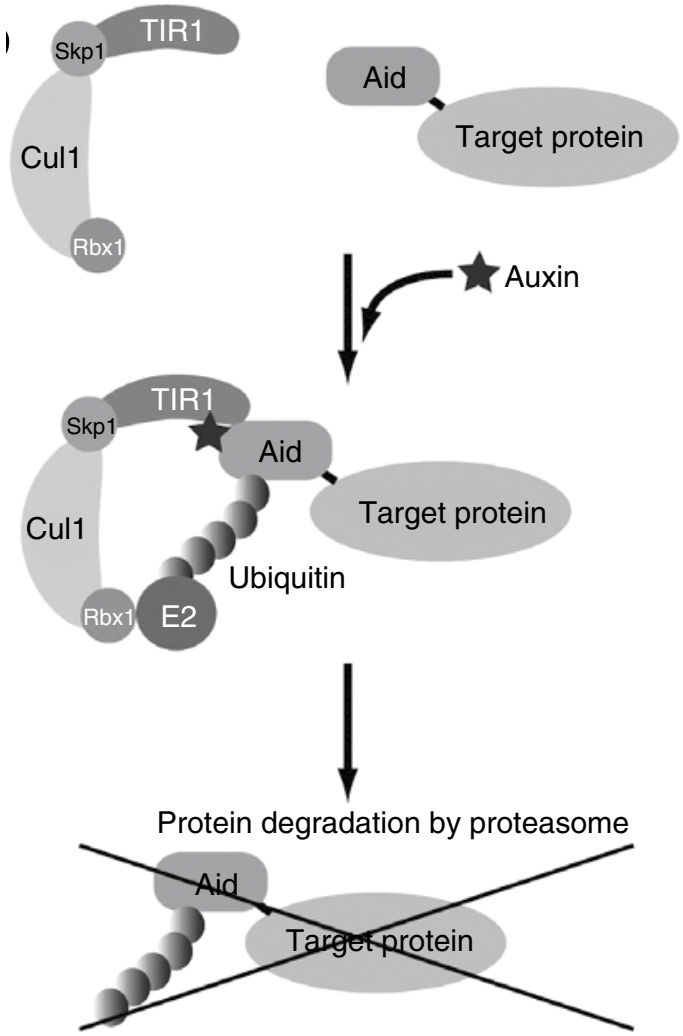

Figure 4. AID/TIR1 System Mode of Action.

Treatment with auxin (IAA: indole-3-acetic acid, represented by star) promotes binding of the E3 ubiquitin ligase SCF-TIR1 (Skp1, Cul1, Rbx1 plus TIR1) to an AID-tagged protein target leading to the recruitment of an E2 ubiquitin ligase to induce proteasomal degradation of the tagged protein (Figure by Nishimura et al., 2009).

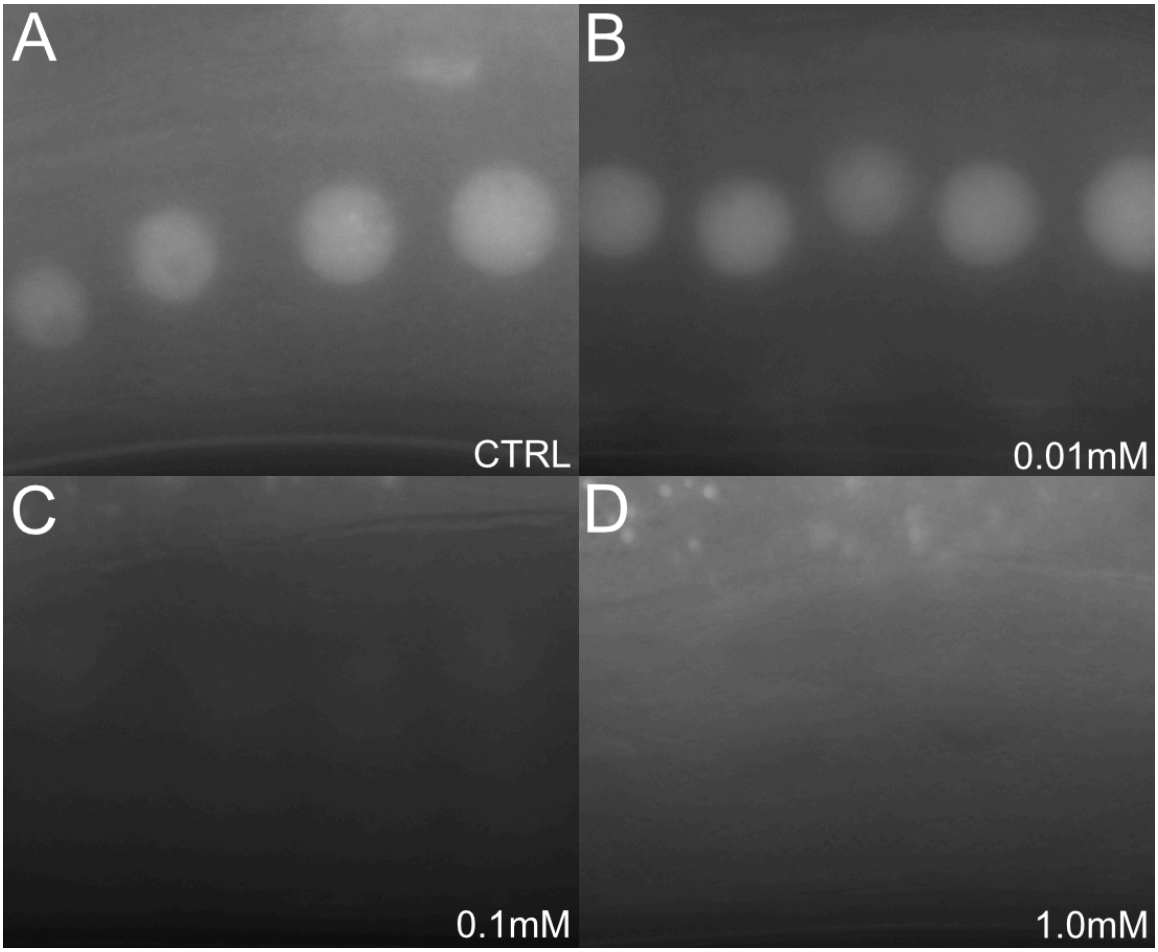

Figure 5.1 SET-16 Germline GFP Intensity Across Auxin Concentrations.

Germline nuclear GFP expression of oocytes in day 1 adult animals raised under four conditions: A) no auxin (control, CTRL). B) 0.01mM auxin. C) 0.1mM auxin. D) 1.0mM auxin. Images taken using DeltaVision Core imaging system at 60X magnification.

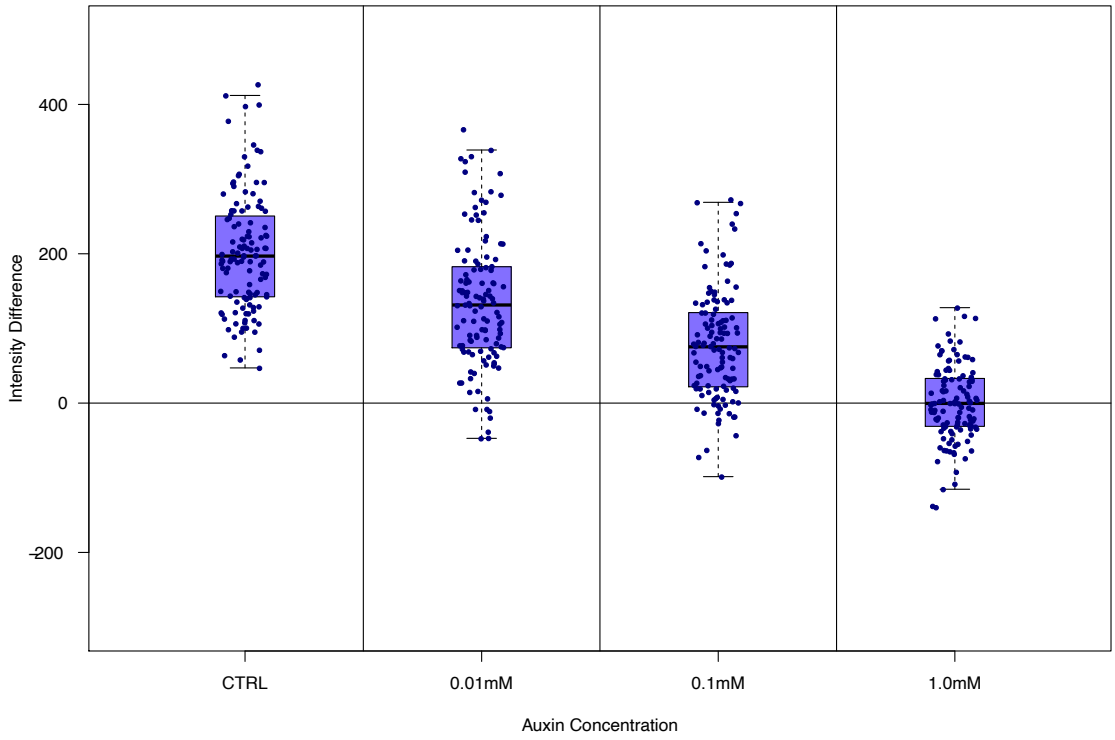

Figure 5.2 SET-16 Germline Depletion Across a Range of Auxin Concentrations.

GFP fluorescence intensity across auxin concentrations of ieSi64 II; set-16(syb1046) III oocyte nuclei (n=120 per condition). Individual replicates shown at right (n=40). Data points indicate mean pixel intensity calculated by the difference in nuclear GFP from background. 0.01 mM auxin vs. control: p-value = $3.297x10^{-9}$. 0.1 mM auxin vs. 0.01mM auxin: p-value = $3.679x10^{-7}$. 1.0 mM auxin vs. 0.1 mM auxin: p-value = $<2.2x10^{-16}$. P-values calculated using Wilcoxon Rank-Sum Test. (RStudio v1.2.5001)

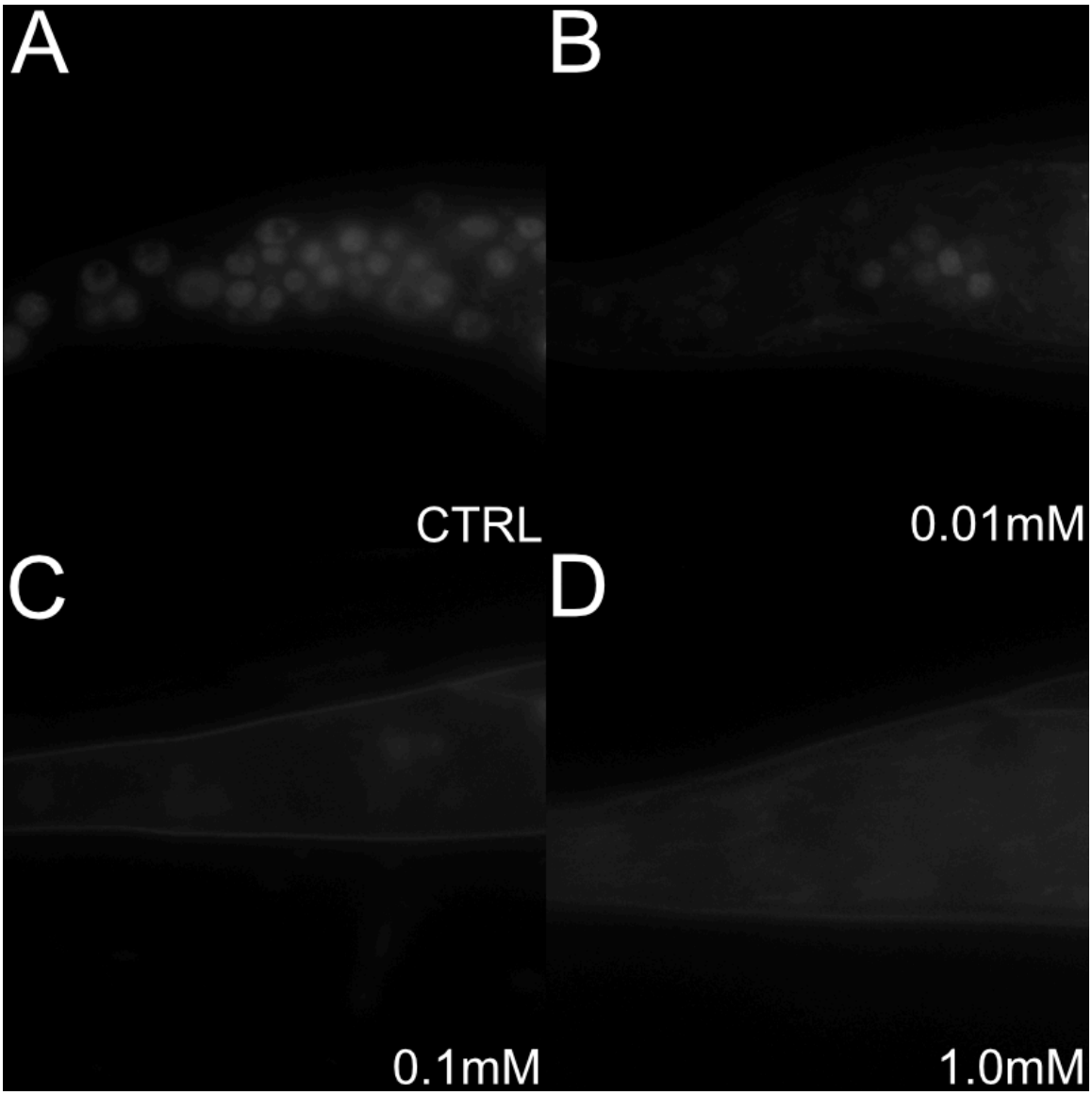

Figure 6.1 SET-16 Somatic GFP Intensity Across Auxin Concentrations.

Somatic nuclear GFP expression in tails of L3 stage larvae raised under four conditions: A) no auxin (control CTRL). B) 0.01mM auxin. C) 0.1mM auxin. D) 1.0mM auxin. Images taken using DeltaVision Core imaging system at 40X magnification.

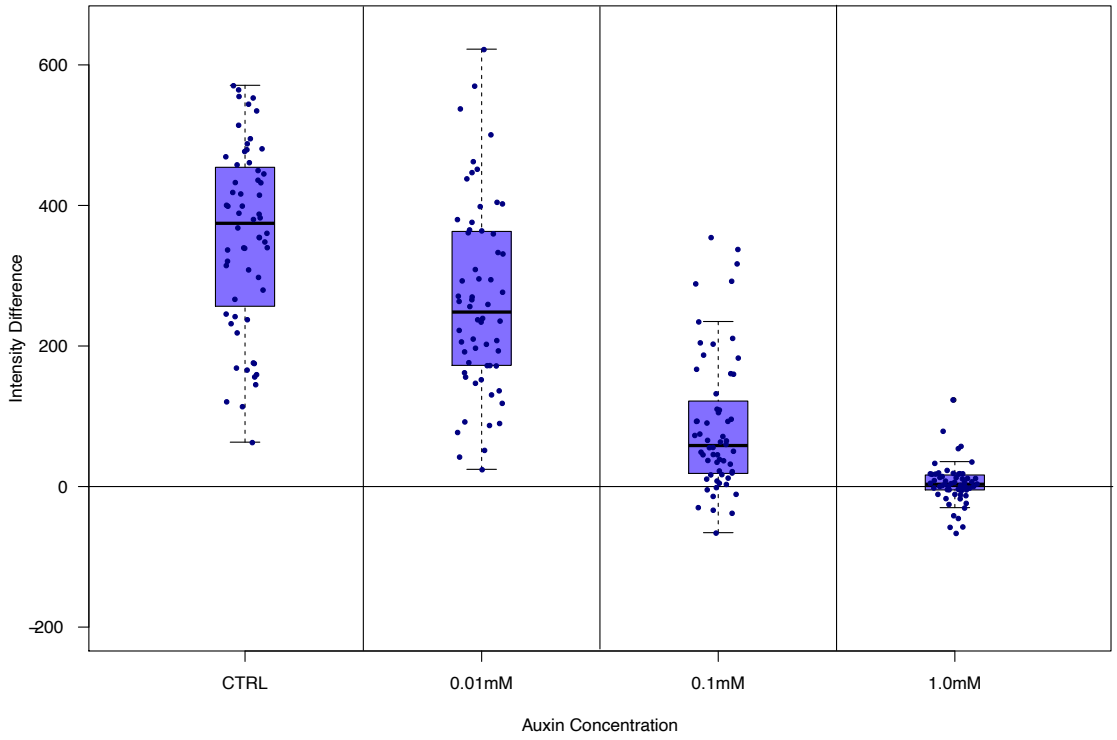

Figure 6.2 SET-16 Somatic Depletion Across a Range of Auxin Concentrations.

GFP fluorescence intensity across auxin concentrations of ieSi57 II; set-16(syb1046) III somatic nuclei (n=60 per condition). Individual replicates shown at right (n=20 per condition). Data points indicate mean pixel intensity calculated by the difference in nuclear GFP from background. 0.01mM auxin vs. control: p-value = $2.565x10^{-4}$. 0.1mM auxin vs. 0.01mM auxin: p-value = $4.184x10^{-12}$. 1.0mM Auxin vs. 0.1mM auxin: p-value = $1.159x10^{-9}$. P-values calculated using Wilcoxon Rank-Sum Test. (RStudio v1.2.5001)

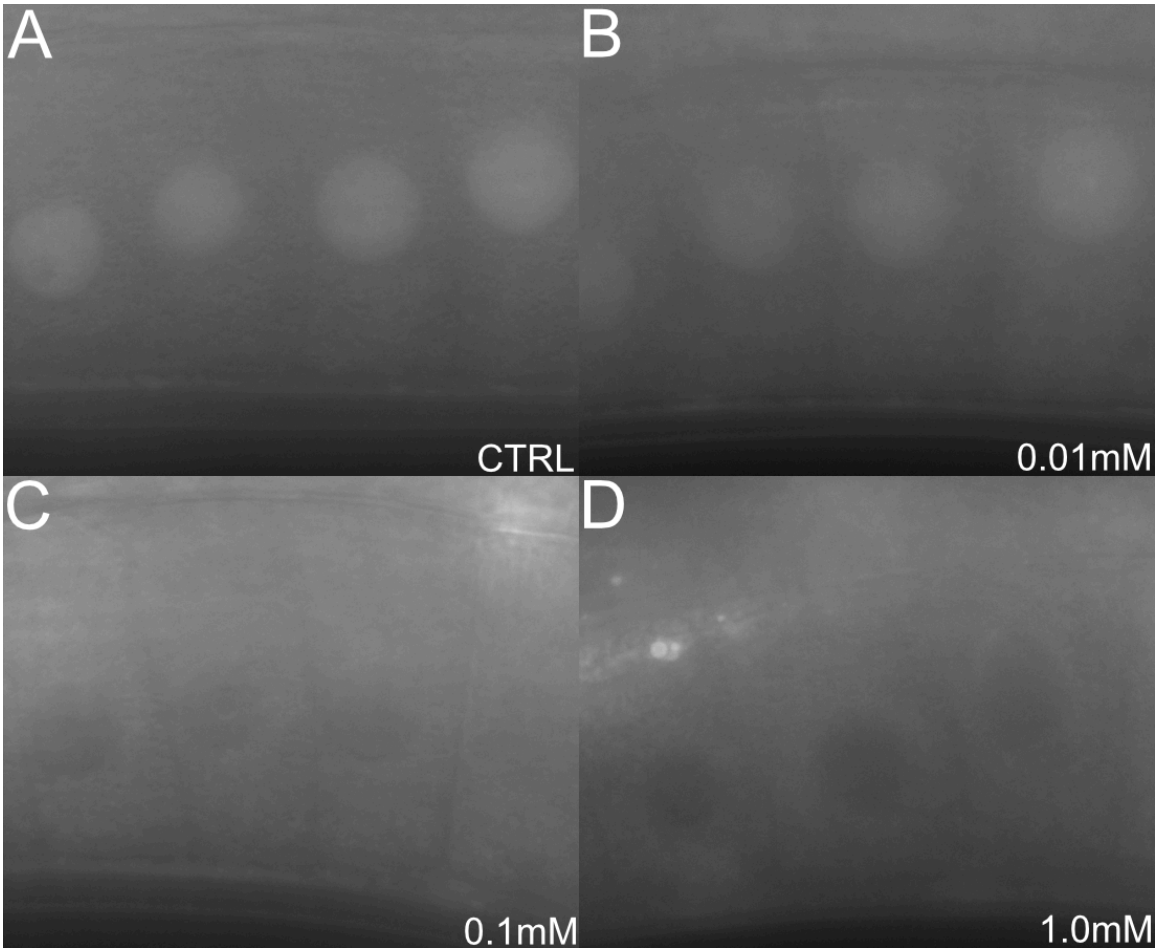

Figure 7.1 UTX-1 Germline GFP Intensity Across Auxin Concentrations.

Germline nuclear GFP expression of oocytes in day 1 adult animals raised under four conditions: A) no auxin (control, CTRL). B) 0.01mM auxin. C) 0.1mM auxin. D) 1.0mM auxin. Images taken using DeltaVision Core imaging system at 60X magnification.

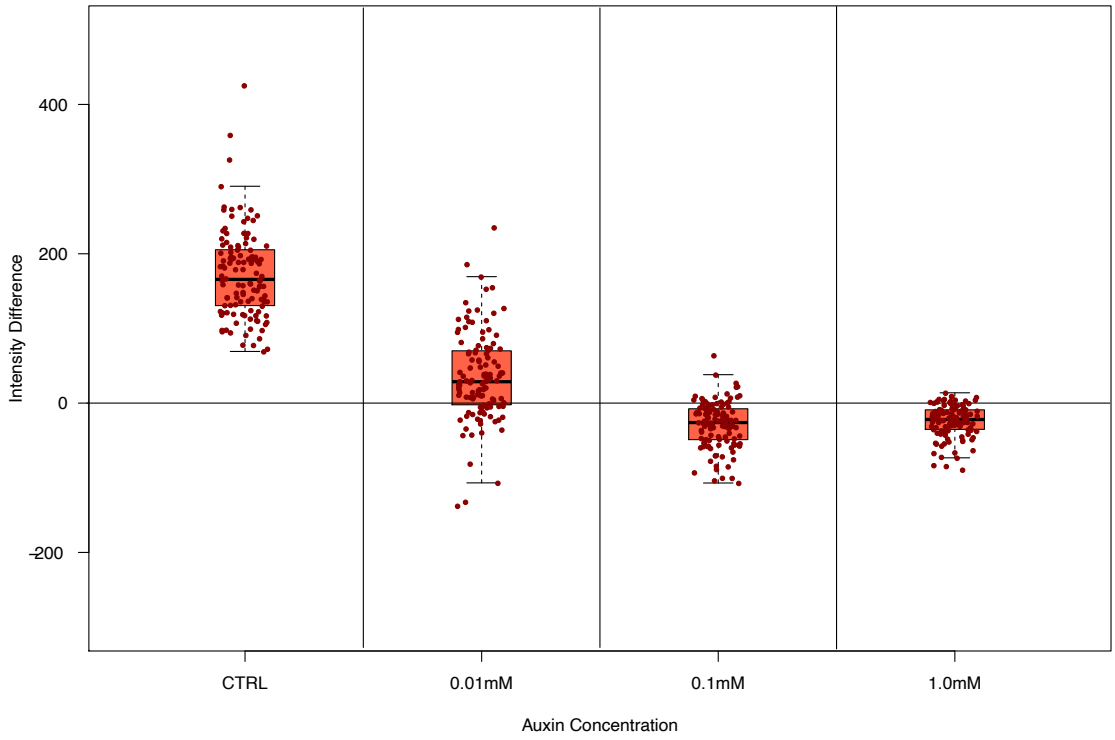

Figure 7.2 UTX-1 Germline Depletion Across a Range of Auxin Concentrations.

GFP fluorescence intensity across auxin concentrations of ieSi64 II; utx-1(syb1026) X oocyte nuclei (n=120 per condition). Individual replicates shown at right (n=40 per condition). Data points indicate mean pixel intensity calculated by the difference in nuclear GFP from background. 0.01mM auxin vs. control: p-value = $<2.2x10^{-16}$. 0.1mM auxin vs. 0.01mM auxin: p-value = $<2.2\ x10^{-16}$. 1.0mM Auxin vs. 0.1mM auxin: p-value = 0.1918. P-values calculated using Wilcoxon Rank-Sum Test. (RStudio v1.2.5001)

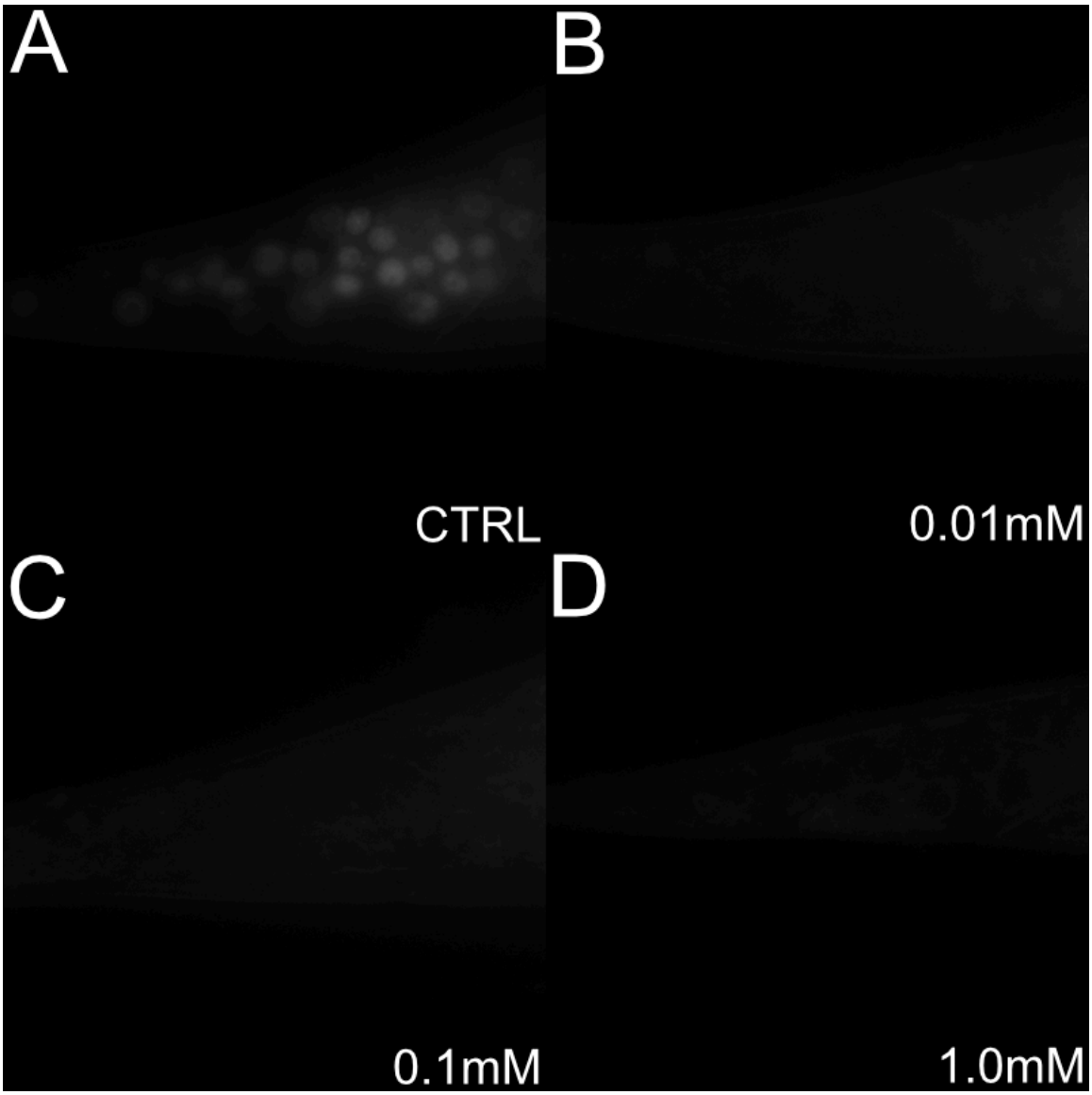

Figure 8.1 UTX-1 Somatic Depletion Across a Range of Auxin Concentrations.

Somatic nuclear GFP expression in tails of L3 stage larvae raised under four conditions: A) no auxin (control, CTRL). B) 0.01mM auxin. C) 0.1mM auxin. D) 1.0mM auxin. Images taken using DeltaVision Core imaging system at 40X magnification.

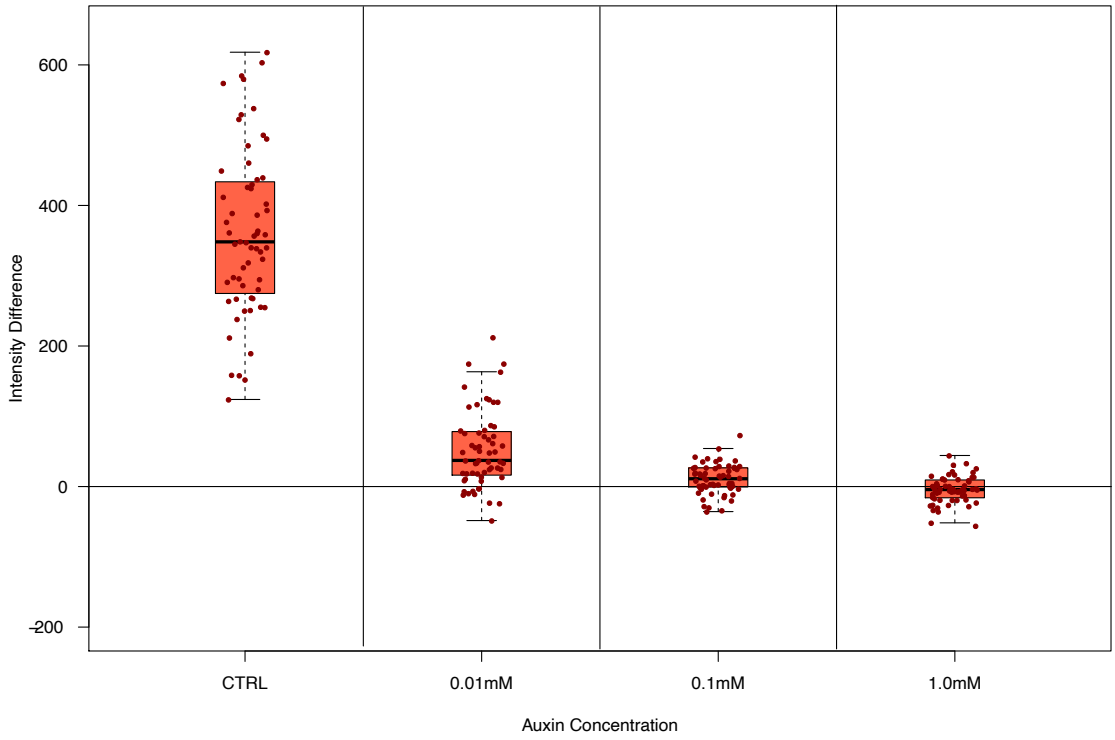

Figure 8.2 UTX-1 Somatic Depletion Across a Range of Auxin Conditions.

GFP fluorescence intensity across auxin concentrations of ieSi57 II; utx-1(syb1026) X somatic nuclei (n=60 per condition). Individual replicates shown at right (n=20 per condition). Data points indicate mean pixel intensity calculated by the difference in nuclear GFP from background. 0.01mM auxin vs. control: p-value = <2.2x10^{-16}. 0.1mM auxin vs. 0.01mM auxin: p-value = <2.008 x10^{-6}. 1.0mM auxin vs. 0.1mM auxin: p-value = 6.006x10^{-5}. P-values calculated using Wilcoxon Rank-Sum Test. (RStudio v1.2.5001)

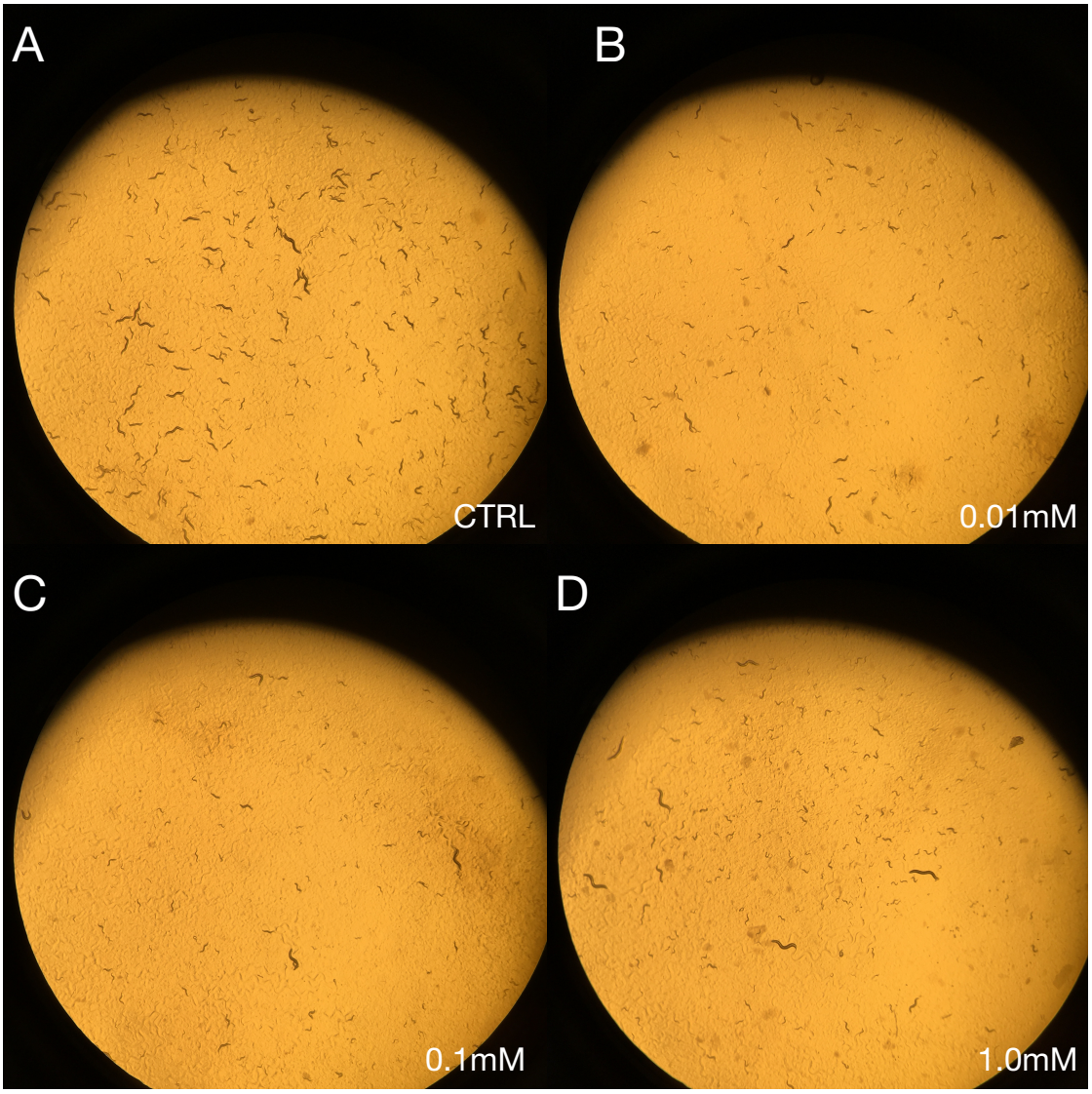

Figure 9.1 Colony Formation After SET-16 Somatic Depletion.

Somatic Depletion of SET-16 has a drastic effect on population growth at higher concentrations of auxin. Images were taken using a dissection microscope 5 days after seeding each plate with an initial 10 animals at the L4 stage.

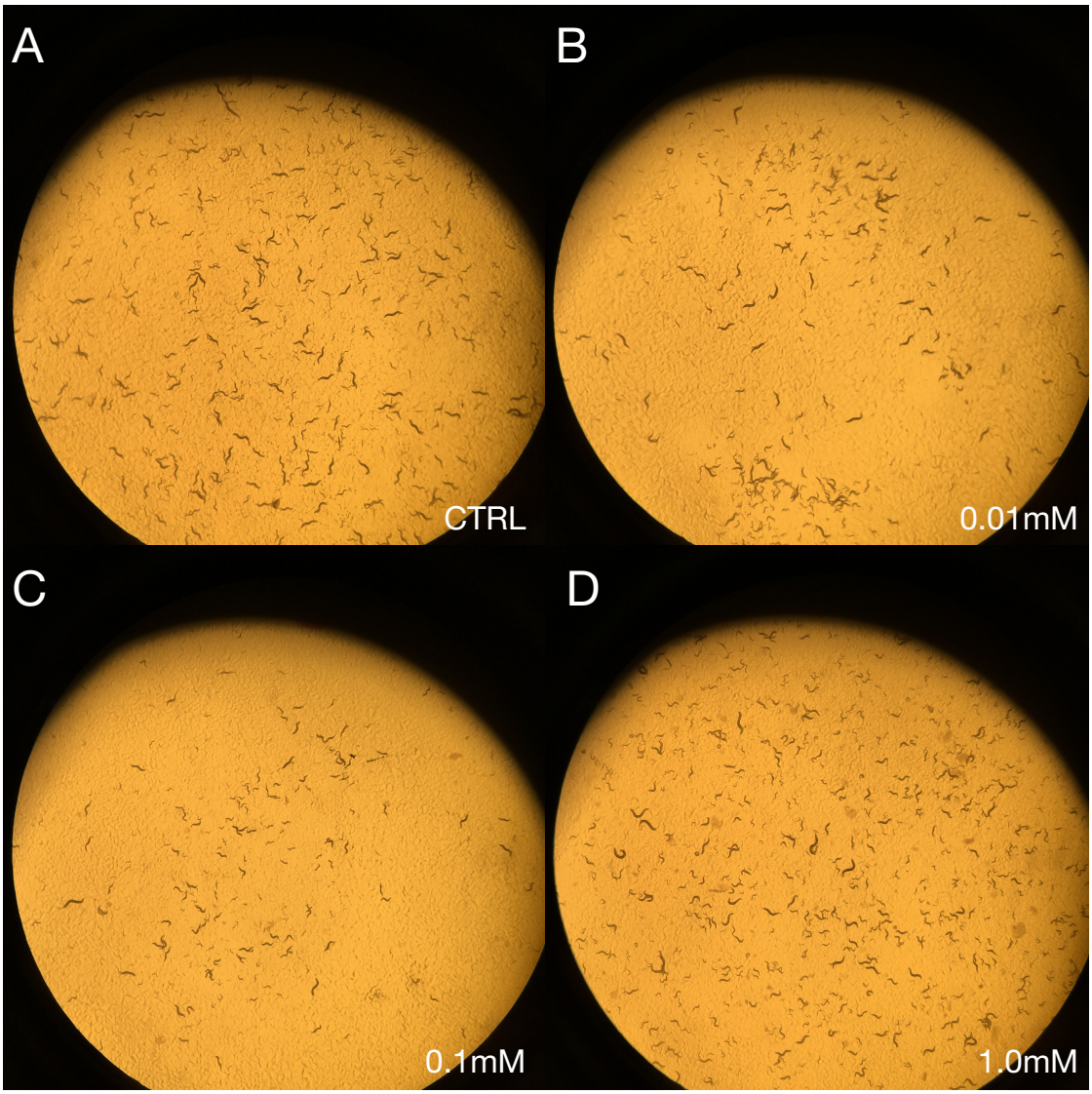

Figure 9.2 Colony Formation After UTX-1 Somatic Depletion.

Somatic depletion of UTX-1 appears to have only a subtle effect on population growth. Images taken using a dissecting microscope 5 days after seeding each plate with an initial 10 animals at the L4 stage.

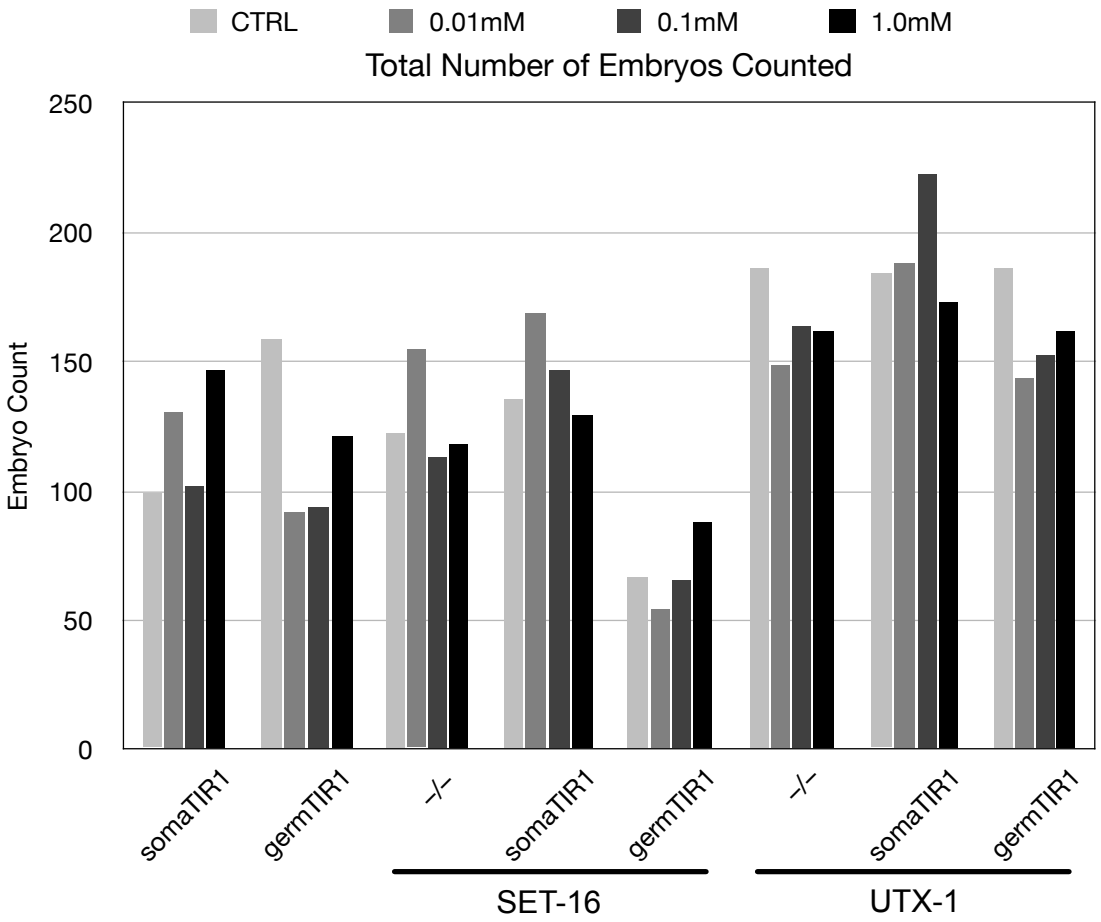

Figure 10.1 Total Embryo Counts Across a Range of Auxin Concentrations

Total number of embryos counted for both somatic and germline depletion strains after seeding with a total of four L4 progenitors across four auxin concentrations. Embryos were counted 24 hours after initial transfer of animals. The SET-16 germline depletion strain produced the fewest number of embryos at any concentration, including 0.0mM auxin.

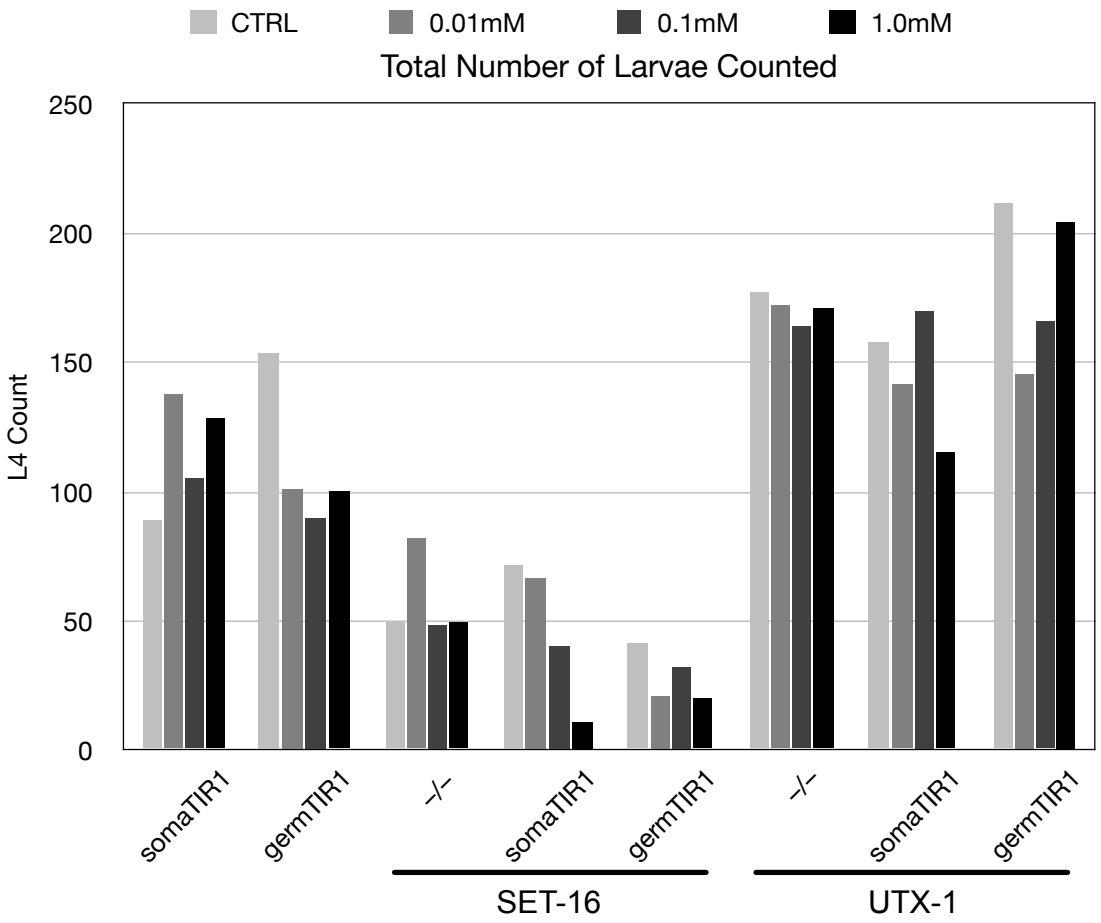

Figure 10.2 Total Larvae Count Across a Range of Auxin Concentrations

Total number of larvae to reach the L4 stage of development counted for both somatic and germline strains after seeding with a total of four L4 progenitors across four auxin concentrations. AID-GFP tagged SET-16 animals produce the fewest viable larvae overall and show the most significant response to elevated concentrations of auxin.

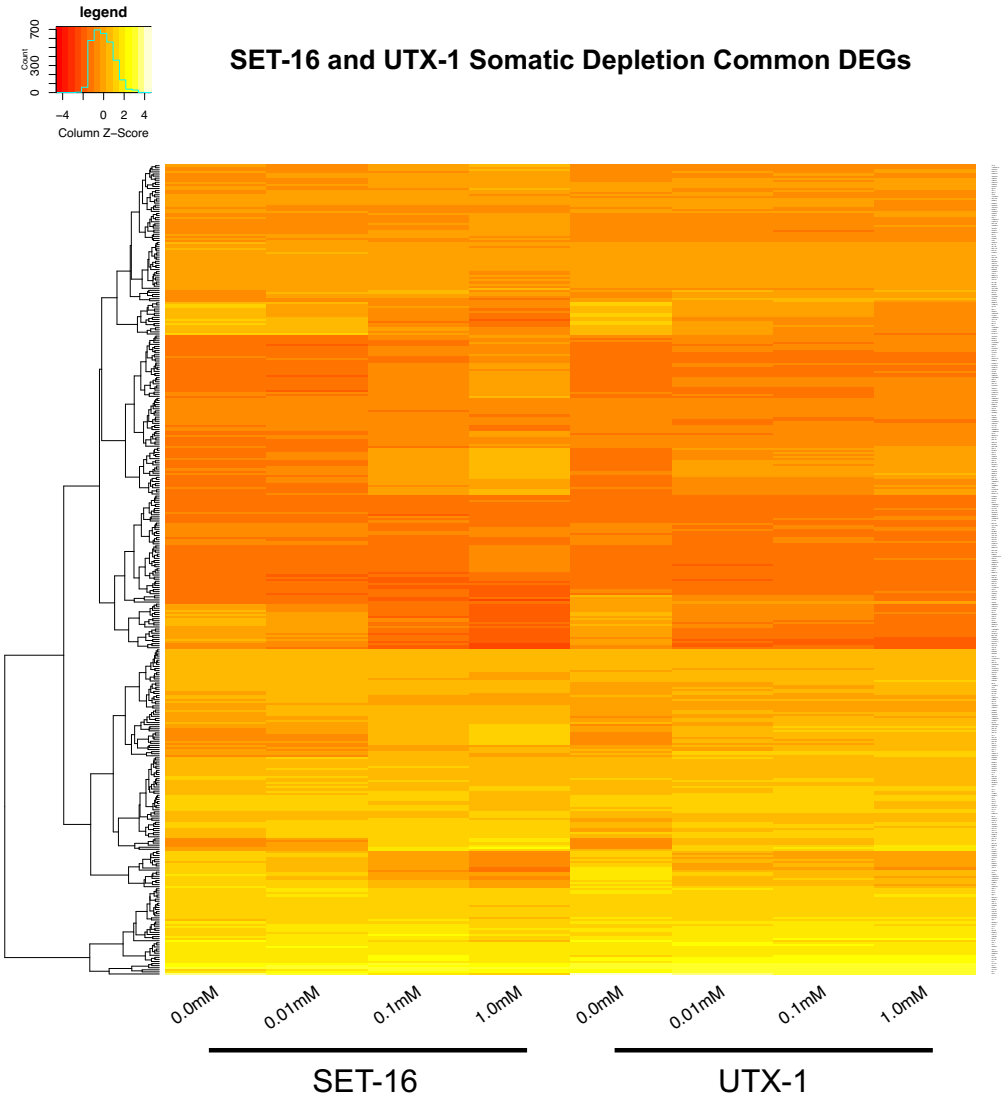

Figure 11. Somatic Depletion of SET-16 and UTX-1 Identifies Common Differentially Expressed Genes (DEGs).

Normalized baseline gene expression of 390 common DEGs (differentially expressed genes) per three auxin conditions compared to control standard of genomic expression. 61 common DEGs were found to be significantly down-regulated as a result of auxin induced depletion of either SET-16 or UTX-1 while 329 common DEGs were found to be significantly up-regulated as a result of the same induced depletion. Figure and statistical data compiled using RStudio v1.2.5001.

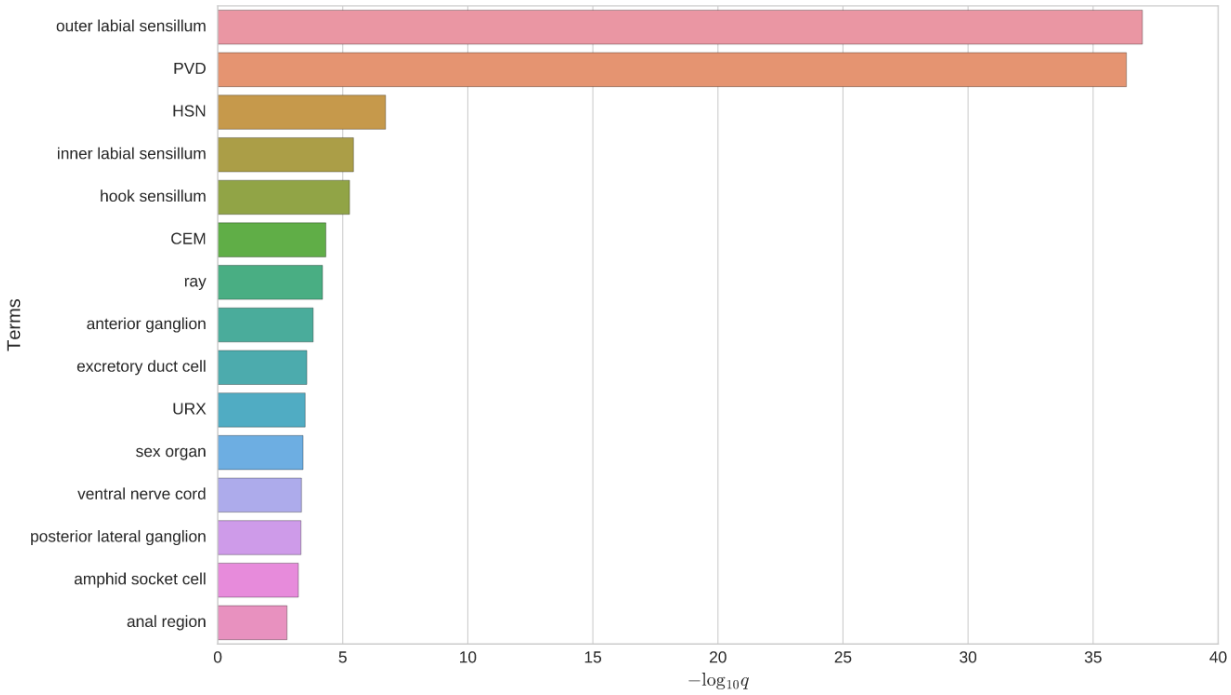

Figure 12.1. Up-Regulated Gene-set Enrichment for Somatic Depletion of SET-16.

Gene-set enrichment test for up-regulated DEGs in response to somatic depletion of SET-16 show a higher number of genes related to development of the outer labial sensilla and PVD neurons are effected. Scales indicate log10 q-values. Figure compiled via wormbase.org enrichment test program, courtesy of Dr. Jaejoon Choi and Dr. Alice Lee.

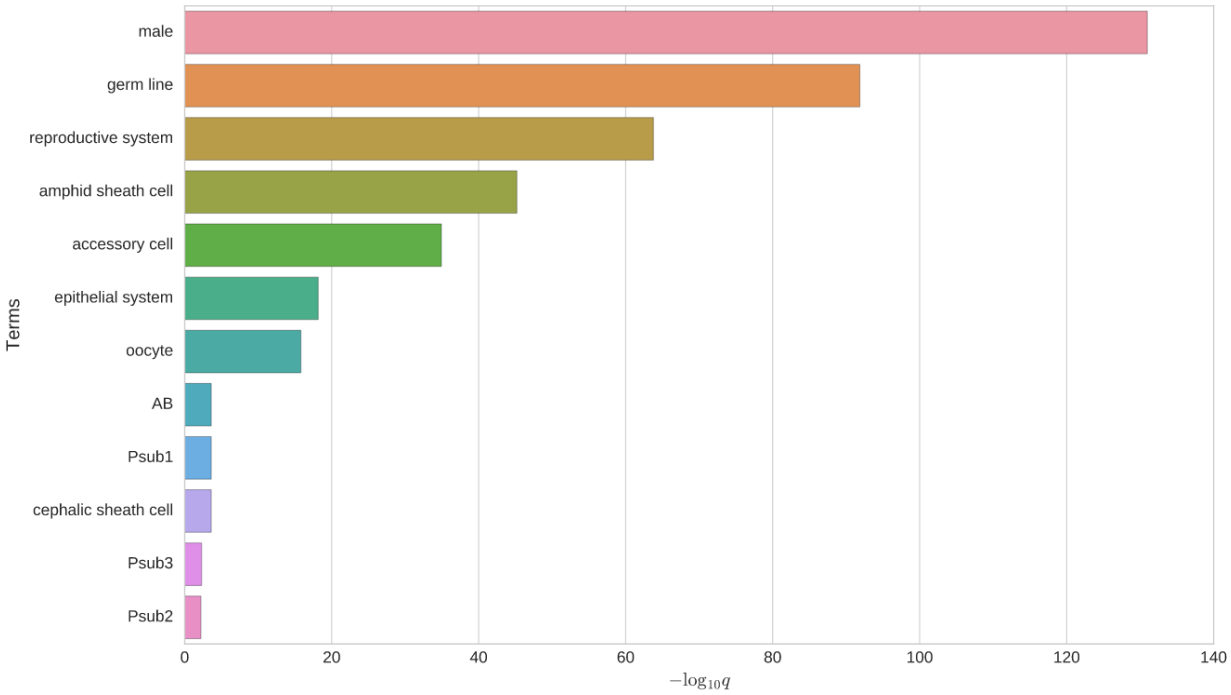

Figure 12.2. Down-Regulated Gene-set Enrichment for Somatic Depletion SET-16.

Gene-set enrichment test for down-regulated DEGs in response to somatic depletion of SET-16 show a high number of genes related to male phenotypes as well as germline and reproductive system development are effected. Scales indicate log10 q-values. Figure compiled via wormbase.org enrichment test program, courtesy of Dr. Jaejoon Choi and Dr. Alice Lee.

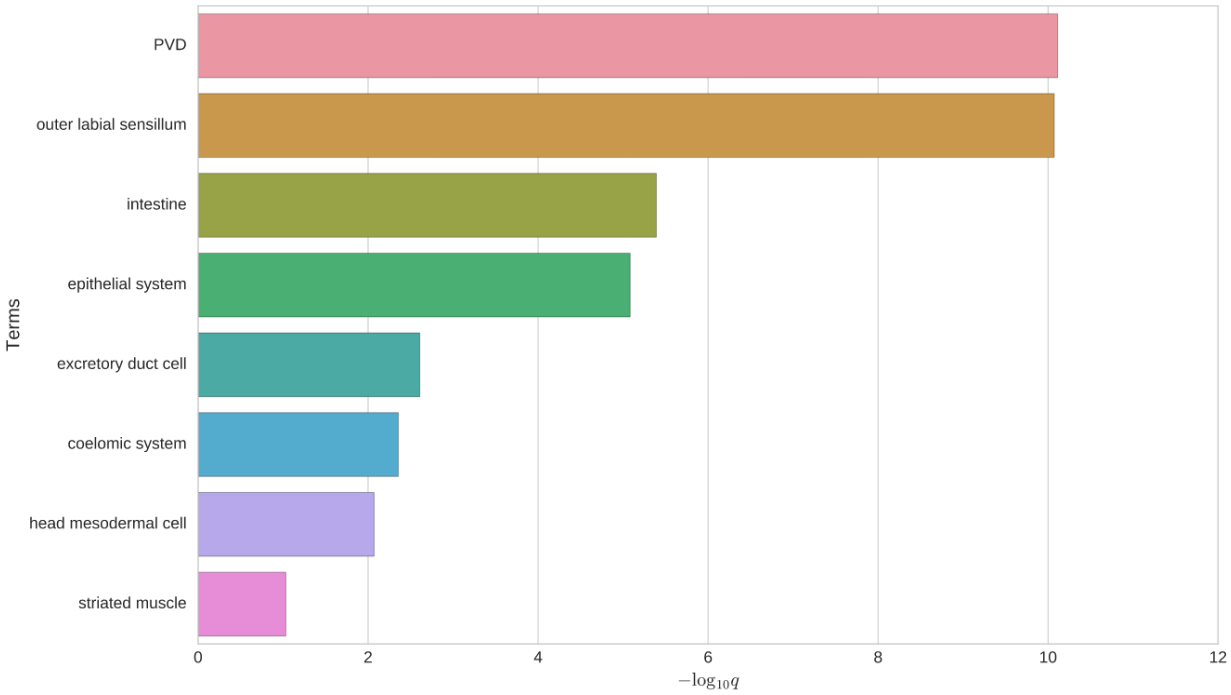

Figure 13.1. Up-Regulated Gene-set Enrichment for Somatic Depletion of UTX-1.

Gene-set enrichment test for up-regulated DEGs in response to somatic depletion of UTX-1 show a higher number of genes related to development of the outer labial sensilla and PVD neurons are effected, similar to somatic depletion of SET-16. Scales indicate log10 q-values. Figure compiled via wormbase.org enrichment test program, courtesy of Dr. Jaejoon Choi and Dr. Alice Lee.

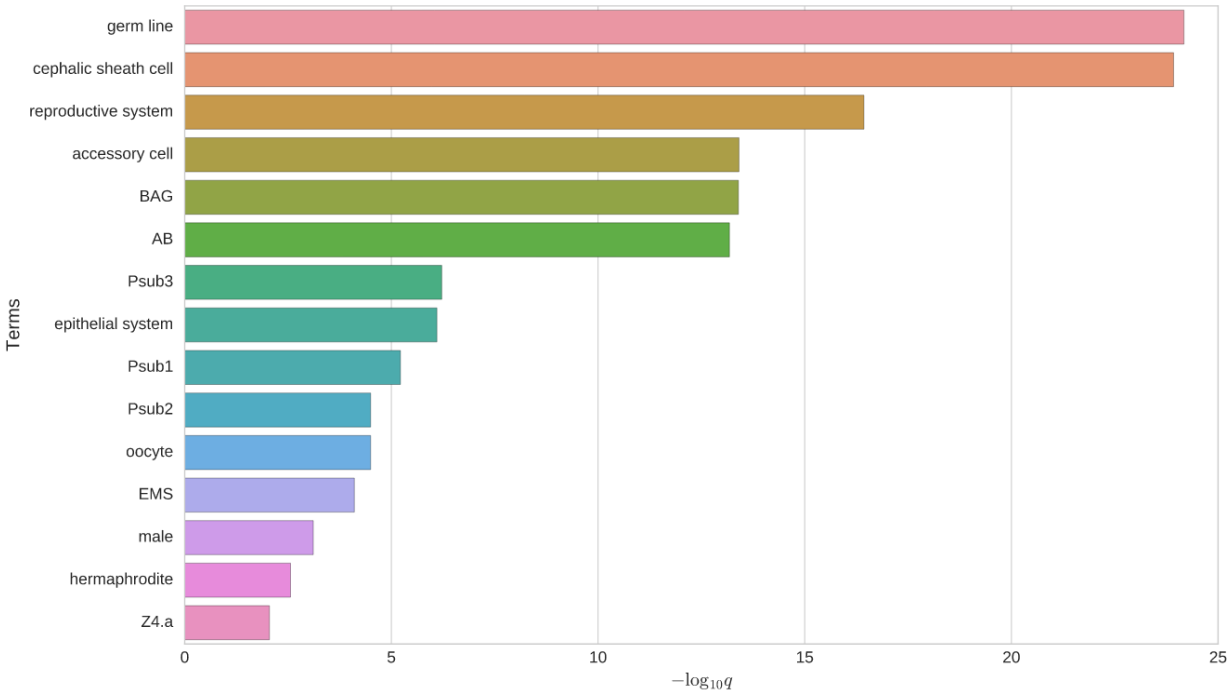

Figure 13.2. Down-Regulated Gene-set Enrichment for Somatic Depletion UTX-1.

Gene-set enrichment test for down-regulated DEGs in response to somatic depletion of UTX-1 show a higher number of genes related germline and reproductive system development, as well as cephalic sheath are effected. Scales indicate log10 q-values. Figure compiled via wormbase.org enrichment test program, courtesy of Dr. Jaejoon Choi and Dr. Alice Lee.

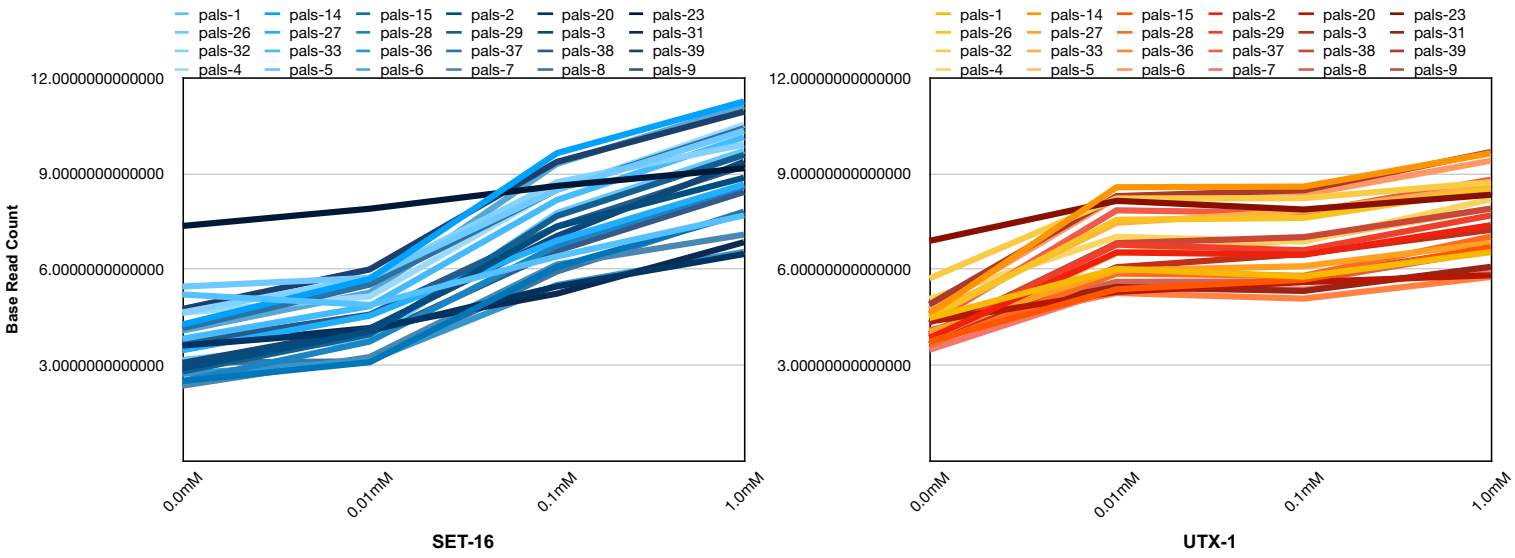

Figure 14. SET-16 and UTX-1 Somatic Depletion Commonly Upregulates 24 out of 39 Members of the Protein Containing ALS2cr12 Signature ("*pals*-") Family.

Line graphs depicting similar response curves from members of the pals family of genes between SET-16 (left) and UTX-1 (right) somatic depletions across a range of auxin concentrations. SET-16 somatic depletion has a greater effect, producing a steeper response curve than UTX-1 somatic depletions. Base read counts calculated from the average base reads per three replicates. Individual values can be found in Supplemental Table Data S1. below. Figures compiled using Numbers v10.1 (6913).

Supplemental Table Data.

Table S1. SET-16/SomaTIR1 and UTX-1/SomaTIR1 Common DEGs.

Gene ID	Gene Name	SET-16 0.0mM	SET-16 0.01mM	SET-16 0.1mM	SET-16 1.0mM	Log2Fold Change	UTX-1 0.0mM	UTX-1 0.01mM	UTX-1 0.1mM	UTX-1 1.0mM	Log2Fold Change
WBGene00000005	aat-4	8.08620578	7.89986610	7.37466642	6.23286365	-0.6453627	8.15434510	7.86491855	7.75017135	7.35132638	-0.2827123
WBGene00000120	aly-1	8.58497123	8.79633628	9.28963624	9.55753001	0.34576361	8.39064367	8.84458274	8.89771308	9.31105913	0.28135252
WBGene00000212	asm-2	9.39853385	9.12069049	8.38257634	7.15487835	-0.7648102	9.12396454	7.99886011	8.13206283	7.52538558	-0.5363745
WBGene00000213	asm-3	9.02613486	7.82342821	6.97907651	5.71626078	-1.2487356	9.78688345	6.38213623	6.83274600	6.23342312	-1.2828087
WBGene00000458	ceh-37	7.45802873	7.74443163	8.33007404	8.84347166	0.48932547	7.45174217	8.04179974	8.11360320	8.24366246	0.26779038
WBGene00000700	col-126	3.50962018	4.43387636	6.27053738	5.66532864	1.53021451	5.10756921	5.78952065	6.04640608	6.38801350	0.66383865
WBGene00000701	col-127	3.90017919	4.25442054	6.04399825	5.32610892	1.03792184	4.96122280	5.27891300	5.91045472	6.33137719	0.78164445
WBGene00000714	col-141	6.40844529	6.67643169	10.8675618	10.2272498	1.86296002	7.12533324	8.95929256	9.33797382	10.3733647	1.04996558
WBGene00000719	col-146	10.2996240	10.6317655	12.2208977	11.3540719	0.57001963	10.7902760	11.5919979	11.9247714	11.9283402	0.38790459
WBGene00000720	col-147	11.8844184	12.1984202	13.7136697	12.8987267	0.58959974	12.3283985	12.8358818	13.2267907	13.1648234	0.29747771
WBGene00000742	col-169	9.92550130	11.0577592	12.6163578	11.5440588	0.77946820	10.5731576	11.5568612	11.9216272	12.1000906	0.48617885
WBGene00000749	col-176	9.07761980	10.8855435	14.1285528	13.5400921	1.86044731	10.5426767	12.6720934	13.0552202	13.6535736	0.88517842
WBGene00000784	cpr-4	12.0264859	12.6693643	12.9924671	13.6687980	0.51772243	12.0821575	12.3207187	13.0439535	12.9732448	0.33195911
WBGene00000830	ctl-1	7.46473139	8.16345085	8.77617505	8.80002407	0.48452382	7.32632959	8.00879176	8.41348334	8.56411265	0.44753446
WBGene00000831	ctl-2	10.3880071	11.0950640	11.6843022	11.6101127	0.44074057	10.2170127	10.9706688	11.1343426	11.1731106	0.30652093
WBGene00000841	cul-6	6.97336033	7.36810699	7.86931443	8.90894498	0.65605304	6.53778120	7.53887619	7.21099746	8.12714165	0.49366519
WBGene00001063	dpy-1	7.79384960	9.57441546	10.5975477	10.0353215	0.93672981	8.36004499	9.45317999	9.57677466	10.2327172	0.57360087
WBGene00001164	efn-3	6.42018952	5.69832492	4.46399140	4.06756801	-1.1489443	6.91563853	6.27912586	6.14085628	5.73064490	-0.4786681
WBGene00001495	F31B12.3	6.06721429	5.45289174	3.60556764	4.00417814	-1.1713160	6.01870857	5.05482584	4.96446928	4.68658196	-0.7646111
WBGene00001772	gst-24	6.97605607	6.55193773	8.09494443	9.40773345	0.88780373	6.72909987	6.67110497	7.84461005	9.12182864	0.93014724
WBGene00001912	his-38	6.64828588	5.19423069	4.30043886	4.04811759	-1.2531248	6.61383007	5.42373107	5.89213780	5.22227841	-0.5986625
WBGene00002055	ifc-1	10.2581063	10.3048973	11.6232661	11.6580936	0.64276269	10.2249268	11.2442271	11.9234703	12.0002310	0.59580533
WBGene00002188	kgb-2	5.07820218	5.88579022	6.58756739	7.18425445	0.78712022	5.34866335	6.49747352	6.26116725	6.79790439	0.54603540
WBGene00003001	lin-12	7.49871526	8.31740783	8.49080447	8.60861215	0.37084416	7.56964374	8.14730713	8.33080438	8.70202753	0.37010037
WBGene00003374	mlk-1	9.30793183	9.79472777	9.93380485	10.1597285	0.28210515	9.24572387	9.62176426	9.79939943	9.98675611	0.24825304
WBGene00003387	mod-5	5.89159476	6.40978275	6.97495445	6.83093243	0.41184721	6.24883202	6.85580472	7.15824255	7.14835019	0.35627383
WBGene00003543	nas-24	3.62210743	3.88263156	3.97785518	4.34245908	0.54315313	6.88537230	5.88213036	5.94649363	5.43393840	-0.7021580
WBGene00003617	nhr-18	6.45082649	6.70653922	7.17955445	7.27634894	0.33207495	6.10595241	6.74343596	6.75471625	6.91585157	0.29906702
WBGene00003727	nhr-137	6.35226299	7.13054094	8.32817129	8.42628420	0.82179849	6.60947479	7.76188185	7.43705587	7.99389305	0.41191757
WBGene00003778	nnt-1	7.21703798	8.71629011	9.59595682	9.24220306	0.71811798	7.18470432	8.49850094	8.86300061	8.94023270	0.59389411
WBGene00003995	pgp-1	9.06123476	9.80471777	9.93246886	10.3432891	0.45451170	8.83590226	9.51916821	9.78606904	10.4246391	0.47739229
WBGene00004002	pgp-8	5.17415277	4.85891574	6.25103382	8.51596136	1.27426620	5.51508720	5.59054872	6.13088849	7.70110397	0.97801477

Gene ID	Gene Name	SET-16 0.0mM	SET-16 0.01mM	SET-16 0.1mM	SET-16 1.0mM	Log2Fold Change	UTX-1 0.0mM	UTX-1 0.01mM	UTX-1 0.1mM	UTX-1 1.0mM	Log2Fold Change
WBGene00004149	trpl-5	3.54465156	3.93947382	5.45006890	7.14368192	1.81654081	4.04457909	5.18906897	5.42921916	5.79271303	1.05728596
WBGene00004172	pqn-92	9.16613900	9.82380658	10.6997930	11.0725719	0.67562889	9.30565871	10.2797664	10.0897126	10.7754605	0.42277114
WBGene00004368	ric-19	6.82696728	7.09086072	7.55943261	7.71132747	0.34324687	6.89039305	7.40429287	7.49707139	7.63048364	0.26760873
WBGene00004402	rom-3	3.68424356	3.39170229	4.96120682	6.96105690	1.65366040	3.98869204	4.71714843	4.81018771	5.49623780	0.82581924
WBGene00004509	rrf-2	7.34149112	8.04200066	9.13313668	11.0528956	1.25978020	7.29126425	8.75036175	8.78394507	9.26277443	0.58491067
WBGene00004809	skr-3	9.89281096	9.98297145	10.6890377	10.8856778	0.38141728	9.19906560	10.1070966	9.95457116	10.4141439	0.34801820
WBGene00004810	skr-4	7.49129255	7.56789546	8.59649130	9.87127950	0.82896740	7.39389342	8.59412306	8.89693726	9.21031582	0.58809665
WBGene00004811	skr-5	5.25734652	5.40681411	7.14665589	8.52541022	1.26178895	4.98173310	5.90818281	5.97949944	6.67430343	0.71748152
WBGene00004949	sox-2	8.45544111	8.91012728	9.22228507	9.29205276	0.28806490	8.43276908	9.10732557	9.00773799	9.27957012	0.25162214
WBGene00005552	sri-40	7.72800457	7.50536974	4.87075744	4.49423851	-1.5060017	8.43149276	6.37883577	6.22466974	6.07260648	-0.9028327
WBGene00005582	sri-70	3.40639711	3.75964075	5.47267689	7.26437547	2.09817432	3.68561749	4.60896080	5.03276334	5.30381073	1.27947388
WBGene00005747	srv-36	2.63178946	3.22129596	5.83300611	5.56611651	2.48750632	3.83381580	4.74984724	5.02691469	5.16520083	1.01709178
WBGene00005832	srw-85	3.39487711	3.72421084	4.34439389	4.51703525	0.77977908	6.11668329	7.19157955	6.99749008	7.67709135	0.49189094
WBGene00005833	srw-86	4.99140654	5.49829947	6.79101074	7.02818794	0.95126170	4.61167592	5.39240612	5.77836908	6.32930473	0.93047944
WBGene00005835	srw-88	2.75263689	3.28620030	3.84876894	3.82200526	1.22112280	3.57272613	4.12457621	4.14848931	4.78862551	1.41511344
WBGene00006429	arrd-3	4.05239893	4.35515338	5.04149897	5.77779471	0.86565516	4.61827189	4.93788298	5.37028298	5.85122643	0.75532460
WBGene00006464	bath-47	6.53768404	6.79681719	6.12603503	5.21015466	-0.5198142	6.10450341	5.35621612	4.88852013	4.96747289	-0.6745793
WBGene00006534	tba-8	6.71102688	7.71031572	8.86429486	8.47929924	0.76969186	6.29310728	7.47366825	7.61444391	8.15986310	0.66956747
WBGene00006539	tbb-6	7.70304954	7.84139666	8.91687021	10.4873891	0.95227528	6.93668298	7.82282392	8.09868616	8.83938992	0.64962391
WBGene00006575	tir-1	9.38029676	10.3334033	11.0393320	11.3921141	0.67482239	9.46277332	10.3370568	10.1857498	10.5924187	0.32115586
WBGene00006718	ubc-23	6.70701102	7.20493556	7.71105405	8.26789575	0.55791433	6.55043688	7.25260183	7.31140434	7.71748674	0.41858298
WBGene00006897	ver-4	6.97236501	6.57214658	5.59677914	3.95355926	-1.2350123	6.22415711	5.75626997	4.94947659	5.29288675	-0.5605480
WBGene00006927	vit-3	14.4795908	13.4754057	11.2832948	10.5237939	-1.2984936	15.4680567	13.2980469	13.3685296	13.0127721	-0.6989750
WBGene00006986	zip-1	7.83170927	8.67889742	9.12759940	9.90020376	0.68441332	7.83265400	8.73602005	8.81205727	9.24516521	0.43317025
WBGene00007131	pals-26	5.46016216	5.73420987	8.48811913	10.3475372	1.82718655	4.48335627	7.55438641	7.61238066	8.51672797	1.23165942
WBGene00007132	pals-27	3.46441983	4.54688834	6.90011109	8.66481287	2.19921382	4.03923952	5.96726080	6.09837242	6.82477174	1.12604610
WBGene00007133	B0284.3	5.60189493	5.29089005	6.22111066	6.34961676	0.35805999	5.67099573	6.11075418	6.22551811	6.54043154	0.36254121
WBGene00007134	pals-28	2.49810320	3.73768250	6.74878041	8.60726179	3.38742397	3.64047541	5.86672921	5.79950958	7.02652669	1.58666544
WBGene00007154	dhc-3	5.10491793	5.96923779	6.72462617	7.56668223	0.95836957	4.91455936	6.06471239	5.92024179	6.28268516	0.56895800
WBGene00007368	C06B8.2	7.34108769	7.61536629	8.02850219	8.37541209	0.41089808	7.02727195	7.85293977	8.20690136	8.76647076	0.62688002
WBGene00007392	fbxa-156	6.45750402	6.44121133	7.30688387	7.31323602	0.40289396	6.50815245	7.17352921	7.42524519	7.81839760	0.48379639
WBGene00007440	C08E8.4	6.57638375	7.24315785	8.25346455	9.39939162	0.97654250	5.90455470	7.54555407	7.44866927	7.93987295	0.66730960
WBGene00007521	C11E4.7	6.91593050	6.66030499	5.42859712	5.33121633	-0.7062611	8.00134622	7.34778688	7.19993496	6.68466248	-0.5348046
WBGene00007565	clec-48	8.24718257	9.18403055	10.0416676	9.65527594	0.57991730	9.27551591	9.70736579	9.99102859	10.3711136	0.33911128
WBGene00007654	C17H1.1	2.63726838	2.82477782	5.02136472	6.48617678	2.62137392	3.57272613	4.78889345	4.82952772	5.24973695	1.20952029
WBGene00007655	C17H1.2	2.35594575	3.22236283	5.50343688	6.57926621	2.79237303	3.47949633	4.90545037	5.13141344	5.64335007	1.54691976
WBGene00007656	pals-2	2.89453044	4.05531079	7.34043712	8.87097376	3.05079259	3.84659657	6.53076015	6.45727476	7.38393619	1.43057620

Gene ID	Gene Name	SET-16 0.0mM	SET-16 0.01mM	SET-16 0.1mM	SET-16 1.0mM	Log2Fold Change	UTX-1 0.0mM	UTX-1 0.01mM	UTX-1 0.1mM	UTX-1 1.0mM	Log2Fold Change
WBGene00007657	pals-3	3.06787357	4.14452059	7.04279067	9.37449857	2.96059461	3.64821809	6.06732939	6.48398880	7.23849849	1.88352456
WBGene00007658	pals-4	4.63898054	5.15037513	8.51316760	10.5291656	2.33782804	5.07573848	7.02032161	6.87265272	8.19597515	1.02796270
WBGene00007659	pals-5	3.15607176	3.82388717	7.76409951	9.71709780	3.07814280	3.66509405	6.51246257	6.92093939	7.90619011	1.78538138
WBGene00007660	pals-6	4.07830963	5.27214105	9.30836301	11.1188412	2.88547483	4.75261638	8.24162606	8.34376624	9.40489813	1.49842812
WBGene00007661	pals-7	2.35594575	3.25161150	6.15066461	7.08848692	3.20662638	3.47949633	5.39487509	5.36761243	6.01180746	1.52573185
WBGene00007662	pals-8	3.08017230	3.11564771	5.93253306	7.80938183	2.90539113	4.08727772	5.61002441	5.62243057	6.60196570	1.31882831
WBGene00007674	C18D4.4	2.35594575	2.65741494	4.69868512	6.63374347	3.31790166	3.59910494	5.16082506	5.64500388	6.08834683	1.60199962
WBGene00007745	C26D10.4	6.68033943	7.20462175	7.60352340	7.66572669	0.37831824	6.51509474	7.30250117	7.27038033	7.64852895	0.39080471
WBGene00007751	C26G2.2	8.19140038	7.80508549	6.54899454	6.56858610	-0.6126840	8.47011296	7.40829385	7.59069162	7.12929649	-0.4465625
WBGene00007835	oac-7	4.87414596	6.13596401	7.02870804	7.36948635	0.96131857	5.50124582	6.30169570	6.50786422	6.73595711	0.50954870
WBGene00007904	C33G3.4	8.25368162	8.47903467	7.43430481	6.82980055	-0.5684308	8.17868888	7.39337730	6.97923372	7.17899411	-0.3867657
WBGene00008010	C38D9.2	4.17033747	4.94922426	5.55980856	6.24510141	0.91930898	4.59407975	5.26227628	5.19930032	5.83629034	0.61812409
WBGene00008043	C40H1.8	7.01841187	8.29715978	9.32202656	9.39888220	0.89672952	6.63529632	8.42341617	8.17784128	8.90058865	0.68680832
WBGene00008067	C43D7.4	2.79679471	3.09058992	6.14164443	7.67406105	2.96047841	3.57272613	5.14433066	5.21190578	6.19389014	1.66582873
WBGene00008068	sdz-6	4.09317923	3.61421065	6.73153954	8.22142765	1.90329324	4.42023982	5.80425932	5.93595023	6.63147330	0.95000775
WBGene00008211	C49F5.7	9.50619054	8.39204532	7.80367708	7.28827974	-0.7604086	9.42834002	8.74263896	8.34596694	8.19488244	-0.4369639
WBGene00008267	C53A5.9	3.40927049	4.17854651	7.23321421	8.65076328	2.53670904	3.80629355	6.32962702	6.52093654	7.32776324	1.50089357
WBGene00008269	C53A5.11	3.25309522	3.20635464	4.53136646	6.44629556	1.99717254	3.74144788	4.40316230	4.30051441	5.36748127	1.33497448
WBGene00008301	pals-39	4.75863024	5.99844171	9.36902927	10.9417228	2.38170556	4.89989210	8.29603922	8.48118713	9.67831634	1.52371171
WBGene00008302	pals-38	3.71174224	4.58179706	7.33837305	9.24281067	2.45877793	3.97836766	6.81970271	7.00967789	7.90335232	1.45242605
WBGene00008476	E03H4.8	7.42951988	7.67896773	8.39473915	9.11842965	0.59272688	7.49209224	8.03768740	8.00691981	8.33672953	0.27556633
WBGene00008477	clec-17	7.52032851	8.67308158	10.3655695	9.93965456	1.12192970	6.65297616	8.49112895	8.94642917	9.43651081	0.92765847
WBGene00008483	E04D5.4	5.60015095	6.05510180	7.04817037	7.83916015	0.85467322	5.82657761	6.63385245	7.11505685	6.79130727	0.44818215
WBGene00008507	F01G10.4	2.63726838	3.68720452	5.64294815	7.37020441	2.65878533	3.57272613	5.24786301	4.92990449	5.57163141	1.12778946
WBGene00008572	F08B12.4	10.3684091	10.5164285	11.2202568	11.6762227	0.45469323	10.2015956	10.5975647	10.9303347	11.1995356	0.32881303
WBGene00008577	F08G2.5	6.49093744	6.50469313	7.56870970	8.37844128	0.70023969	5.49173971	6.95266738	7.00047450	7.15840349	0.61341536
WBGene00008597	clec-55	3.85202589	4.11147274	4.63019103	5.38486808	0.90224573	4.45154765	5.20362381	5.72748766	5.86276935	0.84892190
WBGene00008602	oac-14	8.12608516	9.61536856	10.1682475	10.4793855	0.69797795	7.48182290	8.90883910	8.56099283	9.39566589	0.55322866
WBGene00008842	chil-28	2.63726838	3.61421065	5.62417219	7.70125784	2.86661058	3.68561749	4.74997174	4.97694156	5.91407472	1.58512112
WBGene00008858	pals-1	5.21305486	4.88389088	6.40156617	7.69013067	1.02201557	4.47412843	6.01729738	5.77513042	6.53938729	0.81833745
WBGene00008872	F15H10.5	2.63726838	2.64301077	6.11682984	7.67663850	3.13602227	3.68561749	5.14832773	5.13251017	5.78491074	1.31689994
WBGene00008873	F15H10.6	2.55626806	3.44874733	5.42777960	7.04522628	2.80762418	3.57272613	5.44496037	5.32981350	6.26639142	1.54457236
WBGene00008891	clec-42	7.65493423	8.71830805	10.0024749	10.7775159	1.15354260	6.71012651	8.16070744	8.68351918	9.42393466	0.85634314
WBGene00008905	F17B5.1	6.82401545	8.70306131	10.3536443	10.0143043	1.24869127	7.44291605	9.08669806	9.32596123	10.1875197	0.87066047
WBGene00008945	F19B2.6	6.53329263	6.96686204	7.27103006	7.72635317	0.42339579	6.55269519	7.06897591	7.35202847	7.59181216	0.40302670
WBGene00008988	F20G2.5	6.40656880	7.26284453	8.33796194	8.86278947	0.90181316	5.58776716	7.52440031	7.62457633	7.99598041	0.83910637
WBGene00009061	pals-14	4.27329517	5.69986651	9.64119985	11.2626144	2.84441503	4.60274723	8.57369236	8.59412923	9.64090919	1.47366040

Gene ID	Gene Name	SET-16 0.0mM	SET-16 0.01mM	SET-16 0.1mM	SET-16 1.0mM	Log2Fold Change	UTX-1 0.0mM	UTX-1 0.01mM	UTX-1 0.1mM	UTX-1 1.0mM	Log2Fold Change
WBGene00009077	F23B2.10	2.96734116	3.38998274	5.47784519	7.29836076	2.48181742	3.90048960	5.18043252	5.05936599	5.49628926	0.90202450
WBGene00009168	F26F2.3	2.98552531	3.64812965	5.50724210	6.95849419	2.27233030	4.00717969	5.50315791	5.46613390	6.28628367	1.19432142
WBGene00009169	F26F2.4	2.69447203	2.35594575	4.15010813	5.20218786	2.32235821	3.47949633	4.70670585	4.65501474	5.17515084	1.34511572
WBGene00009295	fbxa-180	5.77584206	5.51728414	4.55197224	3.43506377	-1.1889722	5.94381602	5.15302552	4.69986526	4.88105908	-0.6846924
WBGene00009393	clec-62	9.42378348	9.87993776	10.5025120	10.6550646	0.45047351	9.03234983	9.61958401	10.1038623	10.0397765	0.35961197
WBGene00009515	clec-170	7.99610459	7.59591270	5.64568529	4.37090804	-1.4845750	7.64725413	5.74282921	5.46090535	5.75941404	-0.8311796
WBGene00009517	clec-167	4.14290020	4.49785756	4.57590163	6.09902180	0.88142838	4.37144962	4.88862724	4.97049673	5.49021244	0.71999981
WBGene00009518	clec-166	7.69579659	8.62420071	9.61939858	10.8870020	1.05837189	8.22553816	9.21779025	9.83715663	10.1163107	0.63298972
WBGene00009523	clec-165	5.54848086	5.95107921	6.51948841	7.53333123	0.76163706	5.73388848	6.44714176	6.66985690	6.83288408	0.42885496
WBGene00009803	F47B8.2	7.74320888	8.29023397	9.21255871	9.74324544	0.70845550	7.29572222	8.38165153	8.37127663	8.61247260	0.39599815
WBGene00009835	F47H4.2	6.78944034	7.41527830	7.99421375	8.98147785	0.78004667	6.28782644	7.32929663	7.64942513	8.02441351	0.63358482
WBGene00009839	fbxa-188	3.91740788	3.64651450	5.06090125	6.12892899	1.17438633	4.85706335	6.32737626	6.30996783	7.02258314	0.84562042
WBGene00009840	fbxa-189	5.94487988	6.05891526	7.09727189	7.99827907	0.78415598	5.65681585	6.88946165	6.84237962	7.34101219	0.56815610
WBGene00009895	scl-2	10.2330020	11.0591998	12.1789944	12.2264957	0.76616473	9.21686634	10.3293204	11.0775120	11.5175541	0.73318655
WBGene00009908	F49H6.5	3.81509988	4.88375700	7.61267286	9.58115970	2.46184586	4.06758903	5.81911997	6.28003833	7.34691865	1.38386644
WBGene00009945	bath-38	8.01297447	8.33216704	8.59152603	8.68715022	0.23555630	7.91987013	8.25986260	8.25346118	8.62624336	0.22317689
WBGene00009957	F53B2.8	8.90125307	9.55202156	10.3431735	11.0034196	0.67576499	8.07672974	9.47403610	9.38012254	9.81934500	0.51448947
WBGene00010004	F53H2.1	3.21540169	3.89608322	7.14093769	8.74663278	2.82655696	3.97780770	6.94681744	7.46310564	7.89349506	1.53607989
WBGene00010118	F55F3.4	5.74584450	6.08406766	7.47156646	6.79592101	0.73354037	5.69249773	6.74243480	6.57788605	7.04977121	0.51267385
WBGene00010157	oac-34	4.64098303	7.00714693	8.00843795	7.28626705	1.19080168	4.94222739	7.11736908	7.01699017	7.61925765	0.94237484
WBGene00010508	K02E2.7	3.12107435	3.22221228	4.75650215	6.28907448	2.17881355	3.92872946	4.94428231	4.77799912	5.60436716	1.11750872
WBGene00010545	cbp-2	7.44476012	8.00226236	8.44698963	9.18226756	0.57819156	6.97832567	8.01991438	8.14497122	8.40140838	0.46745370
WBGene00010605	K06G5.1	12.7520059	13.1894046	13.8761021	14.1225383	0.48473707	12.5723287	13.0106337	13.3564781	13.5352621	0.32556738
WBGene00010744	K10D6.4	7.41767401	8.23606716	9.03302172	9.06260961	0.61213137	7.51410329	8.60029547	8.40387075	8.84309372	0.38723290
WBGene00010754	K10G4.5	3.47743206	3.90185475	4.46355205	5.39168159	1.24585284	3.78470265	4.35687109	4.67584166	5.03778912	1.15555452
WBGene00010850	M04C3.1	8.97425033	9.65956559	9.96334607	10.4307885	0.49493149	8.68384613	9.74428411	9.67277992	10.2289212	0.46240533
WBGene00010893	cutl-9	5.83742817	6.02888496	6.77555813	6.74543712	0.39000928	5.51544037	6.52649409	6.31237270	6.73266698	0.43454025
WBGene00010897	lact-3	9.38261371	9.68418968	10.0905862	10.6437817	0.42426453	9.30596747	9.46640661	9.80497530	9.88464282	0.21533512
WBGene00010989	R03D7.2	8.51434015	7.84980816	6.83314277	6.86964843	-0.6085486	8.55952625	7.37700967	7.65511070	7.21155340	-0.4453500
WBGene00011003	R04B5.5	7.58367743	6.66436082	4.99157687	4.53586997	-1.3118018	6.56999655	4.95278504	5.26793675	5.04523939	-0.7111461
WBGene00011161	chil-18	3.50600531	4.35399588	6.00438991	8.74533005	2.42014846	3.79715316	4.98047860	5.23471773	6.22096701	1.31474725
WBGene00011162	chil-19	4.57934942	4.84949321	5.41650729	6.33470952	0.75696641	4.90249656	5.82896328	6.22506972	6.36366946	0.73944889
WBGene00011166	chil-22	7.19349161	7.45862825	8.45861859	9.37096005	0.78268333	6.85558675	8.20077515	8.27342760	8.46631849	0.51601006
WBGene00011209	R10E8.3	4.84208678	5.58088792	7.05059886	7.31744342	1.07676243	4.78829090	6.92482592	7.20882725	7.11763601	0.95477482
WBGene00011539	fbxa-135	4.15529485	4.77253842	6.58802831	7.41376628	1.42872784	4.38295165	6.19547521	5.94229290	6.71874818	0.97108923
WBGene00011571	ttr-46	11.0801556	10.8178623	10.3571194	9.41088768	-0.5421799	11.0158426	9.95554999	9.76447425	9.81533150	-0.3960838
WBGene00011672	cyp-13A5	6.02323047	6.74463814	7.20935049	8.78961875	0.92037520	5.21357663	5.79105374	5.90928778	6.92496958	0.71875987

Gene ID	Gene Name	SET-16 0.0mM	SET-16 0.01mM	SET-16 0.1mM	SET-16 1.0mM	Log2Fold Change	UTX-1 0.0mM	UTX-1 0.01mM	UTX-1 0.1mM	UTX-1 1.0mM	Log2Fold Change
WBGene00011673	cyp-13A6	4.82765737	5.31334239	5.64704348	6.41040076	0.65267628	4.94868719	5.58612298	5.53496006	6.13523623	0.57148431
WBGene00011677	cyp-13A1	4.32775071	4.44549027	4.94961467	5.76427142	0.66929067	4.44933130	5.05192898	5.26512348	5.33714287	0.56377638
WBGene00011737	sqst-1	10.2146065	10.9099159	11.4341937	12.1119417	0.62174691	10.1264417	10.6759218	10.7597883	11.1443976	0.30689150
WBGene00011753	T13F3.6	9.43498347	8.03266936	6.34768626	5.61053531	-1.4051530	9.76145531	8.52146305	8.42634683	8.09450335	-0.5296767
WBGene00011879	pho-7	7.38711939	6.67052850	6.03903207	5.71931992	-0.6280436	7.35783065	6.63743345	6.67272751	6.32974478	-0.3881323
WBGene00012069	T26H5.4	4.00192182	4.87572444	5.84173255	5.89123801	0.86093458	4.25765830	5.03280861	5.14529942	5.63506710	0.83390094
WBGene00012091	pals-29	2.79679471	3.96190431	7.67152053	9.58674180	3.46158261	3.91223797	6.77493852	6.59863007	7.69222509	1.40068225
WBGene00012101	zip-10	6.50237390	6.90296362	7.82592495	8.14073870	0.61966644	6.08450767	7.34402495	7.23434159	7.43238360	0.45291518
WBGene00012144	T28H10.3	10.4569511	10.8941559	11.5347499	12.0098642	0.52844917	9.80387392	10.5680485	10.6512707	11.0126227	0.37178136
WBGene00012239	W04A8.4	7.82899296	8.46565032	8.87938046	9.07896589	0.42054203	7.24874648	8.68130824	8.16237940	9.08095551	0.48785627
WBGene00012252	W04E12.7	7.65274006	6.68218165	4.45399957	3.86592291	-1.7761202	6.82605919	5.24856034	5.14425000	5.21070615	-0.7854351
WBGene00012381	Y2H9A.4	6.17970719	6.91803384	8.41503427	9.34428590	1.21799401	6.30513361	8.00440056	7.81551761	8.78209797	0.78832025
WBGene00012398	Y6E2A.4	4.13873384	4.77191845	6.70126335	8.02816442	1.66422244	4.42306613	6.40176671	6.34801843	6.92737092	0.99569754
WBGene00012399	Y6E2A.5	4.23198986	5.04993870	6.95979863	8.33698588	1.70780794	4.52269642	6.63807066	6.66060321	7.25604462	1.02185143
WBGene00012400	Y6E2A.7	2.89190302	3.40696960	5.46976167	6.98515132	2.41937487	3.77986009	5.03330929	5.01848904	5.61943025	1.10373447
WBGene00012404	Y6G8.2	6.49789284	7.25188572	7.79362574	7.48071313	0.41505182	6.43583178	7.73178572	7.78680828	8.13596783	0.56630660
WBGene00012491	Y20C6A.1	6.14132080	6.43302650	6.98745990	6.99250025	0.36878962	6.10652565	7.02352369	7.11586055	7.44730148	0.49090587
WBGene00012501	Y26D4A.3	3.42911903	3.36304280	3.51823039	4.56816570	0.80791849	4.06919773	4.35461032	4.41037425	5.04960791	0.95341573
WBGene00012593	nspe-7	4.50054539	4.65773641	5.00093554	6.18384919	0.78540033	4.65335602	5.22130574	5.21623664	5.84725734	0.66001573
WBGene00012680	Y39B6A.21	7.67737882	7.19286083	6.02568854	4.71160915	-1.0941458	7.06877138	6.22706750	6.08835695	5.86734207	-0.5270287
WBGene00012683	asp-17	5.72297954	5.44121969	7.15586090	9.28335119	1.31967397	6.81282495	7.30995452	8.35698268	8.46617647	0.68876525
WBGene00012726	Y39G8B.5	3.36897967	3.61421065	6.18775127	8.40652725	2.45219048	3.97603622	5.81748750	5.88556504	7.03388233	1.32869209
WBGene00012822	Y43F8B.12	4.88037767	4.95747792	6.08530241	7.57542500	1.10656804	4.64339932	5.72990751	5.64627550	6.20976463	0.67625235
WBGene00012880	Y45F10C.4	9.16987012	8.31381051	7.19234418	6.92665657	-0.7736077	9.27896707	8.10588012	8.37530229	7.73315406	-0.4878303
WBGene00012910	Y46G5A.20	6.12442417	6.58430952	8.59951239	9.44006786	1.22495154	6.14709818	8.02760309	8.29880959	8.54714167	0.82879929
WBGene00012947	Y47H9C.1	8.06061218	9.55956006	9.91638004	10.9903894	0.78224820	7.65371786	8.68976555	9.10787786	9.00873457	0.48902619
WBGene00012961	Y47H10A.5	7.75842157	7.66708980	8.16698041	9.61100007	0.62908294	6.74352136	7.42607940	7.53630562	8.04525622	0.42962849
WBGene00012980	efhd-1	9.30622629	9.91169367	10.1045650	10.4728668	0.36937712	9.07289147	9.77073864	9.67858268	10.0521573	0.28801847
WBGene00013119	Y51H4A.25	7.59260019	8.14921911	8.75913722	9.14749993	0.54257382	7.08160027	7.97962364	8.02452662	8.38004241	0.43550354
WBGene00013125	clec-92	3.37411736	3.39330058	2.73750200	2.35594575	-1.2692649	6.07709567	5.57859038	5.57911732	4.92783265	-0.6674437
WBGene00013215	Y54G11A.4	5.55203936	6.22056005	7.17599201	7.73896302	0.85421997	5.89991173	7.02830263	6.95149261	7.49186765	0.55837622
WBGene00013275	btb-14	8.46212898	8.00507402	5.88625830	5.49731756	-1.1597573	8.20567851	6.51471002	6.40820252	6.49607709	-0.6491863
WBGene00013372	Y61B8B.2	2.35594575	2.57083219	3.67570740	5.11504122	2.69485445	3.47949633	3.91671576	4.24972591	4.92229964	1.77887893
WBGene00013540	cest-12	8.34695484	9.05410250	9.28681162	9.33796956	0.33146773	7.90624790	8.70806973	8.75525451	8.92282739	0.33415523
WBGene00013614	clec-237	3.11534383	2.85506771	4.09076078	3.83217850	0.99092009	4.67749996	5.17047801	5.10773027	5.85289250	0.60554583
WBGene00013637	Y105C5A.13	5.00396399	5.37384211	7.17802592	8.15661838	1.28871412	4.64424708	5.78990452	5.91860696	6.40084527	0.82721550
WBGene00013650	Y105C5B.9	7.53873961	7.40682381	7.29094915	6.11182301	-0.4460377	6.99747692	6.42909204	6.16688248	6.18950650	-0.3514568

Gene ID	Gene Name	SET-16 0.0mM	SET-16 0.01mM	SET-16 0.1mM	SET-16 1.0mM	Log2Fold Change	UTX-1 0.0mM	UTX-1 0.01mM	UTX-1 0.1mM	UTX-1 1.0mM	Log2Fold Change
WBGene00013754	fbxa-116	2.63726838	3.02455952	4.54314989	6.62337192	2.66745841	3.61113833	4.72978530	4.36923057	5.20116138	1.16675760
WBGene00013755	fbxa-115	6.61900701	6.57357431	7.23660971	7.54151167	0.37523354	6.34609565	6.69936904	6.96033556	7.34564200	0.39522759
WBGene00013763	Y113G7B.14	7.76267681	8.14375282	8.52278743	9.22578531	0.49164615	7.40387420	8.15151362	8.09289070	8.33589719	0.28991162
WBGene00013837	fbxa-30	3.64363599	4.02126218	4.64318612	5.51985453	0.96735247	4.48130758	5.12986035	5.41996552	5.45137020	0.63352814
WBGene00013870	ZC373.5	7.14473791	7.45077673	8.19464497	8.09850905	0.38940101	7.27039253	8.03588996	7.88270790	8.25390398	0.30221484
WBGene00013898	ZC443.3	7.65585205	8.47540135	9.15503913	9.34854977	0.58549547	7.22333417	8.27191165	7.99569232	8.61032375	0.39294693
WBGene00013939	ZK218.5	4.49131429	5.02806778	4.26001052	3.06592778	-1.1587503	5.71317141	3.63371970	3.95853526	3.60765189	-1.9841100
WBGene00014046	clec-60	4.98395776	6.13293369	8.04617244	9.77007795	1.85853227	5.86751289	7.52386936	9.33158880	9.59049419	1.37213319
WBGene00014047	clec-61	4.41131758	5.70984793	7.16435547	8.74762608	1.71002531	5.83336210	6.79101634	7.59277915	8.30782633	0.84168565
WBGene00014821	R10E8.7	8.19490341	8.30452062	7.62527938	6.82143477	-0.4989724	8.09815963	7.60018780	7.19710504	7.33660880	-0.3036358
WBGene00014944	Y68A4A.12	3.00824724	3.18055204	4.85952633	5.82346128	1.66263434	4.06278320	4.43412623	4.59697371	5.05618881	0.80794687
WBGene00015077	B0238.13	3.83407876	5.27619941	6.77226563	7.63756210	1.65098834	4.23651823	5.54952982	5.42330951	6.00568704	0.89752255
WBGene00015100	B0280.2	4.82517831	4.98617585	5.64576905	6.91932784	0.88472044	5.01462227	5.76450768	5.63072818	6.08144121	0.48239704
WBGene00015152	B0348.2	4.08693874	4.58803731	5.15902479	6.31090946	1.05727375	4.89937273	5.37924778	5.90525264	5.90274788	0.62067108
WBGene00015223	B0507.6	3.97918254	4.91239548	7.60913270	9.28189267	2.28417368	4.75076555	7.12331192	7.16090601	8.04696229	1.15604579
WBGene00015224	B0507.7	3.37417239	3.34797717	6.16863043	7.54054875	2.25532067	3.96132246	5.75851459	5.90761392	6.46687088	1.17822490
WBGene00015225	B0507.8	4.50475137	5.77461725	10.0167969	11.9203899	2.94796543	4.62229748	8.89919668	9.28932861	10.3496618	1.61892382
WBGene00015227	ddn-1	5.17493491	6.55735714	10.9336474	12.6988656	2.87974136	5.25897927	9.71203923	10.0285794	11.0909173	1.54765999
WBGene00015259	dod-20	4.30833022	4.86366781	5.65062176	5.75984527	0.90788719	4.76654592	5.27896703	5.88628911	6.25809389	0.83134769
WBGene00015295	acl-12	8.18720987	8.49349078	9.18721221	9.56957834	0.49576924	8.63129516	8.95033229	9.03422803	9.35686778	0.23503772
WBGene00015537	C06E4.8	4.76906755	4.75595028	6.54255339	7.72469815	1.23654261	4.96819665	6.05250551	6.06703018	6.88035218	0.79151151
WBGene00015552	C06G3.6	8.79784459	8.83157496	9.32789613	9.38377217	0.22306419	8.39728993	8.95455539	8.75695166	9.25469758	0.24656511
WBGene00015600	fbxa-165	2.35594575	3.02243058	4.86359621	6.90411042	3.19576785	3.57272613	4.56491424	4.78129043	5.29637974	1.40786261
WBGene00015602	fbxa-158	3.59537156	4.33740915	6.85910599	8.28185397	2.18727599	3.84855418	5.86323561	6.05255084	6.75794614	1.37346954
WBGene00015605	C08E3.13	4.49102446	5.50225319	7.31759721	7.98997340	1.48035021	5.05343322	6.28738560	7.05281969	6.69699777	0.75684669
WBGene00015665	C10A4.4	5.68604782	5.40933405	4.32855813	4.41588353	-0.6232708	6.12904474	5.52673705	5.70808304	5.02491663	-0.4888889
WBGene00015828	math-14	6.19977883	5.66108622	6.94136805	8.08043670	0.74743789	6.06348355	7.17642189	7.49381063	7.78044260	0.63533721
WBGene00015829	math-15	5.29941418	5.27275503	6.41359751	7.63809978	0.94383702	4.66029149	6.62593470	6.28891707	6.95703826	0.85802757
WBGene00015834	math-5	2.74616374	2.78646308	4.82001637	6.76577739	2.76140533	3.57272613	4.82660717	4.84491180	5.79486675	1.46254402
WBGene00015839	math-10	3.37775735	3.82799444	5.76777001	7.04638076	1.82711468	4.45496395	5.65672717	6.11643958	6.78335873	1.19152473
WBGene00015879	C17B7.5	4.63209988	5.21619831	6.49472786	5.66057155	0.70478978	6.38885774	7.83192570	7.58728503	8.50000066	0.63308182
WBGene00016023	prmt-6	6.91075850	6.46679762	5.84553062	4.10085457	-1.0203723	7.02766160	5.89306747	5.67424104	5.43109664	-0.7181837
WBGene00016058	nspd-3	6.11790003	5.61042239	3.72041453	3.43831599	-1.5290970	6.59529002	6.00946545	6.01503772	5.22066851	-0.6203642
WBGene00016064	acd-1	5.38063395	6.34440618	8.53586501	8.58781627	1.40117291	6.59572723	9.06761258	9.13223294	9.39141577	0.83966067
WBGene00016190	rcs-1	9.06149164	9.10088301	9.81063426	9.95904909	0.36365787	8.29505403	9.14486273	9.14359381	9.44355259	0.34732527
WBGene00016191	C28G1.6	6.65143720	6.57474075	7.12851283	7.32118305	0.28644728	6.23390197	6.80406288	6.88773297	7.11250520	0.33155480
WBGene00016218	pals-23	7.36049175	7.90003009	8.61495375	9.16802863	0.62908973	6.89305022	8.14812839	7.87549365	8.33901629	0.42858104

Gene ID	Gene Name	SET-16 0.0mM	SET-16 0.01mM	SET-16 0.1mM	SET-16 1.0mM	Log2Fold Change	UTX-1 0.0mM	UTX-1 0.01mM	UTX-1 0.1mM	UTX-1 1.0mM	Log2Fold Change
WBGene00016221	C29F9.6	5.03221909	5.56740944	7.04735669	7.51175125	1.07483656	5.63185448	6.59434545	6.82262895	7.37221389	0.70501584
WBGene00016274	C30G12.2	9.87288885	8.85230158	7.98210277	7.41522975	-0.8682616	10.0182534	9.64806048	9.34271714	8.81674314	-0.4286132
WBGene00016281	pals-32	4.65138427	5.74098967	8.72960880	9.91445340	2.10295166	5.71569051	8.22171277	8.23156810	8.72945608	0.85966050
WBGene00016301	fbxc-6	3.43651340	4.06242589	4.38826177	5.75265513	1.15903245	3.80919716	4.85957713	4.85433745	5.09772274	0.86679517
WBGene00016407	unk-1	10.3096133	11.1316407	11.7909880	11.9316888	0.57393555	10.0972944	10.9852149	11.0092515	11.3943683	0.38823429
WBGene00016424	C34H4.1	7.98789921	8.18630872	9.02412296	9.40577026	0.53758876	7.68808901	8.42364225	8.40894704	9.00614073	0.42325436
WBGene00016425	C34H4.2	9.05875907	8.99735117	9.40947989	10.0725361	0.35190709	8.62922566	9.22488415	9.48061230	9.72603533	0.37025162
WBGene00016451	clec-6	2.91311209	3.64940151	3.94476444	4.27067007	0.86418692	4.41602967	4.98689260	5.23514659	5.50581513	0.70578438
WBGene00016473	C36C5.4	2.55231458	2.57083219	4.83379917	4.13353023	2.26191975	3.77986009	5.02049715	4.93827295	5.34105098	1.01276704
WBGene00016483	C36C5.14	5.12314508	5.62175243	9.01583327	7.96954031	1.58465602	7.24086118	9.22112478	9.05121746	9.78964916	0.74871007
WBGene00016484	C36C5.15	4.18614152	5.24271543	8.19418301	7.33499373	1.77581670	6.70029477	8.49347814	8.53615082	9.22839229	0.81806901
WBGene00016642	chil-10	8.53301712	8.71684951	9.01083449	9.07892714	0.20389598	8.39270009	8.85041378	8.99306705	9.02992047	0.21479302
WBGene00016762	ugt-24	6.28031465	6.48569695	7.02597180	7.36775649	0.42814570	6.45043050	7.27231056	7.02365384	7.68289315	0.41469393
WBGene00016763	C49A9.9	8.76863293	9.02771066	9.78542841	9.72820335	0.40779183	8.69721588	9.21078848	9.20703078	9.65608910	0.30416958
WBGene00016769	C49C8.5	9.88193591	10.3531460	11.2313567	10.9420429	0.43972567	9.61891614	10.8259740	10.5548731	11.1694819	0.42864360
WBGene00016849	acs-21	6.45606217	6.82632709	7.46589872	7.46759162	0.40719698	6.61250000	7.02665687	7.20586447	7.34197344	0.27656125
WBGene00016862	cest-32	9.25067110	9.30596442	9.92963334	10.4110898	0.41003138	8.80714543	9.34997585	9.36691538	9.74469240	0.29091168
WBGene00016920	C54E4.5	8.22544527	8.18844707	8.96129720	9.53670553	0.48863020	8.12011769	8.53176245	8.78601165	9.03833748	0.30810656
WBGene00016997	cebp-1	8.88226254	9.52019553	10.1054677	10.8557901	0.65013111	8.67398977	9.28508213	9.40620531	9.66809151	0.31244321
WBGene00017089	poml-2	7.94852321	7.82751343	7.54252316	6.77134785	-0.3889045	7.91969350	7.54176598	7.36359622	7.12298283	-0.3031928
WBGene00017103	klo-2	7.93710969	7.53957509	6.18756113	5.66308421	-0.9119419	7.95524443	6.69781357	6.73506884	6.68717188	-0.4632372
WBGene00017128	E04F6.9	8.56581392	9.26699232	10.7859574	10.8700117	0.86633746	9.01376223	10.3438385	10.4130148	10.4905673	0.42253716
WBGene00017214	F07E5.9	2.75263689	4.01116898	7.39125804	8.85728191	3.21530507	4.03179832	6.34313742	6.41387784	7.24509136	1.42566147
WBGene00017467	F14F9.4	7.42845976	8.02662270	8.75606613	9.48511444	0.70310694	7.34435510	8.51951008	8.34009138	8.69623419	0.40162476
WBGene00017586	F19B10.4	4.41066939	4.91950232	5.91990058	6.77739520	1.05497859	4.65133140	5.63001375	5.63336992	6.44709239	0.87898157
WBGene00017592	F19C7.2	7.63231493	7.55466819	6.03148993	6.42289152	-0.5758612	7.73423412	6.48862398	6.03176246	6.04211486	-0.7066586
WBGene00017705	F22E5.6	3.26023953	3.49456383	4.21371466	5.60038708	1.44428660	3.78470265	4.50043804	4.78129043	5.05119605	0.97835777
WBGene00017786	F25E5.5	7.73120854	8.19677300	8.66369183	8.79415283	0.36565962	7.49606471	8.28360941	8.12162805	8.55548980	0.31867178
WBGene00017788	F25E5.7	3.56692355	3.99973812	3.79823104	4.67618747	0.67059842	6.37249337	5.65323359	5.66938195	5.07373398	-0.6625194
WBGene00017839	F26G1.3	4.69175967	5.10487195	6.95437861	7.83180260	1.36335114	4.43405932	5.38171899	5.26026952	6.04225723	0.84028615
WBGene00017961	nhr-180	5.91728045	6.60097506	7.02808499	7.08594882	0.45294560	6.08369924	6.52018158	6.60863718	6.92990605	0.33879566
WBGene00017973	ift-81	4.94345941	5.91038766	6.19165643	6.55952837	0.59446494	4.99013569	5.89989638	5.73781644	6.24533574	0.48147914
WBGene00018266	nhr-183	5.87898174	6.16562553	6.86956910	7.30583084	0.55231849	6.00991697	6.61867524	6.56015409	6.88544486	0.32225141
WBGene00018345	F42C5.3	4.30747374	5.05555245	8.29708402	10.0056347	2.35592759	4.62496432	7.49589473	7.08601011	8.50277254	1.25988461
WBGene00018353	fbxa-182	5.60483800	6.51585172	8.89924399	10.4315178	1.79966035	5.97587430	8.49815332	8.84214428	9.41154740	1.07292738
WBGene00018354	F42G2.5	5.26514944	5.36888956	6.08002244	7.17960380	0.78101831	5.30387427	5.87874559	6.09873958	6.57020554	0.56881947
WBGene00018433	ceh-82	4.32121844	3.69763685	3.44887175	3.06451026	-1.0287511	5.25830923	4.61252954	4.48250083	4.08373415	-0.8041514

Gene ID	Gene Name	SET-16 0.0mM	SET-16 0.01mM	SET-16 0.1mM	SET-16 1.0mM	Log2Fold Change	UTX-1 0.0mM	UTX-1 0.01mM	UTX-1 0.1mM	UTX-1 1.0mM	Log2Fold Change
WBGene00018614	pals-31	3.59959694	4.16107985	5.23674760	6.85149630	1.46139417	4.40774707	5.44815595	5.32306579	6.07991378	0.81903010
WBGene00018645	F49F1.5	6.59490733	8.35689886	9.23253308	10.1336367	1.08138658	6.67647573	7.52301814	8.19814044	8.48510328	0.67544320
WBGene00018702	F52E4.5	7.96802198	8.12806704	9.22978700	9.40792993	0.55576870	7.91416677	8.83417931	8.83194855	9.02798433	0.33312713
WBGene00018704	ztf-13	8.46263993	8.66393496	9.14551219	9.22559640	0.28216650	8.34355911	8.71759236	8.76891827	9.07714462	0.24181491
WBGene00018758	F53E10.1	8.42603087	8.92968950	9.56947385	9.59066178	0.43336661	8.23973086	8.77838189	8.92069105	9.10097255	0.28819317
WBGene00018921	sago-2	7.58370501	7.72670244	8.39455426	9.14978882	0.57060258	7.52796720	7.93476674	8.20882453	8.45145530	0.32349097
WBGene00018997	F57B9.3	4.30993969	4.14985213	5.26424602	6.23572592	0.91843448	4.22955092	4.91342545	4.75242247	5.24318871	0.71620907
WBGene00019047	F58E2.3	5.58943733	5.82058925	6.84821986	7.62484030	0.81525586	5.55994927	6.37874652	6.52385735	6.58972831	0.43020057
WBGene00019057	F58F9.3	7.90449242	7.83772365	8.79578710	9.39080743	0.54722380	7.41014480	8.36912940	8.53886493	8.83875387	0.48244966
WBGene00019146	H02F09.3	6.02349053	6.18685602	7.10995438	7.83612988	0.71549869	6.05316643	7.02422167	7.45340283	7.87545631	0.67743517
WBGene00019279	K01A2.4	6.51861568	7.06869992	8.17032117	8.43099596	0.73954662	6.42066337	7.90815455	8.12355216	8.58300819	0.70318576
WBGene00019309	K02E7.4	2.92599842	3.51830559	3.84634628	4.12864128	0.88451184	3.97780770	4.36856464	4.49468408	4.95569022	0.82014965
WBGene00019314	K02E7.10	5.46354355	5.43998009	7.21959787	7.65498980	1.06394985	5.48210484	6.89331595	6.55257680	7.60967103	0.70027977
WBGene00019426	cutl-16	7.03434170	7.48926937	7.92180939	8.18840573	0.42009265	7.06906203	7.78702549	7.75766259	8.19457801	0.37583260
WBGene00019437	K06A9.3	5.26328363	5.07915105	4.07054210	3.48372263	-1.0546397	5.36478801	4.79339458	4.64897045	4.44948401	-0.6822047
WBGene00019472	cyp-35B1	4.38193858	5.79619702	7.25964450	6.48591076	1.04467599	5.41995242	6.84909482	7.12395964	6.96545934	0.63861825
WBGene00019495	sdz-24	9.27210801	9.93978679	11.3240992	10.6040431	0.67314185	9.61984550	10.7177762	11.2069786	11.6603894	0.68286063
WBGene00019550	K09C4.5	7.07897868	7.73655944	8.43845768	8.44943113	0.56255663	7.46498009	8.18084975	8.68653099	9.19910333	0.59362976
WBGene00019592	K09F6.9	7.96338925	8.79175777	9.36866323	10.9276152	0.96244170	7.74448309	9.18817093	9.24348067	9.54763038	0.50439403
WBGene00019593	K09F6.10	7.40510863	8.24607910	8.77844895	10.4028137	0.98272454	7.18947177	8.39694087	8.68485498	9.03304145	0.56279724
WBGene00019887	R05D8.11	3.47932487	3.50408660	5.62528696	5.17031772	1.43515530	4.21910012	5.19855703	5.17947334	6.06304317	0.90166998
WBGene00019908	R05H11.2	5.76091665	6.52666691	7.38971543	6.95160137	0.57815775	5.58806982	6.88078707	6.59670902	7.50256471	0.63325462
WBGene00019917	clec-43	6.31510779	6.14680721	4.37928674	3.97524022	-1.2208180	5.84012488	4.49786688	4.46974282	4.63758389	-0.8559793
WBGene00019968	R08F11.4	5.57030853	6.20446079	6.89035730	7.22981484	0.65367030	5.97326138	6.87779166	6.80102551	7.47935220	0.52013156
WBGene00019986	R09F10.1	9.32233506	9.37297562	8.90287448	7.69844070	-0.5202575	9.11519829	8.49483791	8.25802069	8.27661175	-0.2949105
WBGene00020220	clec-140	3.25460996	3.90218720	4.06223320	5.01016938	1.11601263	4.14929576	4.65180086	4.94786999	4.94620704	0.71202588
WBGene00020228	T05A8.2	2.75263689	3.05477769	5.36095409	7.27933101	2.68209057	3.47949633	4.76226336	4.68736433	5.21554569	1.30792514
WBGene00020256	T05C3.6	8.68144954	8.43690480	7.78400436	6.26311601	-0.7856585	8.50750563	7.61775180	7.55462358	7.16337238	-0.4841687
WBGene00020276	T05H4.15	4.87145040	5.31798620	6.22202602	6.76558320	0.78113177	5.21264298	6.37168661	6.35979732	6.65023044	0.57488760
WBGene00020315	T07E3.4	8.91955157	9.30695937	10.1463814	10.2109551	0.49222338	8.99264511	9.30827742	9.37020857	9.73704649	0.23900528
WBGene00020357	T08E11.1	3.34706764	4.71900375	7.62260190	9.24224137	2.72261229	3.95225706	6.83743406	7.11389473	7.80831207	1.51760846
WBGene00020393	T10B5.7	9.31751202	8.98728513	8.63415854	7.70985902	-0.5275419	9.34832933	8.28701654	8.38475434	8.12900141	-0.3900121
WBGene00020491	T13G4.4	7.46632451	7.09631354	6.74491418	6.04824007	-0.4913702	7.08757193	6.52265666	6.09990755	6.04712713	-0.4687421
WBGene00020497	T14A8.2	7.39224812	7.95445469	9.54459413	9.09222431	0.77172714	7.64708111	8.67174399	8.74962465	9.04229035	0.46812442
WBGene00020569	lgc-32	8.05967090	6.57208200	6.59118033	6.21819667	-0.6188527	7.57497641	7.28844808	6.77710123	6.80740823	-0.3386619
WBGene00020613	T20D4.7	5.30394852	5.24671006	7.19453070	7.63826685	1.01625491	6.24629237	7.58485493	7.96309308	8.55377129	0.80907482
WBGene00020618	T20D4.12	4.65588196	5.90049045	7.91018804	6.58141983	1.08926067	5.69041430	7.95141160	7.48453577	8.09893030	0.73803249

Gene ID	Gene Name	SET-16 0.0mM	SET-16 0.01mM	SET-16 0.1mM	SET-16 1.0mM	Log2Fold Change	UTX-1 0.0mM	UTX-1 0.01mM	UTX-1 0.1mM	UTX-1 1.0mM	Log2Fold Change
WBGene00020637	fbxa-7	2.35594575	2.85789721	4.40532505	6.02852629	2.81471572	3.77070865	4.72571174	4.70476429	5.38472802	1.29411337
WBGene00020640	fbxa-73	2.86576855	3.04054406	3.94948646	4.44334600	1.36233779	3.64047541	4.21653301	4.48059842	4.92903931	1.18604008
WBGene00020649	sma-10	8.86512829	9.15346921	9.60989734	9.84799578	0.35519892	8.69349634	9.26597011	9.26570875	9.60343630	0.28303220
WBGene00020774	T24E12.5	5.99594905	6.99144994	8.47806249	9.39760714	1.29704168	5.99715579	7.43482699	7.07683716	8.13413523	0.68210016
WBGene00021028	W04C9.6	5.22684892	5.47039289	6.25517231	6.69437250	0.63115589	5.61190004	6.57520143	6.77725795	6.58689116	0.42159205
WBGene00021048	W05H9.1	10.3240975	11.2845682	11.7680322	12.3991070	0.66769637	10.1466733	10.7615305	10.8224051	11.2869337	0.35270064
WBGene00021072	W07B8.4	4.10424288	4.65127867	5.26132424	6.22292714	1.05746112	4.29127726	5.24194817	5.86932591	6.01899173	1.09488571
WBGene00021081	pals-33	3.82515856	4.84670884	8.17313521	10.1452548	2.69615748	4.58095686	7.45960568	7.82814284	8.59795448	1.36696134
WBGene00021179	fbxa-86	3.00069742	3.00134952	3.57119787	5.28766818	1.83714856	3.59910494	4.27170433	4.34008954	4.79781111	1.16721457
WBGene00021235	Y19D10B.6	6.16373221	6.12133232	4.52358073	3.98604470	-1.1585646	6.16878447	4.95623194	4.72421313	4.86992207	-0.7808727
WBGene00021435	Y39A3A.4	4.57953748	5.06195039	5.49827935	6.55200658	0.76767914	4.59407975	5.42897258	5.49841880	5.85745645	0.62027369
WBGene00021448	Y39D8A.1	7.14692579	7.33471373	7.71826599	7.84398087	0.27906024	7.13869134	8.30462108	8.23551847	8.52515412	0.42857079
WBGene00021517	Y41D4B.15	3.94699272	4.96402615	5.81536324	6.42050902	1.09680477	4.28438428	5.12202842	5.51503171	5.44714212	0.80947105
WBGene00021519	Y41D4B.17	5.78112513	5.94885200	6.79051622	7.13500326	0.54185209	5.35963391	5.99551581	6.02715291	6.36610822	0.45232313
WBGene00021529	Y41G9A.5	7.02700733	7.62162843	8.63929012	8.76263788	0.67177093	6.25003765	7.41188733	7.22696282	8.03153213	0.58675665
WBGene00021583	clec-72	9.12181684	10.2998064	11.8467480	11.5480687	1.01017652	8.30372876	9.92716845	10.2107067	10.3365126	0.64093221
WBGene00021587	clec-76	5.58690511	6.82367026	6.96762676	7.17390332	0.64911346	5.68020190	6.63304918	6.79020175	7.41628193	0.68317194
WBGene00021741	Y50D4B.2	6.44936206	7.96506516	8.49668469	8.65163538	0.77852081	6.13486800	6.76757244	7.07689304	7.30739899	0.47774958
WBGene00021865	fbxa-66	4.01030600	4.26013165	5.27812061	6.18361130	1.07884659	4.05641997	4.62301345	4.90108513	5.45558075	0.92062252
WBGene00021873	clec-82	4.08353317	5.39957700	6.28935217	6.71059568	1.21062662	5.78302809	7.01879420	7.89057112	7.93412679	0.70131791
WBGene00022189	Y71H2AR.2	3.16903994	3.27422117	4.97653204	7.18594748	2.19226689	3.95806653	5.24287649	5.13616365	6.08301784	1.22512723
WBGene00022329	fbxa-79	6.37398456	6.37754086	7.13051110	7.53136358	0.44996101	6.11542339	6.93989311	6.78004058	7.19660787	0.35612548
WBGene00022375	Y94H6A.2	3.81575627	4.38634553	6.37449068	7.73226358	1.83816563	4.48952784	6.09449467	6.18948262	7.07215292	1.07930419
WBGene00022487	fbxa-21	4.41558548	4.65618642	5.06176797	5.57011476	0.50891640	4.46834000	5.30684500	5.24748499	5.60866728	0.60444516
WBGene00022545	ZC196.1	3.08169775	3.58158410	5.91202842	7.18658833	2.34527275	4.24830080	6.02092899	5.76412812	6.46539838	0.91694536
WBGene00022546	ZC196.2	3.30228279	3.33901321	5.19206078	6.65113216	1.82218513	4.42482669	5.61144203	5.49117074	6.25538406	0.89033931
WBGene00022547	ZC196.3	4.21181466	4.55367993	6.40872532	8.16816226	1.74072376	4.56263584	5.98930170	5.62485420	6.41508410	0.76022508
WBGene00022548	ZC196.4	5.10403973	5.38852058	7.21856857	8.31666671	1.33823636	5.47373285	7.00902283	7.17634546	7.83904357	0.85481490
WBGene00022550	droe-8	3.52585386	4.49184525	7.38865178	9.02140444	2.53085668	4.07282109	6.18850648	6.30063183	7.21527282	1.38243312
WBGene00022569	ZC239.6	7.44687840	7.78513496	8.53751632	8.75766310	0.47988233	7.24592182	8.05982479	8.17045291	8.48057645	0.41363024
WBGene00022570	sdz-35	3.49464081	3.72739197	4.47840875	5.97621880	1.38720441	4.12467712	4.25952018	4.56651303	5.03226979	0.90956816
WBGene00022584	ZC266.1	6.78076879	6.33093591	5.75248242	5.95157696	-0.3571721	7.07918021	6.54541332	6.63266480	6.19465375	-0.3104173
WBGene00022593	ZC328.3	8.86910650	9.56923556	10.0508743	9.92870236	0.39316674	8.59263489	9.62614673	9.54489432	9.83207907	0.36365258
WBGene00022816	fbn-1	10.6777511	12.2952162	12.8628638	12.4828427	0.69186129	10.8495121	12.1994936	12.2855794	12.6731388	0.53260020
WBGene00022846	ZK1055.5	3.77703892	4.13167296	4.52603783	4.58509820	0.51513554	4.01789846	4.58160241	4.79070232	5.07735625	0.73568298
WBGene00022847	ZK1055.6	7.84835346	8.44817153	9.03717500	9.72025580	0.62936690	7.76934710	8.60381496	8.52579683	9.00336623	0.38104401
WBGene00022848	ZK1055.7	9.54563836	9.69181659	10.3178451	10.8665076	0.47030097	9.40671277	9.78455843	10.0309295	10.3868947	0.32327770

Gene ID	Gene Name	SET-16 0.0mM	SET-16 0.01mM	SET-16 0.1mM	SET-16 1.0mM	Log2Fold Change	UTX-1 0.0mM	UTX-1 0.01mM	UTX-1 0.1mM	UTX-1 1.0mM	Log2Fold Change
WBGene00023395	Y82E9BL.9	4.34344026	4.98432495	6.13580967	5.30642040	0.70963857	4.66124284	5.85104423	5.73550112	5.93047161	0.60789382
WBGene00023401	ZK380.t2	7.98880950	6.98776139	5.94319836	6.17397896	-0.6691536	8.04555891	7.20114970	7.15622448	6.57954545	-0.5612981
WBGene00023483	Y75B8A.39	3.65068957	3.75615360	5.67034305	7.50767984	1.83513291	4.26677259	5.43634673	5.30140391	5.95422355	0.87500058
WBGene00023484	Y54G2A.37	2.75263689	3.41896245	4.51647649	5.39616458	1.91940363	4.21718083	5.01689059	5.49376362	5.72292818	1.06149008
WBGene00043702	Y54G2A.7	5.78819839	5.92771448	6.19036089	6.74790314	0.36044352	5.96466011	6.44670830	6.74435475	6.90515930	0.38287262
WBGene00044013	F15H10.9	2.49810320	3.10906506	6.38306240	7.82583536	3.38539615	3.47949633	5.24916295	5.37600569	6.15360475	1.61730420
WBGene00044014	F15H10.10	2.49810320	3.42394907	6.96920847	8.56406704	3.55653914	3.68561749	5.98410365	6.04639000	6.95821352	1.71899255
WBGene00044150	VB0395L.1	6.02676660	5.22670617	4.73091636	4.21650362	-0.7373795	6.18549320	5.79617528	5.61526276	5.36392291	-0.4260745
WBGene00044206	T26H5.9	8.26795322	9.16216308	10.3225442	10.6435906	0.82067490	7.18283165	8.80555922	8.89488034	9.43960391	0.65393180
WBGene00044207	Y6G8.5	2.69816161	2.80754414	4.35827737	6.09010080	2.18446206	3.76008401	4.80150076	4.77937881	5.25441570	0.94217312
WBGene00044212	Y68A4A.13	5.61740675	6.90478930	9.05881594	10.1384524	1.62911718	4.99455400	6.58925662	7.87020100	8.28347603	1.20140666
WBGene00044237	pals-9	3.09563050	3.87785185	6.57753799	8.42476223	2.64635518	3.97644567	5.96965110	5.76668342	6.65866729	1.09374665
WBGene00044296	F10C1.9	8.41465469	7.90718431	7.22520046	6.13757591	-0.7552268	7.83092519	6.99746255	6.75147236	6.83965196	-0.3922982
WBGene00044331	clec-25	3.80159230	3.93755923	4.50698880	5.18711915	0.75973802	4.44933130	5.02703928	5.29242929	5.22606221	0.56830666
WBGene00044379	F40H7.12	4.24862407	3.97318218	5.26509690	7.45471859	1.37698492	3.61113833	5.26367386	5.02134665	5.93076159	1.31886718
WBGene00044416	C08E3.15	2.49810320	2.52330863	5.49618095	7.69875393	3.49275193	3.61113833	4.63152990	4.73265408	5.34213659	1.22799377
WBGene00044427	F56A6.5	2.75263689	2.72309033	4.19165076	6.31230253	2.52287820	3.73074694	4.02600076	4.24518805	5.20599821	1.48902291
WBGene00044707	pals-15	2.49810320	3.08946385	6.07808177	7.74603661	3.33019472	3.74144788	5.37656938	5.67556083	6.69500800	1.65181580
WBGene00044719	clec-172	4.92813938	4.84932662	3.63139828	2.52905570	-1.6597993	4.90281153	3.85686812	4.21198616	3.60765189	-1.3207114
WBGene00044723	K11H12.11	6.24236133	5.44625205	3.69809494	3.12995763	-1.6138021	5.66662019	4.17885653	4.02468080	4.08660441	-1.4083145
WBGene00044783	T26H5.10	4.36783428	5.51810977	7.31598597	8.25937611	1.55818296	4.40111705	5.92865980	6.31574092	6.64697616	0.99441801
WBGene00044787	pals-36	2.72435470	3.14298188	5.50745517	6.54769535	2.30138776	4.03816456	5.25929203	5.08315355	5.76273949	1.02562708
WBGene00045188	B0284.5	3.08169775	3.91407853	4.66343117	6.51720499	1.97500115	3.69233473	4.99836139	5.10649920	5.61181622	1.30804737
WBGene00045239	Y49E10.29	7.34335771	6.76413241	5.52289758	4.98695480	-0.9310234	8.30240913	6.88047271	7.57268137	6.63040915	-0.5131218
WBGene00045255	nhr-146	6.40977075	6.58692913	6.98014580	7.09351521	0.27914811	6.38526413	6.96173669	6.99156918	7.16510039	0.27498311
WBGene00045338	M01B2.13	3.85377212	4.27396297	5.61130125	7.30161687	1.55072163	4.39345372	5.61335130	5.57050369	6.19554802	0.93009446
WBGene00045393	F26D11.13	3.25857134	4.08900210	5.13342716	6.47771360	1.55693092	4.03179832	5.03530773	4.92642696	5.31423598	0.82313470
WBGene00045399	Y47G6A.33	9.07484261	8.06916124	7.49992226	6.73729203	-0.8072675	9.88066282	8.52710294	9.10161152	8.09463145	-0.5239355
WBGene00045401	eol-1	4.51887609	5.41955426	8.70111353	10.3712430	2.35194902	4.48482216	7.52723233	7.67788119	8.39792032	1.31540358
WBGene00045411	C25F9.11	6.49617700	6.93873106	8.32936224	8.79492750	0.94482988	6.00429200	6.63502387	6.72802704	7.48385469	0.55918095
WBGene00045412	C25F9.12	4.87929223	4.66402526	6.26524923	6.24294629	0.74906964	4.50699778	5.08351483	5.35051701	5.72534870	0.74837424
WBGene00045415	Y43F8B.15	3.15096827	4.58111454	6.53167383	7.77695725	2.05467611	4.07587377	5.52163875	5.74612908	6.33818609	1.23781576
WBGene00045416	Y37H2A.14	7.31960547	7.35320813	8.22433692	9.24205092	0.66802810	6.69682359	7.59662565	7.79585591	8.30430336	0.58727372
WBGene00045457	F33H12.7	4.63475057	5.47788145	6.83993672	8.62401966	1.53383431	5.23696868	6.19626687	5.81437094	7.22723298	0.78076664
WBGene00045475	T07A5.7	4.72599843	4.89614581	6.38242786	7.66257847	1.23610350	4.98253024	5.67718521	6.02682752	7.02884524	0.90931239
WBGene00050904	Y70C5A.3	6.72595587	6.29681280	3.90962139	3.41349679	-1.8759593	6.02198200	4.04827189	3.92261595	3.75590545	-2.2031911
WBGene00050906	F20E11.17	2.94253257	4.14510685	6.77895955	9.09194962	3.07553030	3.86207739	5.32316823	5.69595274	7.06317466	1.77635936

Gene ID	Gene Name	SET-16 0.0mM	SET-16 0.01mM	SET-16 0.1mM	SET-16 1.0mM	Log2Fold Change	UTX-1 0.0mM	UTX-1 0.01mM	UTX-1 0.1mM	UTX-1 1.0mM	Log2Fold Change
WBGene00050914	T12B5.15	8.01257865	6.86110354	5.79622899	5.79810318	-0.8221735	8.15412465	7.28958144	7.11483641	6.56055830	-0.5728958
WBGene00077629	K10G4.13	2.63726838	3.36490928	5.41356602	7.36453845	2.69505985	3.73074694	5.24331858	5.28528979	5.81438481	1.20094352
WBGene00086568	Y2H9A.6	3.52782363	4.53077543	7.46101036	9.06133425	2.39952540	4.52169383	6.75601231	6.66765186	7.83238611	1.26249299
WBGene00138721	pals-37	4.15476850	5.52184374	8.49648638	10.4242739	2.50561919	4.31064820	7.85073435	7.76240083	8.81299415	1.38356297
WBGene00194646	Y105C5A.1270	3.14392214	2.98732486	4.84487135	6.36089475	2.24315387	3.83845793	5.07898402	4.62664995	5.53105338	0.99577515
WBGene00194713	F19B10.13	4.19646945	4.17302389	5.27939173	7.52657962	1.42836742	4.40591130	4.87597011	4.87110034	5.96899317	0.98572769
WBGene00194746	pals-20	3.61114141	4.07622647	5.46395285	6.47983716	1.53902466	4.36458498	5.29452309	5.60068875	5.81566584	0.85140833
WBGene00194815	Y43F8B.23	4.52961562	5.01803465	5.79029067	6.68785271	0.92917049	4.65781617	5.46843554	5.45998281	6.05849635	0.71219211
WBGene00194902	Y39H10B.3	3.11366121	3.39844390	5.99409714	7.72646787	2.40769354	3.92410079	5.83521538	5.50026332	6.39784124	1.05941870
WBGene00195165	F57G4.11	2.55626806	3.18062042	7.52777785	9.63723895	3.94983837	3.73074694	6.35547233	6.42090835	7.50014206	1.61708252
WBGene00195172	K10G4.14	2.35594575	2.89293716	4.23892692	6.09349613	2.81031098	3.47949633	4.23858737	4.11106025	4.71221205	1.27892190
WBGene00195177	Y43F8B.25	2.66939972	3.64903551	4.76794108	5.39824632	1.70752294	3.83845793	4.44483663	4.46078745	4.87237875	0.94936928
WBGene00195183	R04A9.9	6.68956272	5.61334887	4.17202426	4.23507089	-1.1627703	6.77840902	6.01638990	5.61388972	5.39652221	-0.7289330
WBGene00202499	B0507.15	2.55626806	3.00134952	5.02248895	6.06838648	2.41338382	3.47949633	4.76492823	4.47023068	5.38995903	1.35705345
WBGene00206484	C31H2.14	6.28784494	5.37886139	4.62302254	4.10198025	-1.0603457	6.37446742	5.61568956	5.33794803	5.29942324	-0.5562562
WBGene00206537	Y71H9A.10	2.35594575	2.73819506	3.69219061	3.71335649	1.77374383	3.69233473	4.23349108	4.48008752	4.67041889	1.11768557
WBGene00219316	F21A3.11	8.23490068	8.34049864	7.31297253	5.90029920	-0.8437035	7.84452240	6.45633206	5.59439554	4.94364245	-1.3442435
WBGene00219493	C18D4.12	4.51367581	4.27770938	5.88270493	7.12317968	1.19538482	4.80566707	5.48063719	6.09265575	6.76259856	0.89166150
WBGene00219609	linc-7	9.39126489	8.60087179	7.65840812	7.60071605	-0.6503953	9.55190305	8.69143952	8.53774813	7.97565591	-0.5300706
WBGene00219686	linc-125	3.49685580	3.82233340	4.36651082	5.11620081	0.96349469	3.99322322	4.57601972	4.93778756	5.66218650	1.14368828
WBGene00235133	T26H5.14	5.92244772	6.30712513	8.17404695	8.95304242	1.15083297	5.45129815	7.14964307	7.58299342	7.93913356	0.88902867
WBGene00235307	B0507.17	2.63178946	2.80635440	3.84914303	5.72255999	2.44510371	3.69233473	4.73604016	4.63729862	5.22539327	1.13862781
WBGene00249826	F42A9.18	3.99746293	4.60812534	4.49741089	4.88873839	0.41578116	4.66634050	5.01550798	5.08284761	5.49039529	0.52905971
WBGene00255420	Y51F10.15	3.05993894	3.42559596	4.71486097	5.25534181	1.40636370	3.47949633	4.21469025	4.32168969	4.60808838	1.34816979
WBGene00304201	T07H8.11	3.15900585	3.58515517	5.29014884	7.11865749	2.03415058	4.33450053	5.43996014	5.80705366	6.36075476	1.01067561

A total of 61 commonly down-regulated and 329 commonly up-regulated genes from both SET-16/SomaTIR1 and UTX-1/SomaTIR1 depletion experiments are listed in order from SET-16 (left) to UTX-1 (right). Two genes, nas-24 and F25E5.7 (red box), do not share the same response trend per depletion. WormBase Gene IDs are listed at left followed by actual gene name. Numbers indicate mean base read count. Log2FoldChange was calculated from the overall change in expression across three auxin concentrations compared to control. Table data assembled using Numbers v10.1 (6913).

Supplemental Figure Data.

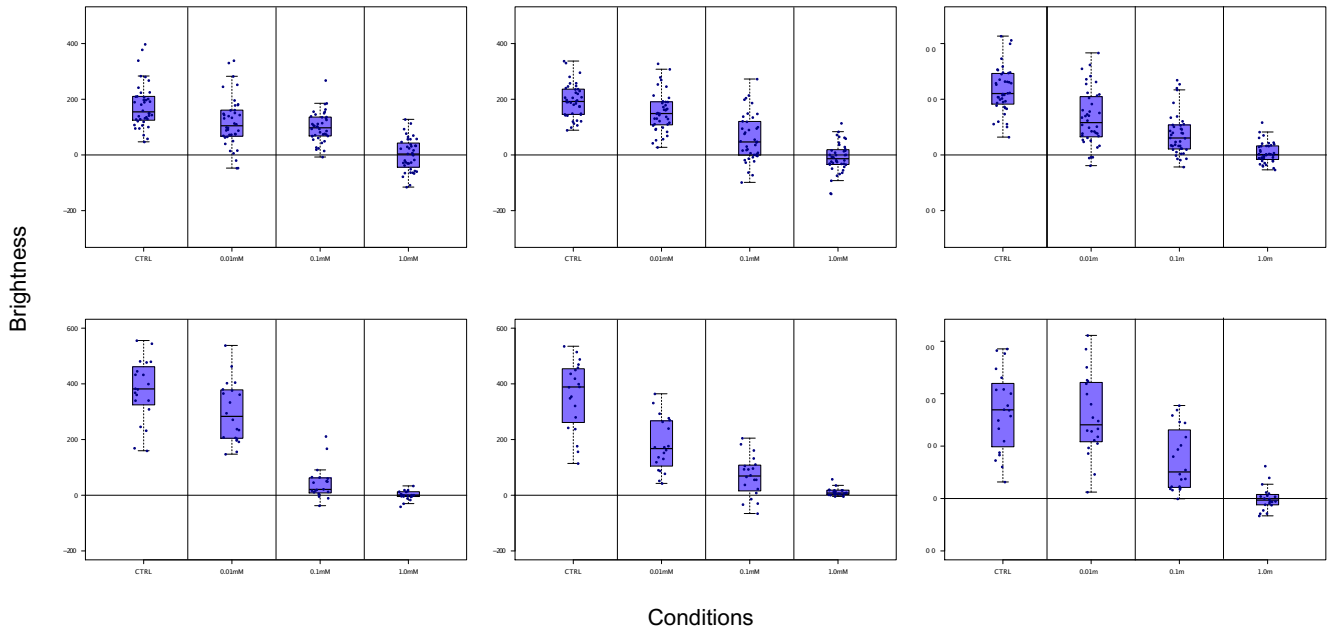

Figure S1. Individual Replicates for Germline and Somatic Depletions of SET-16.

GFP fluorescence intensity across auxin concentrations of ieSi64II;set-16(syb1046)III oocyte nuclei and ieSi57II;set-16(syb1046)III somatic cells (n=40 per condition per replicate for germline and n=20 per condition per replicate for soma). Data points indicate mean pixel intensity calculated by the difference in nuclear GFP from background. Replicates for germline (top) and somatic (bottom) strains are shown in order from left to right.

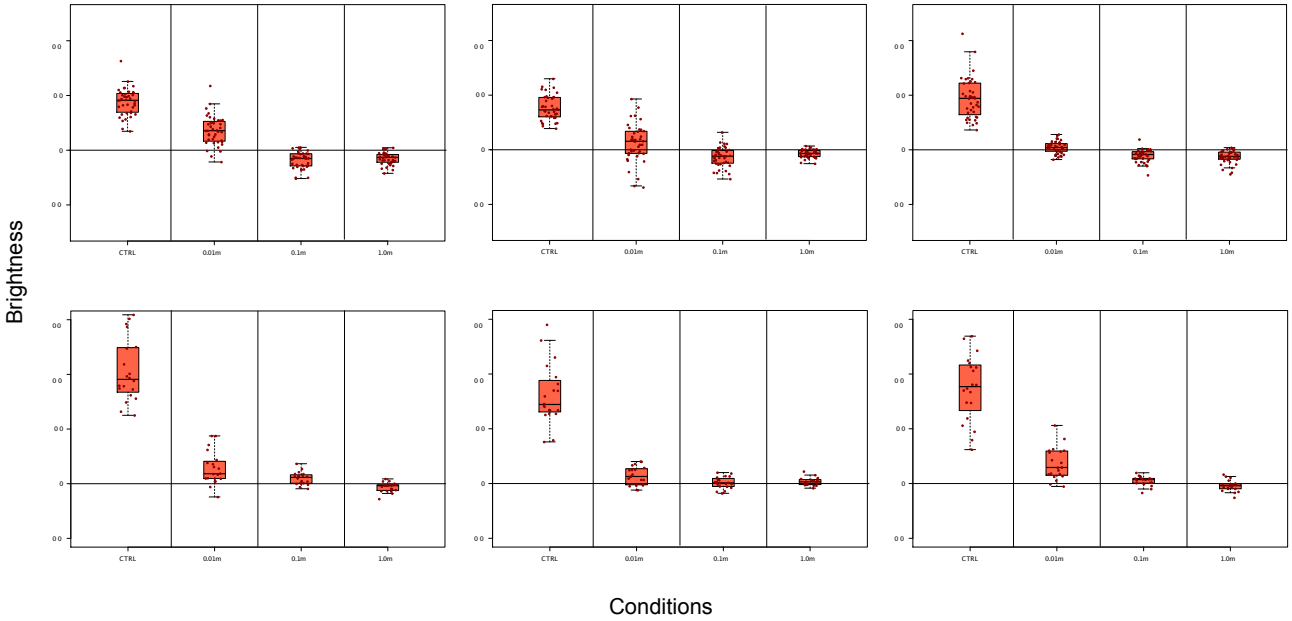

Figure S2. Individual Replicates for Germline and Somatic Depletions of UTX-1.

GFP fluorescence intensity across auxin concentrations of utx-1(syb1026)X;ieSi38IV oocyte nuclei and ieSi57II;utx-1(syb1026)X somatic cells (n=40 per condition per replicate for germline and n=20 per condition per replicate for soma). Data points indicate mean pixel intensity calculated by the difference in nuclear GFP from background. Replicates for germline (top) and somatic (bottom) strains are shown in order from left to right.

References

Works Cited

Anderson EC, Horvitz R. (2007) Two C. elegans histone methyltransferases repress lin-3 EGF transcription to inhibit vulval development. *Development,* 134, 2991-2999.

Aref-Eshghi E., Schenkel L.C., Lin H., Skinner C., Ainsworth P., Paré G., Rodenhiser D., Schwartz C., & Sadikovic B. (2017) The defining DNA methylation signature of kabuki syndrome enables functional assessment of genetic variants of unknown clinical significance. *Epigenetics,* 12(11), 923-933.

Brenner S. (1973) The genetics of caenorhabditis elegans. *Genetics,* 77, 71-94.

Cheon C., & Ko J.M. (2015) Kabuki syndrome: clinical and molucular characteristics. *Korean Journal of Pediatrics,* 58(9), 317-324.

Cao K, Collings CK, Morgan MC, Marshall SA, Rendleman EJ, Ozark PA, Smith ER, Shilatifard Ali (2018) An Mll4/COMPASS-Lsd1 epigenetic axis governs enhancer function and pluripotency transition in embryonic stem cells. *Science Advancements,* 4, eaap8747.

Cocciadiferro D., Augello B., De Nittis P., Zhang J., Mandriani B., Malerba N., Squeo G.M., Roman A., Piccinni B., Verri T., Micale L., Pasqualucci L., & Merla G. (2018) Dissecting KMT2D missense mutations in kabuki syndrome patients. *Human Molecular Genetics,* 27(21), 3651-3668.

Cong L., Ran F.A., Cox D., Lin S., Barretto R., Habib N., Hsu P.D., Wu X., Jiang W., Marraffini L.A., Zhang F. (2013) Multiplex genome engineering using CRISPR/Cas systems. *Science,* 339, 819-823.

Conte Jr. D., MacNeil L.T., Walhout A.J.M, Mello C. (2017) RNA interference in Caenorhabditis elegans. *Curr Protoc Mol Biol,* 109, 26.3.1-26.330.

Corsi A.K., Wightman B., & Chalfie M. (2015) A transparent window into biology: a primer on Caenorhabditis elegans. *Genetics,* 200, 387-407.

Culetto E., & Sattelle D.B. (2000) A role for caenorhabditis elegans in understanding the function and interactions of human disease genes. *Human Molecular Genetics,* 9(6), 869-877.

Daniel K., Icha J., Horenburg C., Müller D., Norden C., Mansfield J. (2018) Conditional control of fluorescent protein degradation by an auxin-dependent nanobody. *Nature Communications*, 3297(9), 1-13.

Dhar S.S., Lee S., Kan P., Voigt P., Ma L., Shi X., Reinberg D., & Lee M.G. (2012) Trans-tail regulation of MLL4-catalyzed H3K4 methylation by H4R3 symmetric dimethylation is mediated by a tandem PHD of MLL4. *Genes & Development,* 26, 2749-2762.

Delaney K., Strobino M., Wenda J.M., Pankowski A., & Steiner F.A. (2019) H3.3K27M-induced chromatin changes drive ectopic replication through misregulation of the JNK pathway in C. elegans. *Nature Communications,* 10, 2529.

De Ley P. (2006) A quick tour of nematode diversity and the backbone of the nematode phylogeny. In: *Community TCeR* (ed) WormBook; http://www.wormbook.org.

Dorighi K.M., Swigut T., Henriques T., Bhanu N.V., Scruggs B.S., Nady N., Still II C.D., Garcia B.A., Adelman K., & Wysocka J. (2017) Mll3 and Mll4 facilitate enhancer RNA synthesis and transcription from promoters independently of H3K4 monomethylation. *Molecular Cell,* 66(4), 568-575.

Dudley N.R., Labbe J.C., Goldstein B. (2002) Using RNA interference to identify genes required for RNA interference. *Proc Natl Acad Sci USA*, 99, 4191–4196.

Ellis H.M., Horvitz H.R. (1986) Genetic Control of Programmed Cell Death in the Nematode C. elegans. *Cell,* 44, 817-829.

Fang F., Xu Y., Chew K., Chen X., Ng H., & Matsudaira P. (2014) Coactivators p300 and CBP maintain the identity of mouse embryonic stem cells by mediating long-range chromatin structure. *Stem Cells,* 32, 1805-1816.

Fisher K., Southall S.M., Wilson J.R., & Poulin G.B. (2010) Methylation and demethylation activities of a C. elegans MLL-like complex attenuate RAS signaling. *Developmental Biology,* 341, 142-153.

Fire A., Xu S., Montgomery M.K., Kostas S.A., Driver S.E., Mello C.C. (1998) Potent and specific genetic interference by double-stranded RNA in Caenorhabditis elegans. *Nature*, 391, 806-811.

Froimchuk E., Jang Y., & Ge K. (2017) Histone H3 lysine 4 methyltransferase KMT2D. *Gene,* 627, 337-342.

Greer E.L., Maures T.J., Hauswirth A.G., Green E.M., Leeman D.S., Maro G.S., Han S., Banko M.R., Gozani O., & Brunet A. (2010) Members of the H3 lysine 4

trimethylation complex regulate lifespan in a germline-dependent manner in C. elegans. *Nature,* 466(7304), 383-387.

Heintzman N.D., Stuart R.K., Hon G., Fu Y., Ching C.W., Hawkins R.D., Barrera L.O., Calcar S.V., Qu C., Ching K.A., Wang W., Weng Z., Green R.D., Crawford G.E., & Ren B. (2007) Distinct and predictive chromatin signatures of transcriptional promoters and enhancers in the human genome. *Nature Genetics,* 39(3), 311-318.

Hedgecock E.M., Sulston J.E., Thomson J.N. (1983) Mutations affecting programmed cell death in the nematode Caenorhabditis elegans. *Science* 220(4603), 1277-1279.

Jang Y., Wang C., Zhuang L., Lie C., & Ge K. (2017) H3K4 methyltransferase activity is required for MLL4 protein stability. *Journal of Molecular Biology,* 423(13), 2046-2054.

Kantidakis T., Saponaro M., Mitter R., Horswell S., Kranz A., Boeing S., Aygün O., Kelly G.P., Matthews N., Stewart A., Stewart A.F., & Svejstrup J.Q. (2015) Mutation of cancer driver MLL2 results in transcription stress and genome instability. *Genes & Development,* 30, 408-420.

Kasimatis K.R., Moerdyk-Schauwecker M.J., & Philips P.C. (2018) Auxin-mediated sterility induction system for longevity and mating studies in caenorhabditis elegans. *G3 Bethesda,* 8, 2655-2662.

Kenyon C., Chang J., Gensch E., Rudner A., Tabtiang R. (1993) A C. elegans mutant that lives twice as long as wild type. *Nature*, 366, 461-464.

Kim D., Rhee J.C., Yeo S., Shen R., Lee S., Lee J.W., & Lee S. (2015) Crucial roles of mixed-lineage leukemia 3 and 4 as epigenetic switches of the hepatic circadian clock controlling bile acid homeostasis in mice. *Hepatology,* 61(3), 1012-1023.

Kouzarides T. (2007) Chromatin modifications and their function. *Cell,* 128, 693-705.

Krüger A.V., Jelier R., Dzyubachyk O., Zimmerman T., Meijering E., & Lehner B. (2015) Comprehensive single cell-resolution analysis of the role of chromatin regulators in early C. elegans embryogenesis. *Developmental Biology,* 398, 153-162.

Kuroki Y., Suzuki Y., Chyo H., Hata A., Matsui I., (1981) A new malformation syndrome of long palpebral fissures, large ears, depressed nasal tip, and skeletal anomalies with postnatal dwarfism and mental retardation. *Journal of Pediatrics* 99(4), 570-573.

Lee J.E., Wang C., Xu S., Cho Y.W., Wang L., Feng X., Baldridge A., Sartorelli V., Zhuang L., Peng W. (2013) H3K4 mono- and di-methyltransferase MLL4 is required for enhancer activation during cell differentiation. *eLife 2:e01503.*

Lin-Shiao E., Lan Y., Coradin M., Anderson A., Donahue G., Simpson C.L., Sen P., Saffie R., Busino L., Garcia B.A., Berger S.L., & Capell B.C. (2017) KMT2D regulates p63 target enhancers to coordinate epithelial homeostasis. *Genes & Development,* 32, 181-193.

Martinez M.A., Kinney B.A., Ashley G., Ragle J.M., Hammell C.M., Ward J.D., & Matus D.Q. (2019) Members of the histone H3 lysine 4 trimethylation complex regulate lifespan in a germline-dependent manner in C. elegans. *Nature,* 466(7304), 383-387.

Matsumoto N., & Niikawa N. (2003) Kabuki make-up syndrome: a review. *American Journal of Medical Genetics,* 117C, 57-65.

Maures T.J., Greer E.L., Hauswirth A.G., & Brunet A. (2011) The H3K27 demethylase UTX-1 regulates C. Elegans lifespan in a germline-independent, insulin-dependent manner. *Aging Cell,* 10, 980-990.

Mohan M., Herz H.M., Smith E.R., Zhang Y., Jackson J. (2011) COMPASS-like complexes in Drosophila. *Mol Cell Biol.* 31(21), 4310-4318.

Moore L.D., Le T., & Fan G. (2013) DNA methylation and its basic function. *Neuropsychopharmacology,* 38, 23-38.

Morawska M., & Ulrich H.D. (2013) An expanded tool for the auxin-induced degron system in budding yeast. *Yeast,* 30, 341-351.

Nagel G., Brauner M., Liewald J.F., Adeishvili N., Bamberg E., Gottschalk A. (2005) Light activation of channelrhodopsin-2 in excitable cells of Caenorhabditis elegans triggers rapid behavioral responses. *Current Biology*, 15, 2279-2284.

Ng S.B., Bigham A.W., Buckingham K.J., Hannibal M.C., McMillin M., Gildersleeve H., Beck A.E., Tabor H.K., Cooper G.M., Mefford H.C., Lee C., Turner E.H., Smith J.D., Rieder M.J., Yoshiura K., Matsumoto N., Ohta T., Niikawa N., Nickerson D.A., Bamshad M.J., & Shendure J. (2010) Exome sequencing identifies MLL2 mutations as a cause of kabuki syndrome. *Nature Genetics,* 42(9), 790-793.

Niikawa N., & Matsuura N. (1981) Kabuki make-up syndrome: a syndrome of mental retardation, unusual facies, large and protruding ears, and postnatal growth deficiency. *The Journal of Pediatrics,* 99(4), 565-569.

Nishimura K., Fukagawa T., Takisawa H., Kakimoto T., & Kanemaki M. (2009) An auxin-based degron system for the rapid depletion of proteins in nonplant cells. *Nature Methods,* 6(12), 917-923.

Placek K., Hu G., Cui K., Zhang D., Ding Y., Lee E., Jang Y., Wang C., Konkel J.E., Song J., Liu C., Ge K., Chen W., & Zhao K. (2017) Mll4 prepares enhancer landscape for Foxp3 induction via chromatin looping. *Nature Immunology,* 18(9), 1035-1045.

Rickels R., Hu D., Collings C.K., Woodfin A.R., Piunti A., Mohan M., Herz H., Kvon E., & Shilatifard A. (2016) An evolutionary conserved epigenetic mark of polycomb response elements implemented by Trx/MLL/COMPASS. *Molecular Cell,* 63(2), 318-328.

Roguev A., Schaft D., Shevchenko A., Pijnappel WW., Wilm M. (2011) The Saccharomyces cerevisiae Set1 complex includes an Ash2 homologue and methylates histone 3 lysine 4. EMBO J. 2001; 20:7137–48.

Ruegger M., Dewey E., Gray W.M., Hobbie L., Turner J., Estelle M. (1998) The TIR1 protein of Arabidopsis functions in auxin response and is related to human SKP2 and yeast Grr1p. *Genes & Development*, 12, 198-207.

Ruthenburg A.J., Allis C.D., & Wysocka J. (2007) Methylation of lysine 4 on histone H3: intricacy of writing and reading a single epigenetic mark. *Molecular Cell,* 25, 15-30.

Schwenty-Lara J., Nürnberger A., & Borchers A. (2018) Loss of function of KMT2D, a gene mutation in kabuki syndrome, affects heart development in Xenopus laevis. *Developmental Dynamics,* 248, 465-476.

Sulston, J (1988) Cell lineage. In Wood, W.B. (ed.), The Nematode Caenorhabditis elegans. Cold Spring Harbor Laboratory Press, Cold Spring Harbor, NY, 123-155.

Sze CC, Shilatifard A (2016) MLL3/MLL4/COMPASS family on epigenetic regulation of enhancer function and cancer. Cold Spring Harb. Perspect. Med. 6(11). pii: a026427

Takahashi Y., Westfield G.H., Oleskie A.N., Trievel R.C., Shilatifard A., & Skiniotis G. (2011) Structural analysis of the core COMPASS family of histone H3K4 methylases from yeast to human. *PNAS,* 108(51), 20526-20531.

Teale W.D., Paponov I.A., & Palme K. (2006) Auxin in action: signaling, transport and the control of plant growth and development. *Nature Review,* 7, 847-859.

Vandamme J., Lettier G., Sidoli S., Di Schiavi E., Jensen O.N., & Salcini A.E. (2012) The C. elegans H3K27 demethylase UTX-1 is essential for normal development, independent of its enzymatic activity. *PLOS Genetics,* 8(5), Article e1002647

Wang S., Tang Z., Chen C., Shimada M., Koche R.P., Wang L., Nakadai T., Chramiec A., Krivtsov A.V., Armstrong S.A., & Roeder R.G. (2017) A UTX-MLL4-p300 transactional regulatory network coordinately shapes active enhancer landscapes for eliciting transcription. *Molecular Cell,* 67, 308-321.

Xiao Y., Bedet C., Robert V.J., Simonet T., Dunkelbarger S., Rakotomalala C., Soete G., Korswagen H.C., Strome S., & Palladino F. (2011) Caenorhabditis elegans chromatin-associated proteins SET-2 and ASH-2 are differentially required for histone H3 Lys 4 methylation in embryos and adult germ cells. *PNAS,* 108(20), 8305-8310.

Yan J., Chen S.A., Local A., Liu T., Qiu Y., Dorighi K.M., Preissl S., Rivera C.M., Wang C., Ye Z., Ge K., Hu M., Wysocka J., & Bing R. (2018) Histone H3 lysine 4 monomethylation modulates long-range chromatin interactions at enhancers. *Cell Research*, 28, 204-220.

Zhang HS, Du GY, Liu Y, Zhang ZG, Zhou Z, Li H, Dai KQ, Yu XY, & Gou XM (2016) UTX-1 regulates Tat-induced HIV-1 transactivation via changing the methylated status of histone H3. *International Journal of Biochemistry & Cell Biology,* 80, 51-56.

Zhang L., Ward JD., Cheng Z., & Dernburg A.F. (2015) The auxin inducible degradation (AID) system enables versatile conditional protein depletion in C. elegans. *Development,* 142, 4374-4384.

Works Consulted

Bayarsaihan D (2018) Modus operandi of COMPASS/MLL epigenetic writers in the mammalian genome. *Epigenomics,* 10(7), 861-863.

Martinez MA, Kinney BA, Ashley G, Ragle JM, Hammell CM, Ward JD, Matus DQ (2019) A water-soluble, synthetic auxin analog for rapid degradation of target proteins during C. elegans development. Manuscript doi: 10.1101/716837.